GEOLOGY OF THE MAD RIVER FAULT ZONE BETWEEN FIELDBROOK AND MCKINLEYVILLE, CALFORNIA BASED ON FIELD OBSERVATIONS AND HIGH RESOLUTION SPATIAL DATA ANALYSIS

By

Paul R. J. Sundberg

A Thesis Presented to

The Faculty of Humboldt State University

In Partial Fulfillment of the Requirements for the Degree

Master of Science in Environmental Systems: Geology

Committee Membership

Dr. Mark Hemphill-Haley, Committee Chair

Dr. Raymond Burke, Committee Member

Dr. Brandon Schwab, Committee Member

Dr. Christopher Dugaw, Graduate Coordinator

December 2013

ABSTRACT

GEOLOGY OF THE MAD RIVER FAULT ZONE BETWEEN FIELDBROOK AND MCKINLEYVILLE, CALFORNIA BASED ON FIELD OBSERVATIONS AND HIGH RESOLUTION SPATIAL DATA ANALYSIS

Paul R. J. Sundberg

Initial mapping of the Mad River fault zone (MRFZ) was at a scale of 1:24,000, over several years and at a reconnaissance level with limited access to land for field verification. My study area is within the MRFZ, approximately 15 km northeast of the city of Eureka, CA. I acquired LiDAR (1 m-resolution) hillshades and land access through an agreement with Green Diamond Resource Company. I used GPS and LiDAR in an effort to refine the original mapping.

I identified three flights of late-Pleistocene marine terraces on the hills between McKinleyville, CA and Fieldbrook, CA. Assuming an average uplift rate of 1 m/ky, these terrace flights correlate to sea level highs of the last inter-glacial period, between approximately 120 ka and 80 ka. Several alluvial terraces are present north of Fieldbrook Valley that correlate to the ages of the marine terraces.

I observed compression features related to the McKinleyville fault adjacent to the previously identified trace. Marine terraces on the footwall of the McKinleyville fault exhibit secondary scarps with up to 5 m of relief that are discontinuous along strike and may be related to compression along the Mad River fault, to the southwest.

The Trinidad fault is identified in Mather Creek, northwest of Fieldbrook Valley. The fault is present as an eroded remnant of resistant ridges, with no apparent scarps cutting the young channel deposits. Expression of the fault diminishes in the 100 ka marine terrace.

ACKNOWLEDGEMENTS

I would like to thank the following people and entities, with out whom this project wouldn't have been possible. First and foremost I would like to acknowledge the HSU Geology department. They have been instrumental in my current understanding of and love for geology and been an incredible resource for me in completing my thesis. Secondly, Green Diamond Resource Company (GDRCo) provided me land access for field verification and LiDAR data for interpretation. Woody at GDRCo acted as the point of contact and helped initiate the current research collaboration between HSU and GDRCo. My advisor Mark Hemphill-Haley was instrumental in helping me with the decision to pursue my idea for this local project. SHN Consulting Engineers & Geologists supported me in my career development and supplied GPS field equipment. Many thanks are due to HSU Geology students for field efforts and discussions. Courtney Kopp helped me see something bright and beautiful in the journey to the next phase in our lives together. I had many great discussions with my friends Christian, Giovanni, Jason, Shaun, Steve, Sylvia, Nick, Dylan, and a variety of others; thanks for helping me work through it.

TABLE OF CONTENTS

LIST OF TABLES

LIST OF FIGURES

INTRODUCTION

The study area is within the Mad River Fault Zone (Figure 1). The Mad River Fault Zone (MFRZ) is characterized by northwest trending folds and parallel northeast dipping thrust faults that have deformed Pleistocene deposits (Manning and Ogle 1952). The thrust faults and folds are the central part of the on-land portion of the southern end of the Cascadia Subduction Zone (CSZ) fold and thrust belt (Figures 1 and 2). The CSZ marks the boundary between the subducting Gorda Juan-de-Fuca plates beneath overriding North American plate (Figure 2). The CSZ fold and thrust belt consists of north-northwest trending east-northeast dipping reverse faults (Figures 1 and 2), fault-generated anticlines, and broad north-northwest trending synclines that extend across a 70-80 km wide belt situated along the western edge of the accretionary margin of the North American Plate (Carver and Burke, 1992). This region is defined by low-lying coastal hills with broad open valleys blanketed by thick vegetation. Uplifted thrust blocks form headlands sculpted by flights of raised glacio-eustatic marine terraces, while down-faulted blocks and synclinal troughs are occupied by lagoons, bays, and estuary-delta complexes (Carver, 1985).

Regional bedrock geology includes Jurassic/Cretaceous Franciscan complex, lower- to middle-Pleistocene Falor formation, and late-Pleistocene marine terrace and alluvial terrace deposits. The Franciscan complex consists of mélange characterized as highly sheared, with a silt and clay matrix and blocks of greenstone, sandstone, chert,

blue schist, greenschist, and other exotic lithologies; and greywacke sandstone with interbedded siltstone, mudstone, and conglomerate (Carver and Stephens, 1984). The Franciscan complex comprises a succession of tectonostratigraphic terranes (Clarke and McLaughlin, 1992). These terranes contain rock assemblages recording diverse histories including subduction, tectonic accretion, and large-scale lateral translation (Clarke and McLaughlin, 1992). Manning and Ogle (1950) describe the Falor formation as locally thick sequences of poorly consolidated inter-bedded shallow marine sands and pebbly sands, estuarine and bay sands, silts, and clays, and fluvial gravels. These marine sediments represent an environment that consisted of a relatively narrow marine basin that became shallower to the southeast, while fluvial gravels represent a terrestrial environment.

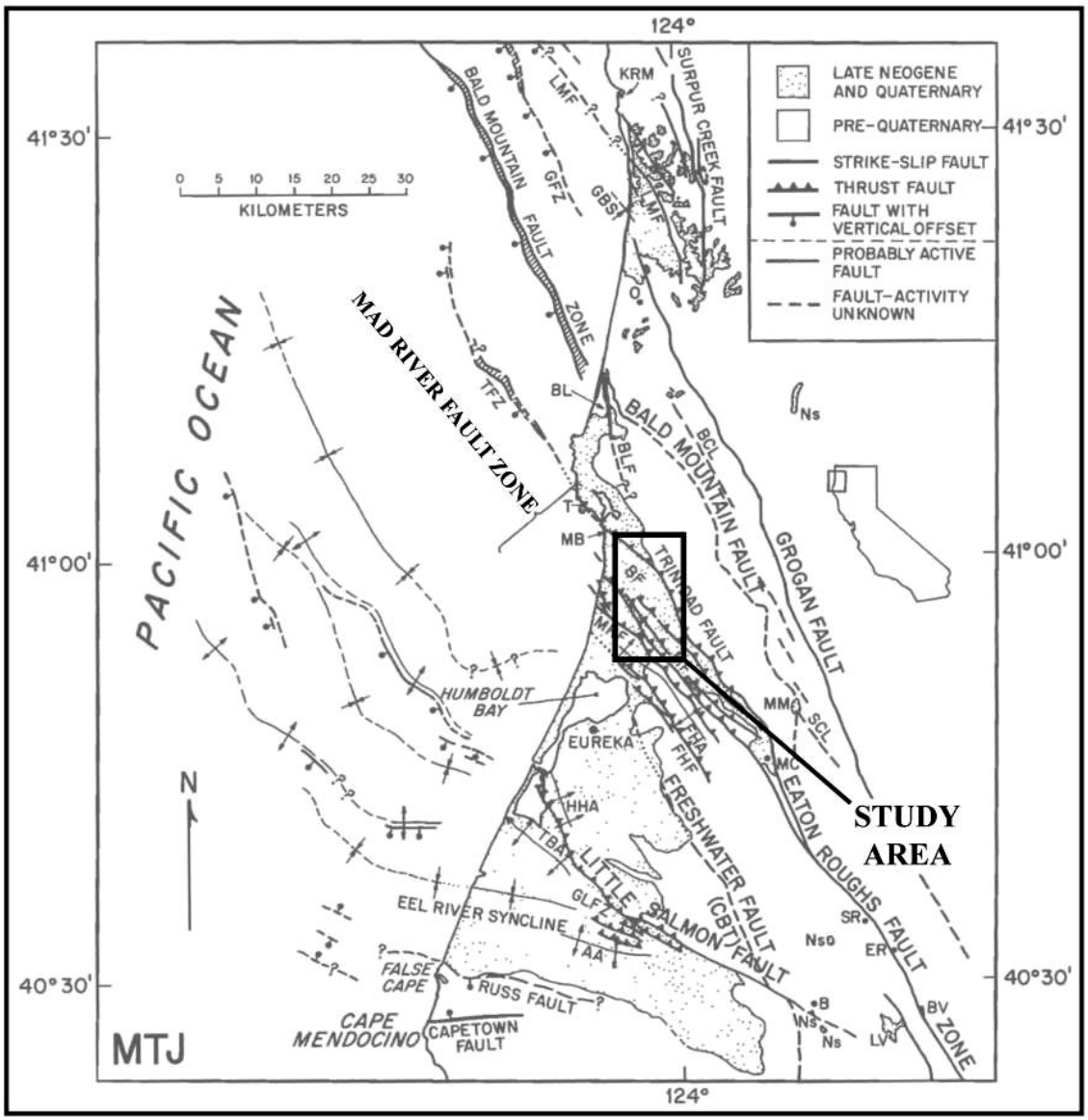

Figure 1: Tectonic map of north coastal California, north of Cape Mendocino, showing study area within the Mad River Fault zone. Modified from Kelsey and Carver (1988)

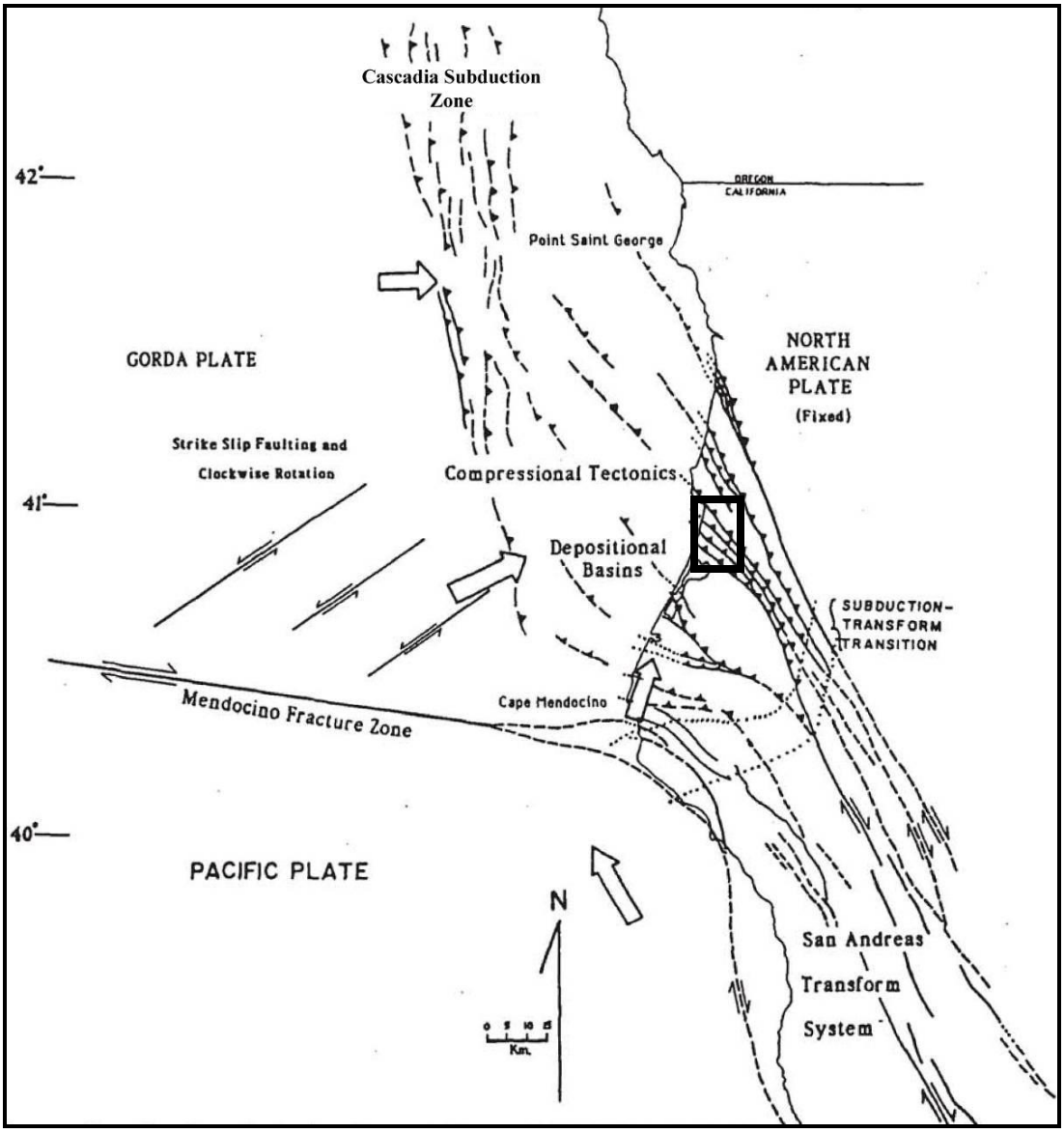

Figure 2: Regional tectonic setting of Northwest California in the vicinity of the Mendocino Triple Junction. General region around the study area is shown in the black box. (Modified from Carver, 1985)

Carver and Burke (1992) note that the MRFZ is a northwest striking, approximately 80-km-long and 15- to 25-km wide, belt of en-echelon thrust faults and

fault-generated folds that dip predominantly northeast (Figure 2). Thrust fault scarps are present west of the study area adjacent to School Road (Mad River fault) and the Arcata/Eureka Airport (McKinleyville fault) in McKinleyville, California (Coppersmith et al., 1982, Carver et al., 1982; Figure 3).

Several faults in the on-land portion of the fold and thrust belt are zoned active by the state of California and include structures within the MRFZ (CGS, 2007). In particular, the McKinleyville fault is considered to have experienced surface displacement within Holocene time (Carver and Burke, 1988; CGS, 2007) and capable of producing up to M_W 7.0 earthquake (Petersen et al., 2008).

Initial mapping efforts of the MRFZ were conducted by Carver et al. (1982) and lead to a subsequent map series produced by Carver and Stephens (1984) on USGS 7.5 minute quadrangles, at a scale of 1:24,000 (Figure 4). These became the base map for the state geologic and geomorphic maps of the area. Most mapping was done over several years and was conducted mainly at a reconnaissance level with limited land access for field verification.

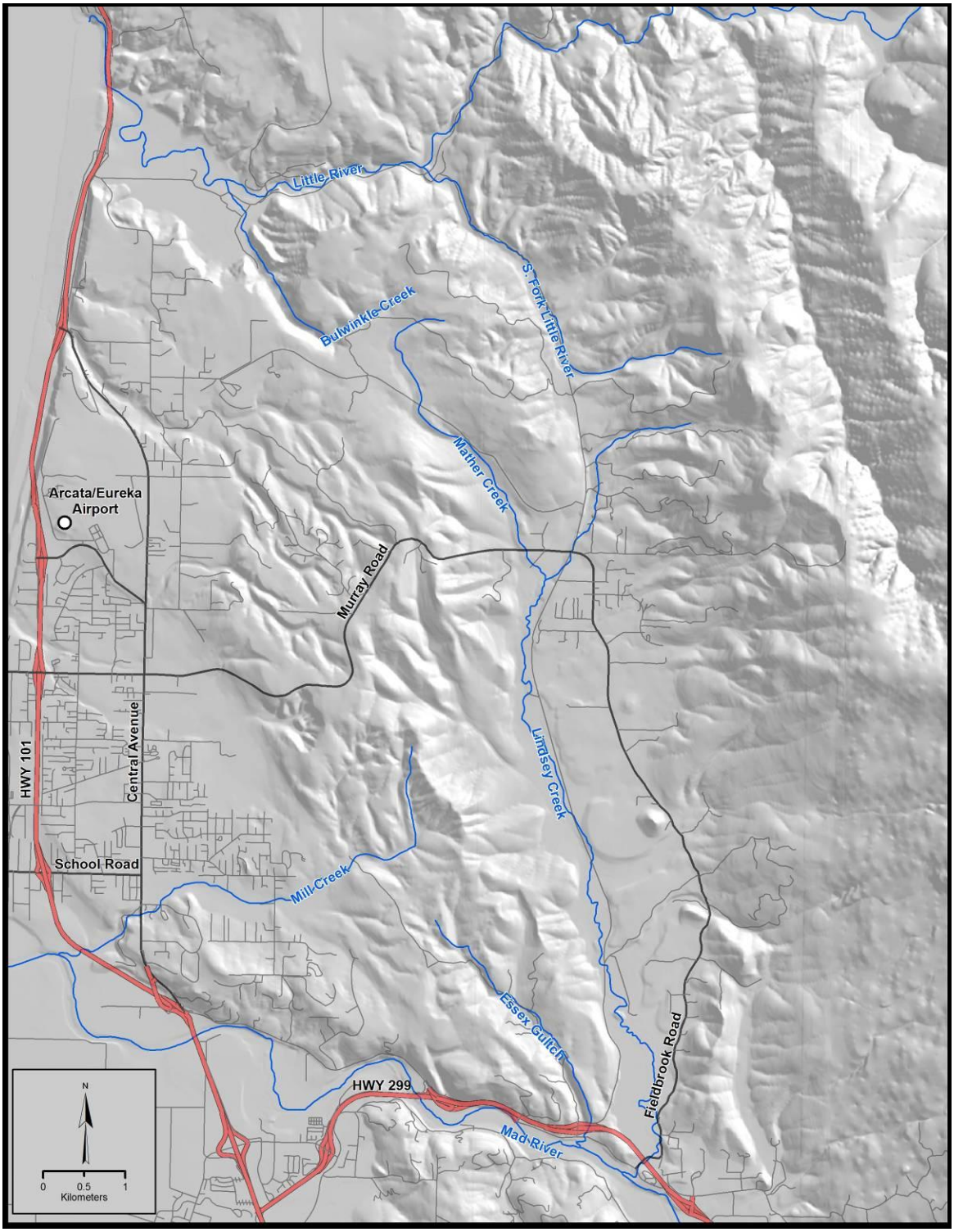

Figure 3: Study area and general vicinity with 10 m, 45 degree sun-angle hillshade.

Detailed mapping of the fault zone (Figure 4) originally took place in the late 1970's and early 1980's combining efforts by members of the Humboldt State University Geology Department and Simpson Timber Company (now Green Diamond Resource Company [GDRCo]). In addition to the early mapping efforts, Carver and Burke (1992) assessed uplift rates associated with faults in the MRFZ with respect to regional uplift rates, using late-Pleistocene marine terrace geomorphology and soil pit data. They identified several flights of marine terraces they believe mainly correlated to the last inter-glacial period (Figure 5). Locating and identifying marine terraces of specific ages and elevations lead to an understanding of regional tectonics and local fault activity.

In the last 30 years, technological advances have led to the development of significantly better topographic data. High-resolution ground imagery or LiDAR has provided researchers an opportunity to map at higher resolutions and led to advances in assessing geomorphology by being able to detect subtle topographic features beneath thick vegetation cover.

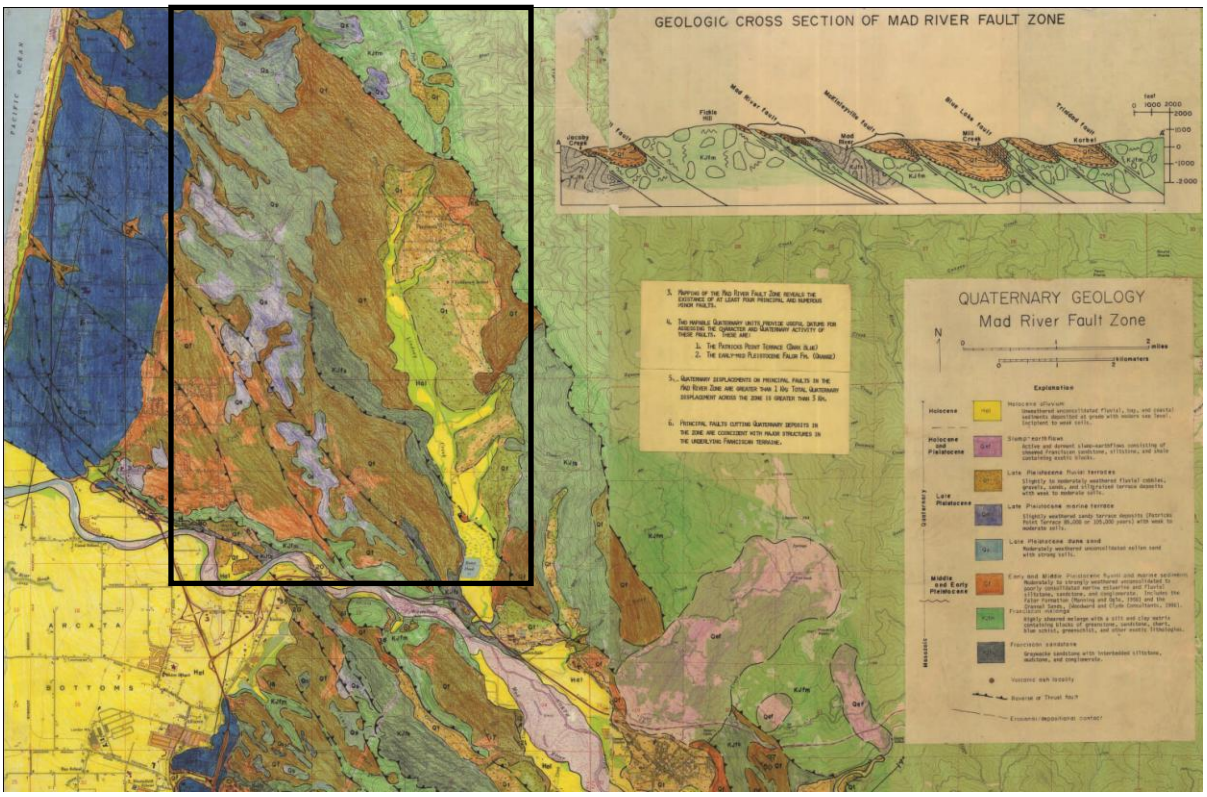

Figure 4: Unpublished geologic map of the Mad River Fault Zone (Carver and Stephens, 1984). Approximate study area boundary shown in black box.

.

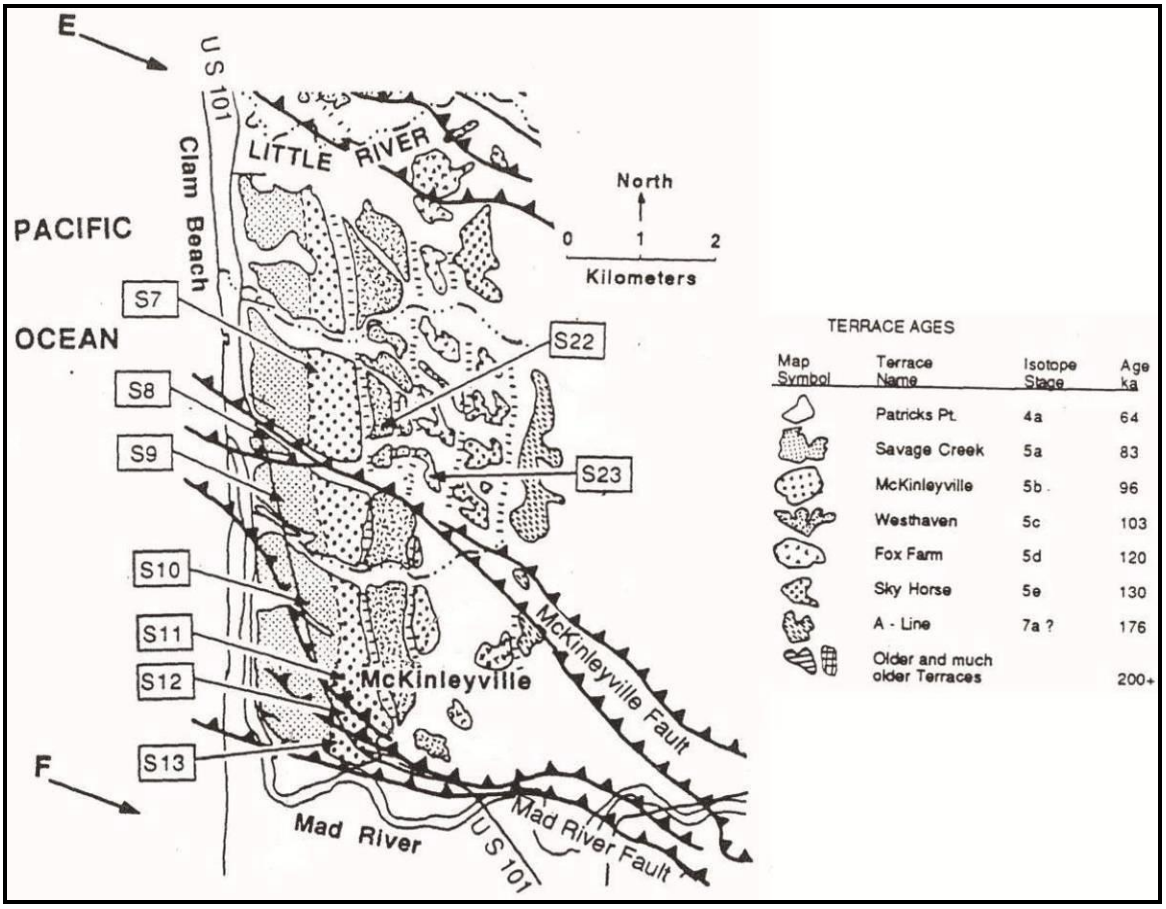

Figure 5: Map of raised, faulted, and folded late Pleistocene marine terraces in McKinleyville, California. The letters and numbers in boxes refer to soil pit locations from their study. (from Carver and Burke, 1992).

The objective of this study was to refine geomorphic mapping of the northwestern portion of the MRFZ in and around Fieldbrook Valley and McKinleyville, California. I used proprietary 1-m resolution topographic data provided by Green Diamond Resource Company (2011). My objectives were to refine the locations of Quaternary faults and geomorphic units in order to produce a more detailed and accurate Quaternary geomorphic map of the MRFZ. This purpose of this study is:

- to investigate elevation and distribution of Pleistocene geomorphic units within the fold and thrust belt and any potential differences resulting from active tectonics;
- gather information relating to late-Pleistocene to Holocene activity along faults and/or folds within the study area; and
- refine fault locations based on field observation and spatial analysis.

METHODS

Data Acquisition and Compilation

Using ArcMap GIS v. 9.3.1, I geo-referenced a digital copy of an unpublished geologic map series generated by Carver and Stephens (1984; Figure 4). For control purposes during geo-referencing of the geologic maps, I used USGS 7.5 minute topographic maps of the Arcata South, Arcata North, Blue Lake, and Cranel quadrangles. I digitized the geologic units from the geo-referenced maps to provide a basis for mapping. A map of raised, faulted, and folded late Pleistocene marine terraces (Figure 5), designated by age (Carver and Burke, 1992), was also geo-referenced and digitized for constraint on marine terrace locations. I acquired a 10 m digital elevation model (DEM) from the USGS Seamless Server (http://nationalmap.gov/viewer.html) for the purposes of generating a slope map, contour sets, and various sun-angle hillshade images.

Through collaboration with GDRCo and Humboldt State University's Department of Geology, I was provided proprietary LiDAR data and land access. The LiDAR data consists of 1 m-resolution hillshade images generated from sun angles of 45°, 135°, 225° and 315°. I was also provided 1 m contour data and a 1 m resolution slope map. I generated several surface profile lines throughout the study area that were best representative of the observed geomorphology (Appendix A). GDRCo used the profiles

lines to extrapolate 1 and 2-m elevation data. The 45° 1 m LiDAR hillshade and study area boundary are shown on Figure 6.

Marine Terraces Delineation

Using the LiDAR hillshades, I delineated terrace sets by differentiating the degree of drainage development, current elevation with respect to sea level, degree of surface rounding, and distribution and extent. I performed field checking to determine type of material present within mapped terrace units and, to confirm locations with respect to LiDAR mapping. The digitized geomorphic features served as basis for locating surfaces with established ages and as reference for the refinement of the terrace boundaries, elevations and ages. Timing of sea level highs in the mid- to late-Pleistocene have been refined since the work of Carver and Burke (1992), therefore, the new sea level curve data of Muhs et al. (2012) are considered here.

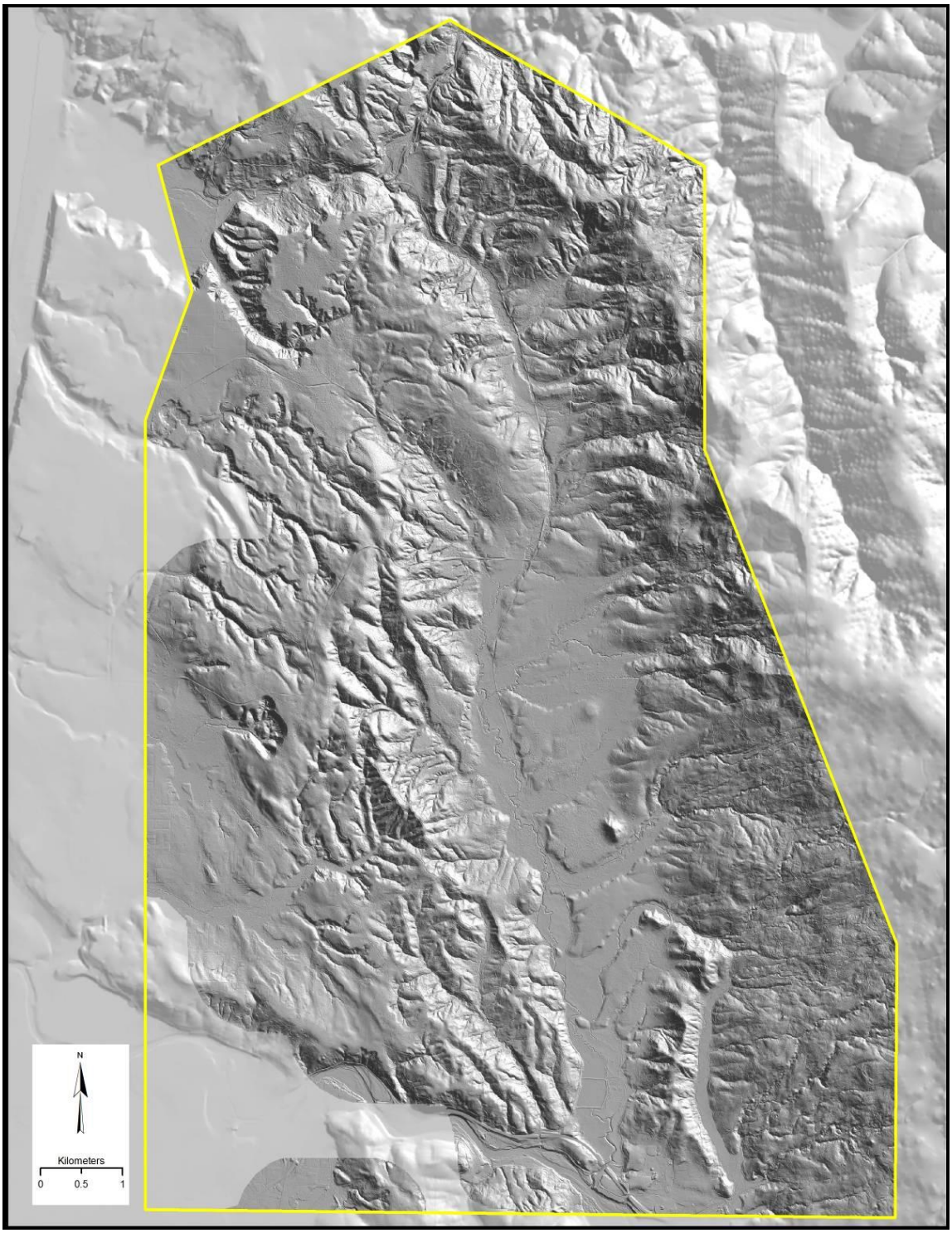

Figure 6: 45 degree, 1 m LiDAR hillshade and study area boundary, shown in yellow.

Field Reconnaissance

I conducted the majority of my field work over a two year period from 2011 to 2013. Field reconnaissance was aided with use of a Panasonic Toughbook CF-19 outfitted with ArcPad 10 GIS field mapping software and a GPS receiver capable of up to 1-m accuracy. GPS data collection, field mapping and sampling were confined to GDRCo property with access through gated entry. The overall focus of the study was confined to the coverage of the LiDAR data. The northern and southern study limits were Little River and Mad River, respectively (Figure 3). I took photos and samples at road cut exposures, and logged GPS waypoints of the sample sites and points of interest. I described the soil samples in general accordance with the USDA method for soil classification, per methods outlined in Birkeland (1999).

RESULTS

Marine Terrace Geomorphology

Marine terraces attributed to a given high sea-level stand period are present at a range of elevations in the study area. Terraces inferred to have been formed at the same time are grouped into what I refer to as terrace sets. Four terrace sets are recognized, and generally identified by large differences in elevation from one set to the next, known as terrace risers. Additionally, terrace surfaces are differentiated by varying levels of geomorphic development. Higher terraces appear as remnant pieces exhibiting a greater degree of surface rounding and drainage development through time, while lower terraces appear generally flatter and more expansive. Several terrace surfaces in the study area are mapped as undifferentiated due to limited access and project scope. Terrace sets are cut into and deposited primarily on clay, sand and gravel of the Falor formation. Terrace thicknesses are undetermined due to limited field exposure and dense vegetation cover. Marine Terrace Profiles A-A' through H-H' illustrate surface morphology (Appendix A). Figure 7 illustrates marine terrace locations identified in this study.

These terrace sets are named Marine Terrace Set (MTS) 1 through 4, from youngest to oldest. The four-part breakdown in this study generally follows the late-Pleistocene terrace breakdown identified by Carver and Burke (1992).

MTS 4

MTS 4 is generally present at elevations greater than 150 m, but is observed as low as 140 m in some locations. Terrace surfaces cap the ridges in the hills east and northeast of McKinleyville and northwest of Fieldbrook Valley. Approximate trends of ridge-lines, on which MTS 4 surfaces are identified, are north-northeast and northwest, respectively. Surfaces are hummocky, rounded, and fragmented into linear segments along the hilltops. Inset features are present within these terraces and appear as relic drainage patterns. The patterns resemble small channels but generally do not have corresponding heads or mouths.

MTS 4 soils are sandy and contain a large fine-grained component consisting of what I interpret to be pedogenic clay. Overall color of the soil is reddish-brown and it has a moist consistency that is generally firm. MTS 4 was identified in the field, north and south of Murray Road. At these locations the surface is blanketed by dark brown silt loam. Road cut exposures show terrace soils that are sandy and consolidated. MTS 4 deposits appear to be confined to the central and northern parts of the mapping area (Figure 7).

MTS 4 is located at elevations generally greater than 150 m in Marine Terrace Profiles A-A' to E-E' (Appendix A). Surface profiles illustrate the rounded nature of these surfaces.

MTS 3

MTS 3 is more extensive than MTS 4 and is observed at elevations between 70 and 150 m, with an approximate average elevation of 120 m (Table 1). The terrace surfaces are more widespread in the western portion of the mapping area and are hummocky, dissected and fragmented. I attribute the hummocky nature of the surfaces to inset features similar to those identified on MTS 4. Small remnant terrace pieces are present along the south-facing hillside, north of Mather Creek at an elevation approximately 125 m. They appear as small, low-gradient pieces dotting the hillside; each covering similar area (Figure 7). The highest observed surfaces for MTS 3 are located north of the Mad River, adjacent to Essex Gultch and in the northern part of the mapping area, southwest of the South Fork Little River (Figure 7). These are preserved only as remnant features. Generally, in the middle of the mapping area, terraces are preserved as features capping small ridges. MTS 3 is lower in elevation than MTS 4, however in the south there are no deposits above MTS 3.

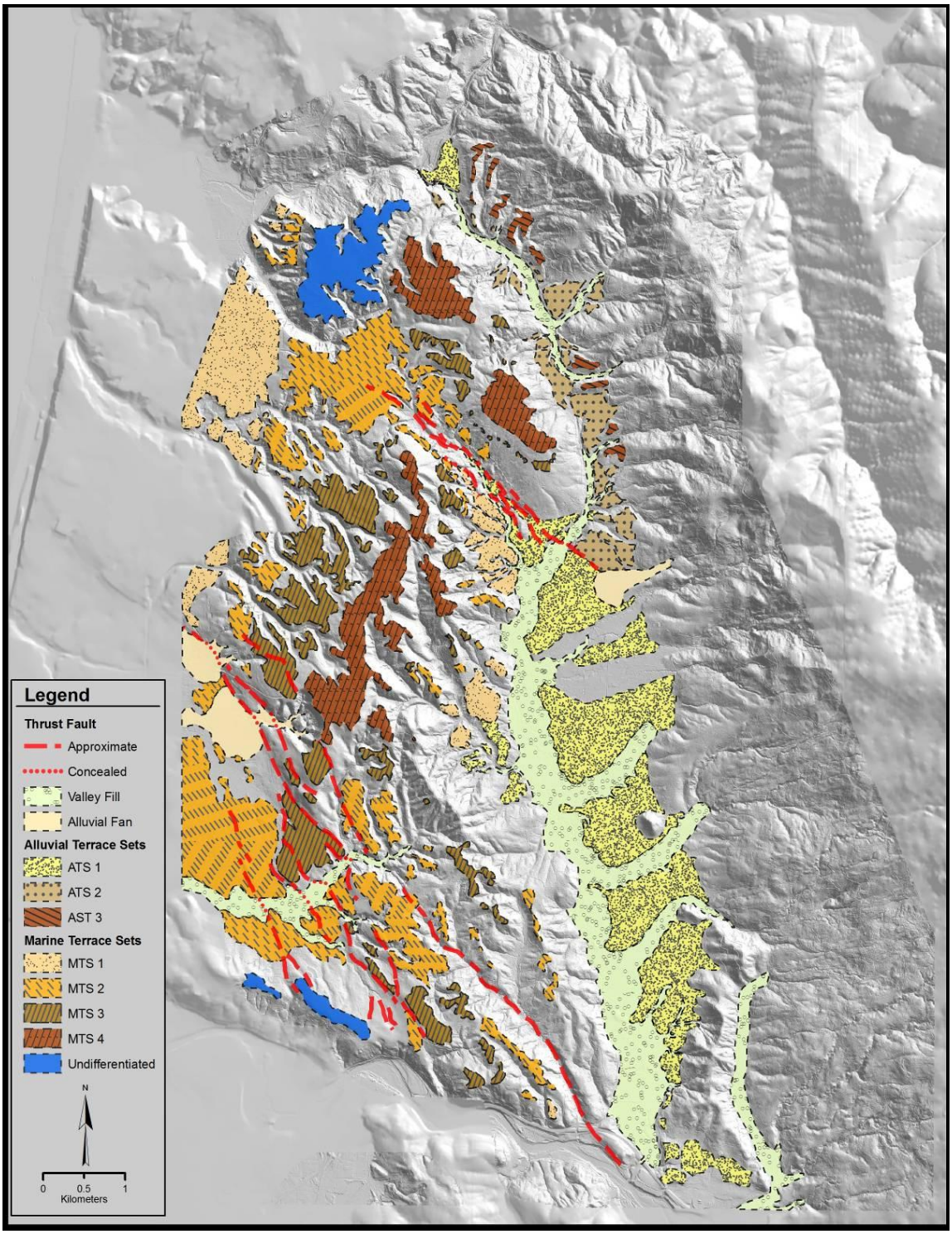

Figure 7: Map of delineated geomorphic units from this study.

MTS 3 soils consist of loamy sand and sand. Colors range from reddish-brown to dark yellow and moist consistency varies from loose to dense (Figure 8). This terrace set was identified in the field mainly in the central portion of the mapping area south of Murray Road (Figure 7). At the surface, MTS 3 is covered by dark brown silt loam, similar to that of MTS 4. However, the underlying terrace deposit contains a larger amount of sand compared to the fine-grained material capping it.

This terrace set is identified in Marine Terrace Profiles A-A' to E-E' (Appendix A) at elevations of approximately 130 m to 140 m (Marine Terrace Profiles A-A' to C-C') in the south, and between 120 m and 130 m (Marine Terrace Profile D-D' to E-E') in the north. Surface profiles illustrate the hummocky, dissected nature of this surface.

MTS 2

MTS 2 is the most extensive terrace set in the mapping area. Surface elevations range from 40 to 130 m (Table 1). The average elevation of this surface is approximately 105 m. Deposits are widespread and surfaces are generally flat. Slopes adjacent to Mather Creek contain terrace surfaces that are generally fragmented, at elevations of approximately 100 m. These fragments are more continuous and adjoined in the northwest and become more dispersed to the southeast. A large broad deposit with little surface morphology and a slight southerly dip is present at the head (northwest) of Mather Creek (Figure 7).

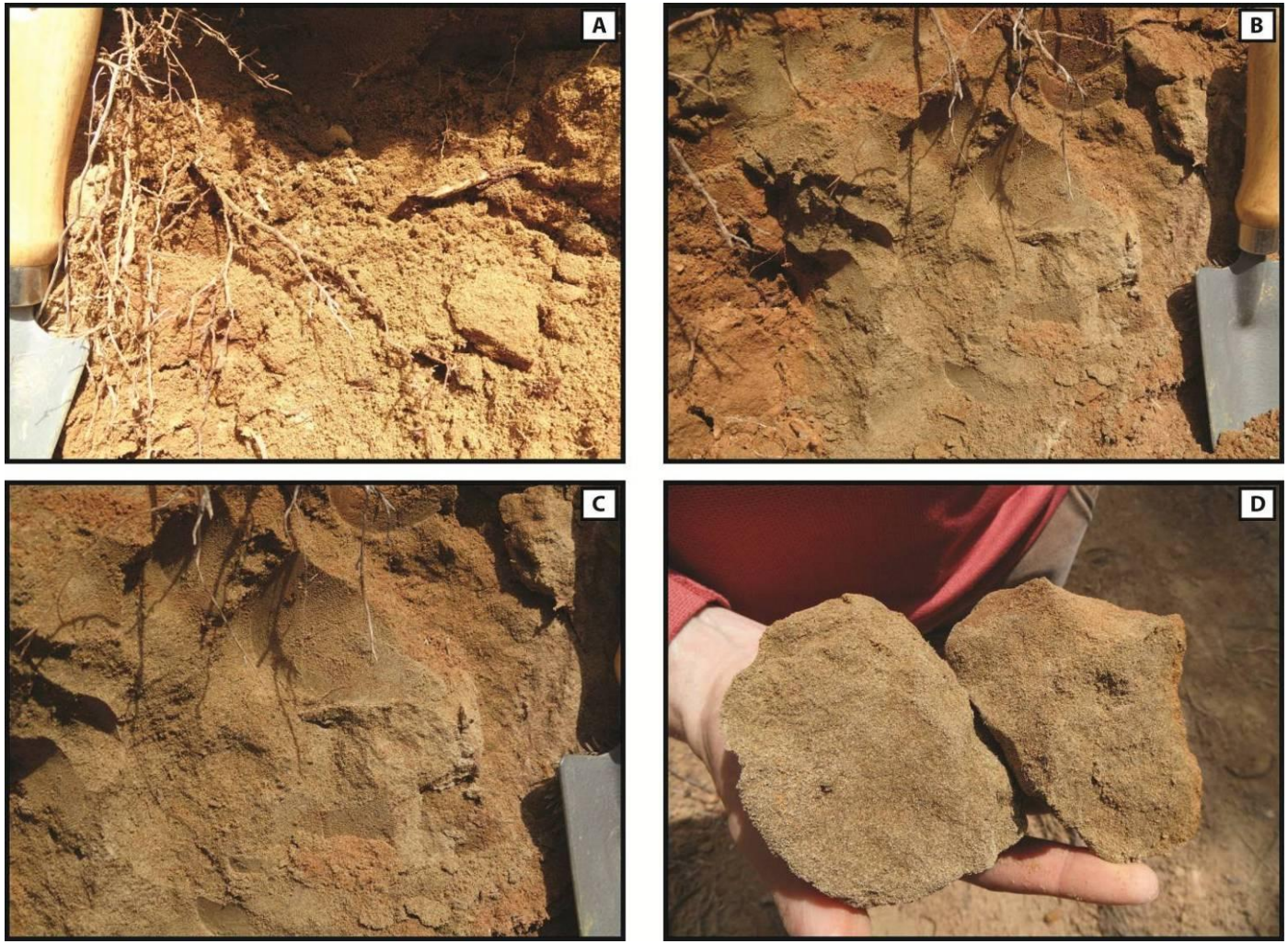

Figure 8: Photos illustrating field exposure of MTS 3 soils. Note the well-sorted sandy texture and dense soil consistency (D). Garden hand shovel for scale

To the south and west, the broad surface becomes northwest trending set of ridgelets (Figure 7) that range in elevation from 90 to 120 m, with average of 107 m. A few small MTS 2 terraces are identified along the western slope of Fieldbrook Valley, and are preserved only on the east facing ridges (Figure 7). MTS 2 deposits are interspersed and at lower elevations than MTS 3 in the southern part of the mapping area. However, in the western central portion of the mapping area the lowest elevation at which MTS 2 is identified is 40 m, but averages 52 m. Four MTS 2 terraces are identified in the northwest portion of the mapping area at the head of the broad Little River valley (Figure 7). They are fragmented and planar, and separated by narrow east-west drainages.

MTS 2 soils consist of sandy loam to sand and are generally yellowish-brown with a moist consistency that is loose to very friable. In the south, MTS 2 is also blanketed by a dark brown silt rich deposit. In field exposure the deposit contains horizontal laminations and cross-bedding. Figure 9 provides an example of the field exposure of MTS 2 soils.

This terrace set is identified in Marine Terrace Profiles A-A' to E-E' (Appendix A) at elevations of approximately 115 m to 125 m (Marine Terrace Profiles A-A' to B-B') in the south, and between 100 m and 110 m (Marine Terrace Profile C-C' to E-E') to the north. Surface profiles illustrate smooth, planar topography.

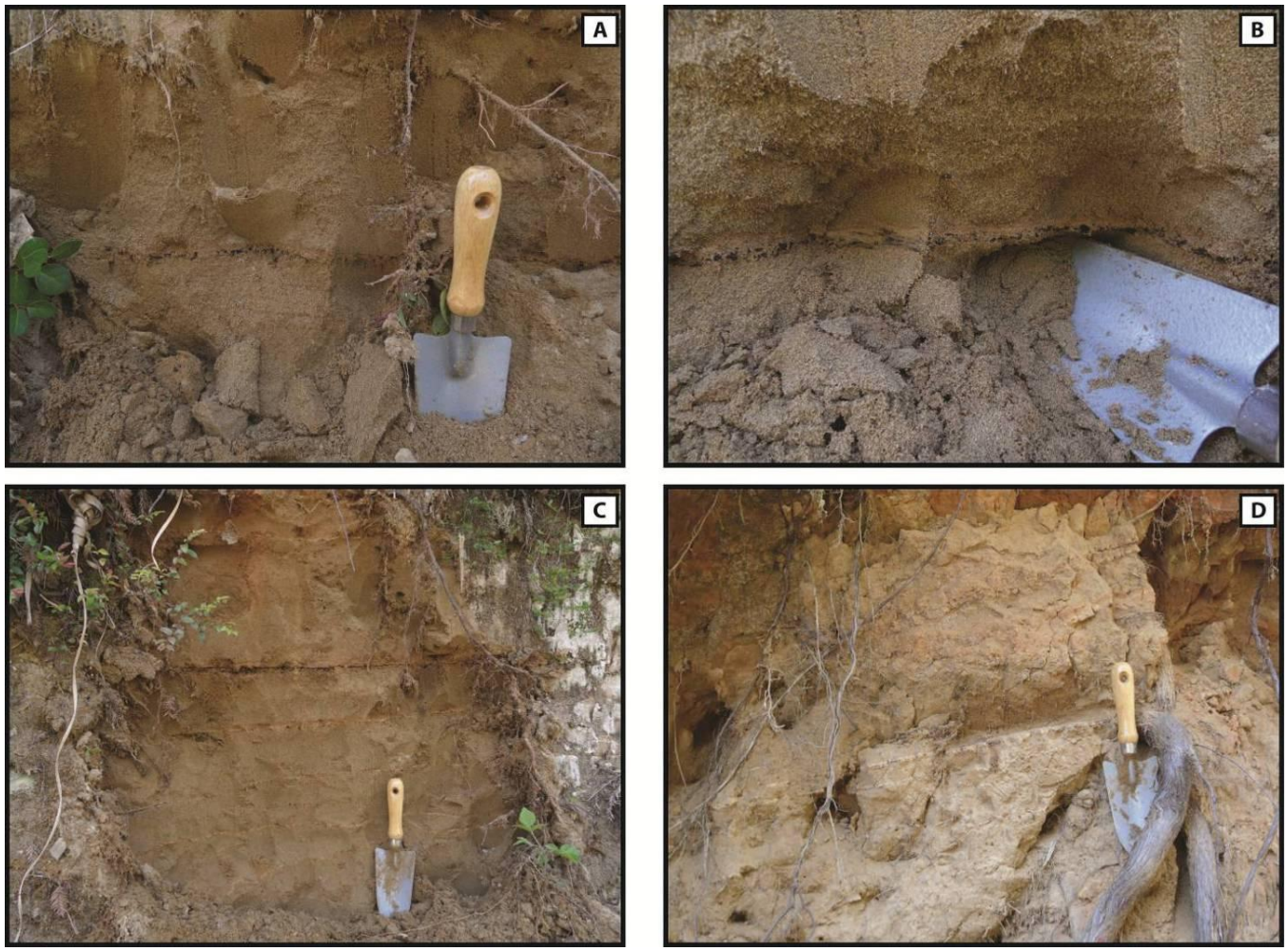

Figure 9: Photos illustrating field exposure of MTS 2 soils. Note the well-sorted, fine-grained texture and sub-horizontal laminations in (A, B and C). Laminations exhibit slight dip in cross-sectional view (D).

MTS 1

MTS 1 contains the lowest identified terrace surfaces and marine deposits in the northern and central parts of the mapping area (Figure 7). Surfaces have an average elevation of 68 m but range from 50 to 90 m (Table 1). I identified surfaces in the northwest and, north and south of Murray Road (Figure 7). In the northwest surfaces are broad, planar and expansive. They are dissected by the larger more established drainages of Strawberry Creek and Norton Creek. Smaller, narrower drainages dissect terrace deposits north of Murray Road, while to the south, MTS 1 surfaces are separated by wider, deeper drainages (Figure 7).

Similar to MTS 2, three MTS 1 terraces are identified in the northwest portion of the mapping area at the head of the broad Little River valley. They are fragmented, generally planar, and separated by narrow east-west drainages.

MTS 1 soils consist of sandy loam to sand, are yellowish-brown, and are generally loose. Deposits were observed adjacent to Mather Creek, north of Murray Road. Figure 10 provides examples for field exposure.

This terrace set is identified in Marine Terrace Profiles A-A', B-B', D-D' and E-E' (Appendix A). Surface elevations range from approximately 70 m to 80 m (Marine Terrace Profiles A-A' and B-B') in the south and between 60 m and 80 m (Marine

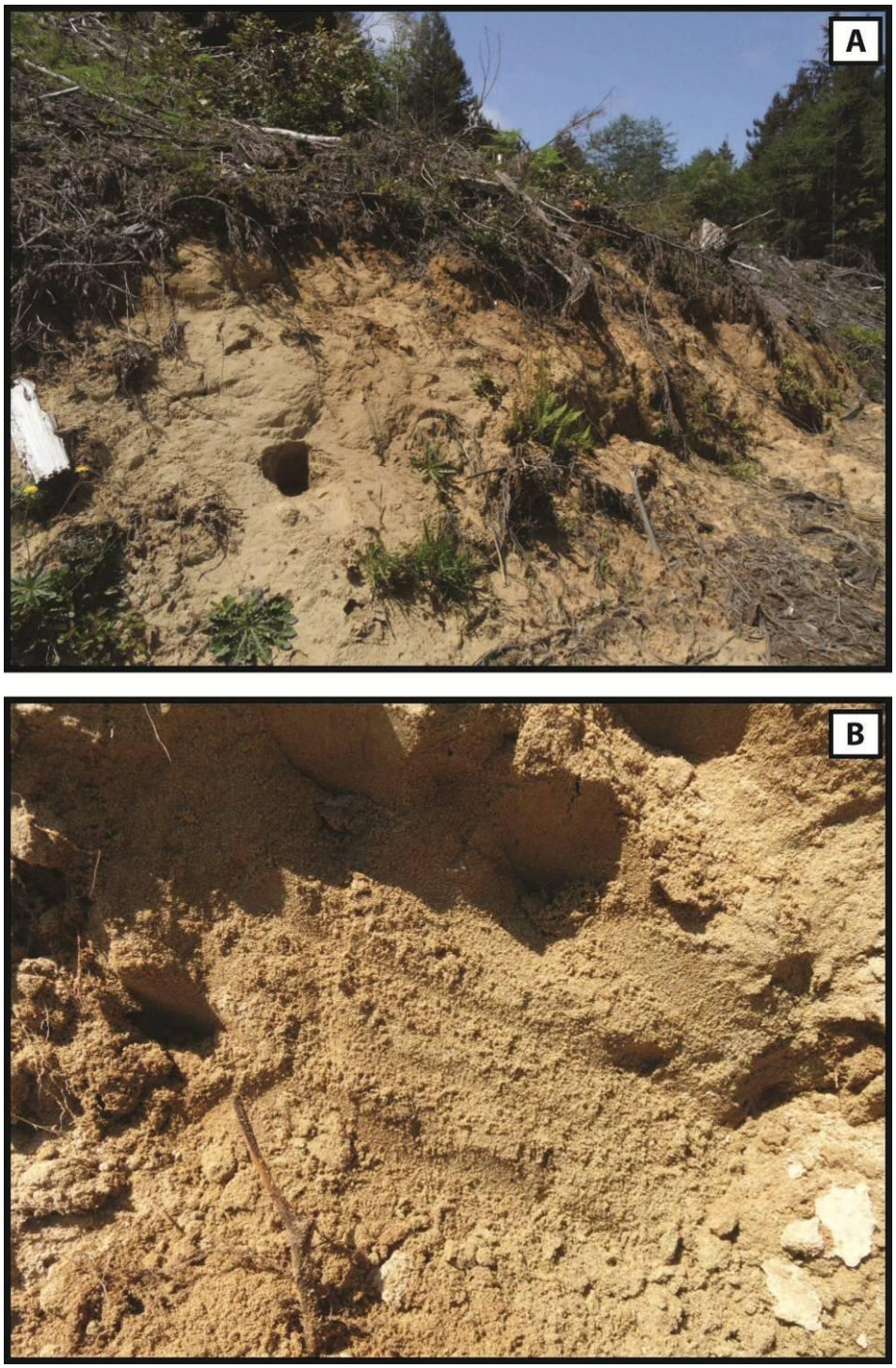

Figure 10: Photos illustrating field exposure of MTS 1 soil. Note the low-gradient nature of the slope (A), and the well-sorted fine-grained texture (B).

Terrace Profile D-D' to E-E') in the north. Surface profiles illustrate the generally planar, broad nature of this surface.

Undifferentiated Terraces

A few surfaces in the mapping area are interpreted to be of marine origin based on surface expression, but are not differentiated into a particular terrace set group or time period. Therefore, three terrace surfaces are mapped as undifferentiated; one in the north and two in the south (Figure 7). The southern two terraces are located north of Mad River and trend northwest-southeast. They are present at an average elevation of 100 m and exhibit a low gradient and rounding. They have similar surface morphology to MTS 2 terraces, but are present at elevations that are inconsistent with other MTS 2 surfaces in the same area. The northern terrace lies west of Bulwinkle Creek and has an elevation range of 110 to 170 m. (Figure 7). Surfaces are generally planar with some moderate lateral drainage incision and exhibit consistent gradient of approximately 5 percent to the south.

There is no access to observe these terrace surfaces therefore it was difficult to differentiate them into a particular terrace set within the resolution of this study. MTS 2 and MTS 1 terraces are present to the west of the northern-most undifferentiated terrace (Figure 7).

Table 1: Table of MTS characteristics.

Terrace Set #	Elevation Range (meters)	Geomorphic Surface Expression	Soil Type	Distribution and Extent in the mapping area	Previous Assigned Age (Carver and Burke, 1992)	Assigned Age (This Study)
MTS 1	50 - 90	Generally planar, little to no surface drainage development	loamy sand and sand	broad and present at lowest elevations	103 ky-OIS 5c	80 ky - OIS 5a
MTS 2	40 - 130	Generally planar, minor level of surface drainage development	loamy sand and sand	Widespread	120 ky-OIS 5d	100 ky - OIS 5c
MTS 3	70 - 150	Broad and hummocky in the west; Fragmented ridge cappers in the east and south. Extensive relic drainage features.	loamy sand and sand	Broad to fragmented	130 ky-OIS 5e	120 ky - OIS 5e
MTS 4	140 +	Ridge topper, fragmented, preserved relic drainage features, rounded	Loamy Sand with Clay	Ridge cap, north-northeast and northwest trend	175 ky-OIS 7	greater than 120 ky

Alluvial Terrace Geomorphology

Alluvial terraces in Fieldbrook Valley and South Fork Little River (SFLR) valley have an approximate north-south trend (Figure 7). Carver and Stephens (1984; Figure 4) initially mapped these features as late Pleistocene fluvial terraces. Deposits consist of slightly- to moderately-weathered fluvial cobbles, gravels, sands, and silt with weak to moderate soils (Carver and Stephens, 1984). Terraces are cut into bedrock of early and middle Pleistocene fluvial and marine sediments of the Falor formation and Jurassic/Cretaceous Franciscan sheared melange (Carver and Stephens, 1984). Alluvial terraces are differentiated in this study based on elevation range, morphology and material type. Similar to the marine terraces, alluvial terraces are divided into three sets (ATS 1 through 3) of youngest to oldest.

ATS 3

ATS 3 surfaces exist as remnant features capping ridges on the east side of SFLR and Lindsey Creek valley (Figure 7). Terrace surface elevations range from approximately 90 to 110 m. The northern most terraces all have a surface gradients and orientations to the south. They are narrow and low-gradient with greater degree of dissection to the north. Southern terraces in this set trend more east-west and are slightly broader. Relief from these terraces to the valley bottom is much less in the south (~20-25 m) than in the north (~40-50m).

Surficial deposits consist of fine to medium, sub-rounded, gravel within a fine- to coarse-grained, sub-rounded sand, silt, and matrix. Soil color has a reddish-brown hue. Photos (Figure 11) illustrate firm to very firm in-place soil consistency.

ATS 3 terraces are identified in Alluvial Terrace Profiles I-I' to K-K' (Appendix A) at elevations of approximately 100 m to 115 m. Terrace surfaces are generally narrow (~150 m wide) and are paired with deeply incised drainages.

ATS 2

ATS 2 surfaces are more extensive than ATS 3 surfaces. These terraces are generally situated relatively low in the SFLR/Lindsey Creek valley, but are above the active fluvial drainage systems (Figure 7). Terrace surface elevations range from 60 m to 100 m.

Surfaces are moderately rounded and have low gradient. The terraces follow a north-northwest trend mimicking the geometry of the larger valley. In the north, adjacent to SFLR, terraces are fragmented and small. Near the confluence with main stem Little River, the terraces are situated higher above SFLR (Figure 7). To the north and east of Lindsey Creek, the terraces cover a large area but are identified at lower elevations in the south. ATS 2 marks the approximate north-south drainage divide separating SFLR and Lindsey Creek; at an average elevation of 90 m (Figure 7).

The surficial deposit consists of fine to medium, sub-rounded gravel in a fine- to coarse-grained, sub- rounded sand, silt and clay matrix. Lithology of the gravel is primarily chert. Soil color grades from dark yellowish-brown to reddish-brown with a moist consistency that is firm. Photos in Figure 12 demonstrate field exposure of soils.

ATS 2 alluvial terraces are identified in Alluvial Terrace Profiles I-I' to L-L' (Appendix A) at elevations of approximately 80 m to 95 m (Alluvial Terrace Profiles I-I' to K-K'). On Alluvial Terrace Profile L-L', set 2 terraces are present at elevations ranging from 75 m to 90 m. Profiles demonstrate that terrace surfaces are generally more broad and expansive than the ATS 3 terraces. They feature relatively small drainages with relief on the order of less than 10 m.

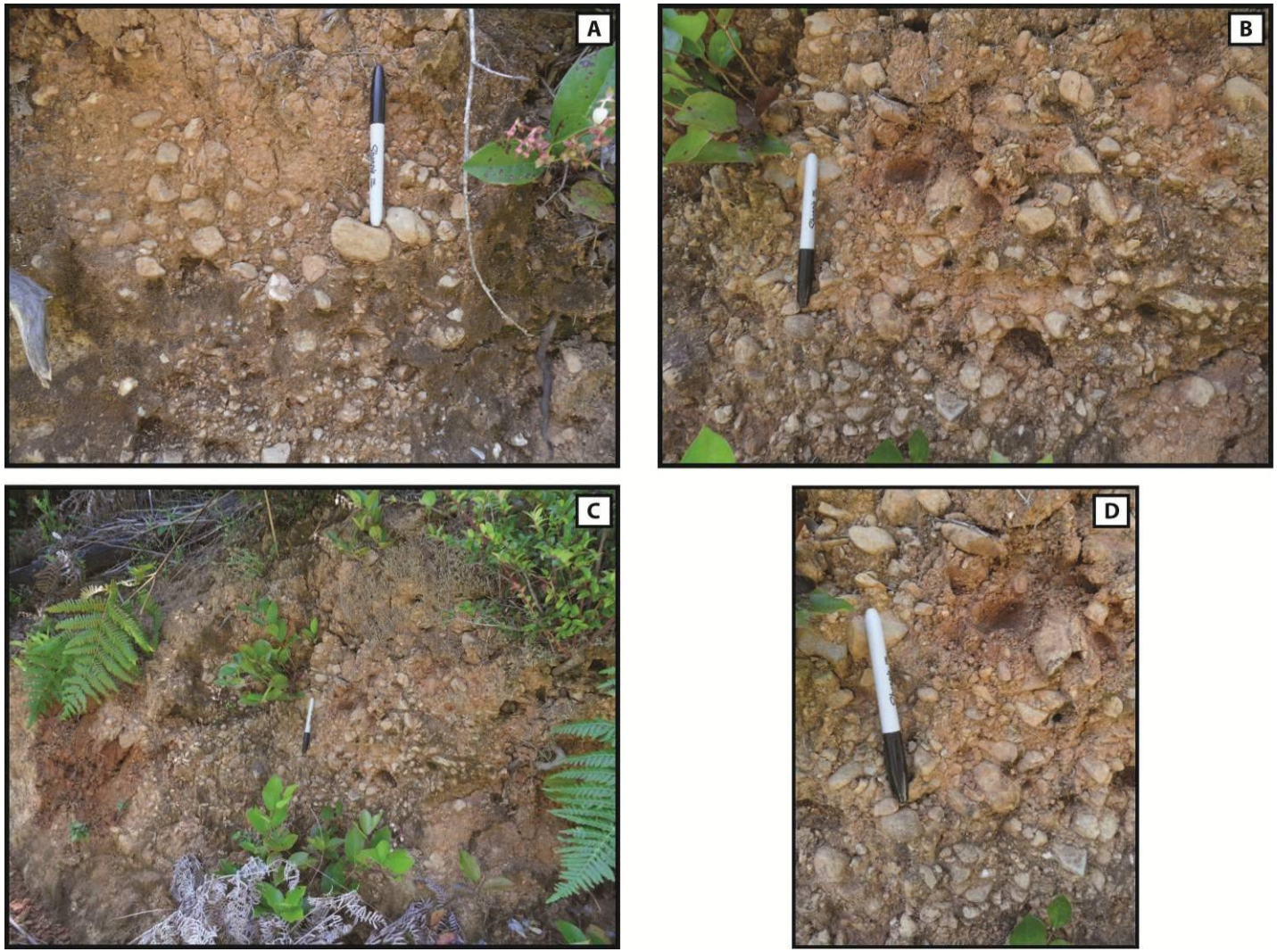

Figure 11: Photos illustrating field exposure of ATS 3 soils. Note the small- to medium-grained sub-rounded gravel.

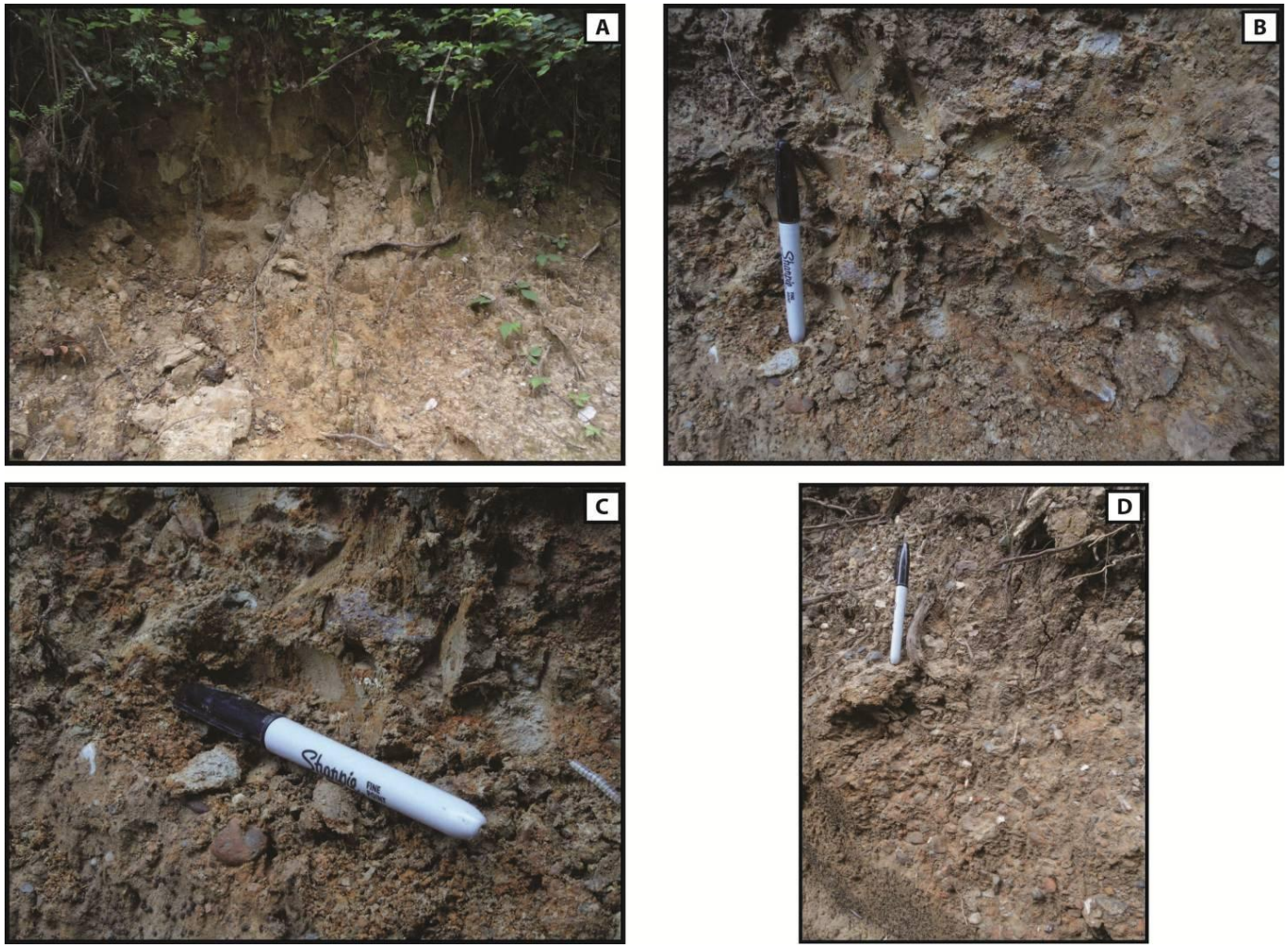

Figure 12: Photos illustrating field exposure of ATS 2 soils. Photo A demonstrates general road-cut exposure. Note the well-sorted medium-grained rounded chert gravel within a clayey sand matrix (B, C, and D).

ATS 1

ATS 1 is observed in Fieldbrook Valley and Mather Creek. These terraces make up the most prominent geomorphology in the valley. Gently sloping, broad and generally low gradient; the surfaces extend laterally from the base of the slope in the east, through the central axis of the valley and become truncated to the west by modern drainage systems of Lindsey creek (Figure 7). Elevations range from 20 m in the south to 70 m in the north. Smaller, remnant terraces are observed to the west of Lindsey Creek, at the base of the western hills of Fieldbrook Valley (Figure 7), and have elevations that range from 40 to 60 m. The large, broad terraces are approximately 15 to 20 m above the younger valley bottom of Lindsey Creek. Four of the terraces are separated by wide, shallow-bottom, northeast-southwest drainages, similar in width and morphology to Lindsey Creek. Terrace morphology is subtle; however descriptions of the geomorphology for the four southern-most terraces in this set are presented by Perry (2012). ATS 1 terraces present in Mather Creek are gently sloping and broad, and on the order of 7 to 10 m above the active channel.

ATS 1 soils in the north consist of sub-rounded cobble, and fine- to coarse-grained, sub-rounded gravel with sand, silt and clay. The southern terraces have a relatively thin sediment cover that is generally fine grained and contains fine- to medium-grained, sub-angular gravel. Dialogue with local consultants reveals that soils throughout Fieldbrook Valley are generally "tight" and fine-grained. However a property owner in

the northern part of the valley revealed coarse-grained sub-rounded to rounded gravel and small cobbles are on the property.

Surface profiles of ATS 1 terraces, generated along general east-west trends, exhibit a gentle concave up nature. The surfaces are somewhat low-gradient in the west with an increase in gradient at the base of the hill to the east. Small topographic inflections are present on the terrace surfaces representing a stair-step pattern. ATS 1 terrace profiles (M-M' to S-S') are presented in Alluvial Terrace Profiles in Appendix A.

Younger Alluvial Deposits

Valley Fill Deposits (Qvf)

Recent alluvium consists of valley fill deposits in the valley bottoms of modern streams (Figure 7). This young valley fill material is present in South Fork Little River, Lindsey Creek, Mather Creek, and Mill Creek. Geomorphic surfaces are gently sloping to flat and demonstrate evidence to suggest channel migration. Valley bottoms are generally wide. The southern part Lindsey Creek has experienced large amounts anthropogenic modification in recent history resulting from agricultural practices. Natural channels were diverted into man-made channels and other channels were dammed to generate ponding, evident at the south end of Fieldbrook Valley. Surficial deposits consist of fine-grained silt and clay "flood" deposits and fine- to medium-grained sand deposited in low-gradient stream valleys.

Alluvial Fan Deposits (Qaf)

Three medium-size alluvial fans are present in the mapping area (Figure 7). Two of the fans are located near the west-central mapping area boundary adjacent to the identified trace of the McKinleyville fault. The other fan is at the northeast end of Fieldbrook Valley adjacent to the previously identified trace of the Trinidad fault. Fans are convex, gently sloping, and lobate, and difficult to identify in the field. These features are apparent in the 1 m contours. Surficial deposits consist of fine- to medium-grained sand and fine, sub-angular gravel. The source material for the western two fans is from marine terrace deposits, upslope.

Tectonic Geomorphology

Tectonic geomorphic features in and around the study area proved to be a challenge to map initially. Rust (1982) noted the general difficulty in precisely locating faults in this region for several reasons:

1. *"They are primarily thrust faults which do not generate a well-defined linear scarp.*
2. *They tend to be represented at the surface as a series of faults following a zone, with individual traces dying out along strike.*
3. *As they propagate upwards through thick sequences of terrace deposits, displacement is taken up along multiple faults and associated fractures and folds so that offset at the ground surface becomes diffused".*

Based on initial mapping by Carver, Stephens and Young (1982),

"faults are expressed geomorphically by linear or curvo-linear scarps, linear ridges, linear depressions, swales, and warping of the surface sediments. Along strike, scarp height and morphology vary considerably. Multiple scarps are common across zones of up to 500 ms wide. Individual scarps occasionally branch or terminate abruptly.

Streams and drainages are commonly aligned along the faults. Where streams intersect faults they are frequently deflected and have disrupted profiles."

Trinidad Fault

A series of northwest-trending linear bedrock ridges are present in the northern part of Fieldbrook Valley, in the Mather Creek drainage (Figure 3, Figure 7, and Figure 13). Thrust faults in this area, initially identified by Carver et al. (1982), are the southeast extent of the Trinidad fault. The fault is expressed in the northern part of Fieldbrook Valley as a wide zone of discontinuous linear bedrock ridges and swales (Figure 7). The zone is approximately 3.5 km long, roughly 400 m wide, and has a general of trend N 40° W. Figure 13 displays 5 m contours demonstrating fault surface character of this area. To the southeast, surface expression of the fault extends across Lindsey Creek and onto the ATS 1 terrace. There, the fault trace becomes obscured by a large low-gradient alluvial fan covering ATS 1 with no discernable topographic evidence of the fault beyond fan to the southeast. To the northwest, the fault trace continues up the head of Mather Creek before terminating in the MTS 2 marine terrace where topographic expression diminishes.

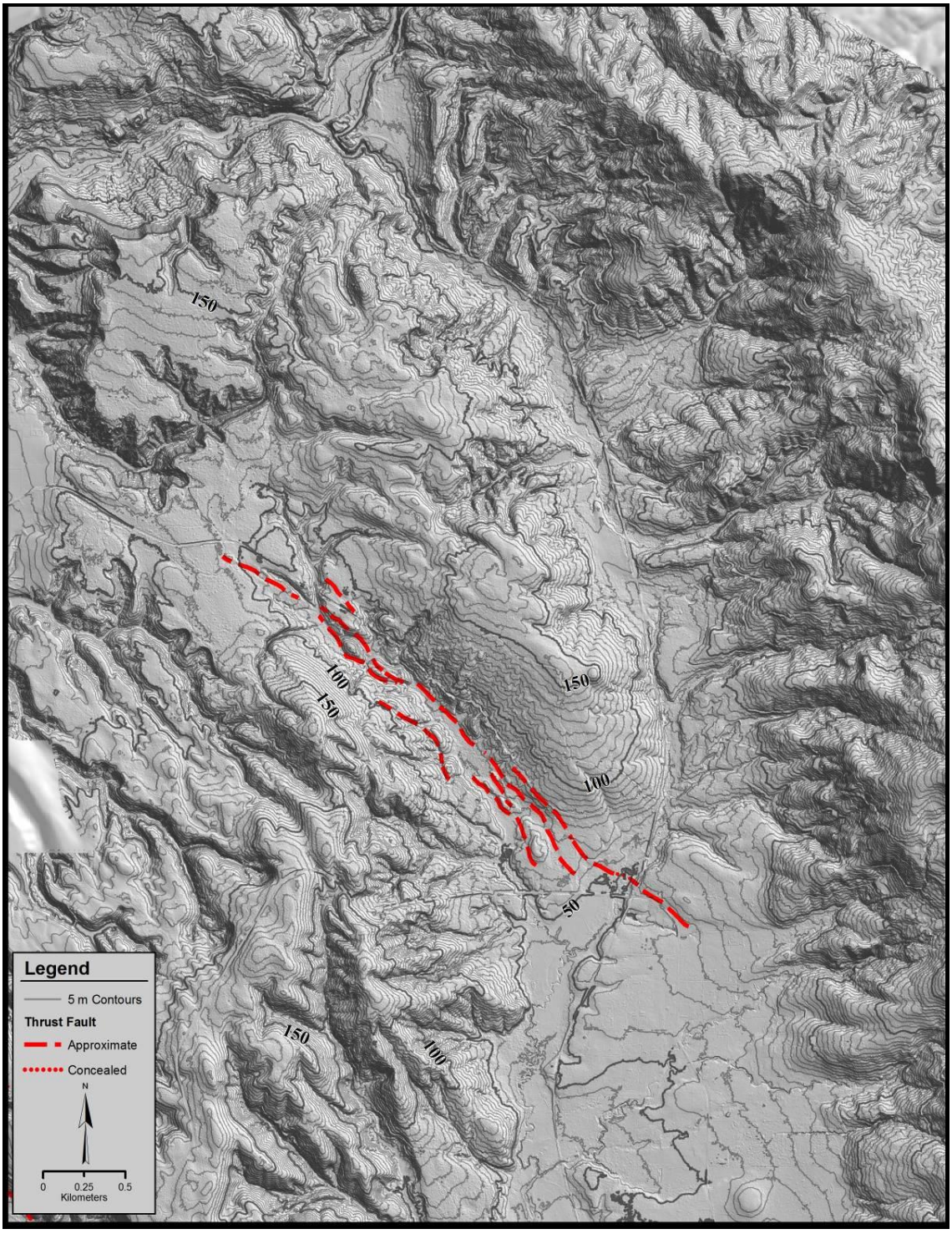

Figure 13: 45 degree LiDAR hillshade and 5 m contours in the vicinity of the Trinidad fault at the north end of Fieldbrook Valley.

The down-stream portion of Bulwinkle Creek, northwest of the MTS 2 marine terraces, follows a trend of N40°W, similar to that of the grain of nearby drainages. However, due to a lack of surface and/or bedrock morphology the fault trace becomes difficult to differentiate to the northwest toward the mouth of Little River valley.

In field exposure, fault traces are identified based on juxtaposition of Franciscan bedrock against Falor formation deposits and younger Pleistocene marine terrace deposits. This juxtaposition is generally obscured by vegetation. Road cuts along the south side of Mather Creek (Figure 3) expose a change in material type from MTS 1 marine terraces to greywacke of the Franciscan formation. The change in material type occurs across a tributary drainage to Mather Creek. Clear fault exposure was not observed. There is no expression of the fault in the younger channel deposits in Mather Creek or Lindsey Creek.

Fault Scarp Profiles CC-CC' through MM-MM' illustrate the degree of topographic relief along the fault structure. The level of topographic expression is observed decreasing to the northwest. Surface profiles are presented in *Fault Scarp Profiles* in Appendix A.

McKinleyville Fault

The McKinleyville fault is mapped as dissecting the hills north of the Mad River, continuing to the northwest along the base of the hills on the east side of the town of McKinleyville where it turns and goes off shore south of the airport (Figures 3, 7, and 14). The McKinleyville fault is expressed as a 1,200 to 1,700 m-wide zone of faults immediately north of the Mad River (Figures 7 and 14). The zone narrows to one prominent fault trace at the western margin of the mapping area. The zone has an average trend of N38°W with individual fault orientations ranging from approximately N25°W to N45°W. Total length of the zone from the north bank of the Mad River to the western study boundary is approximately 8.5 km. Faults are generally linear but exhibit some curvature (curvilinear). Faults offset MTS 2 and MTS 3 surfaces. I found no evidence for the fault in the younger channel deposits of Mill Creek, or the two large alluvial fans near the west-central margin of the study area. A large topographic rise (~140 m tall) on the east side of McKinleyville associated with the "main" fault trace is indistinguishable in the hills on the north side of the Mad River, however becomes distinct near the west central study area boundary (Figure 14).

In the field, surface expression is identified by medium- to low-gradient topographic rises. These rises generally occur in the late-Pleistocene marine terraces deposits (MTS 2 and MTS 3; Figure 7).

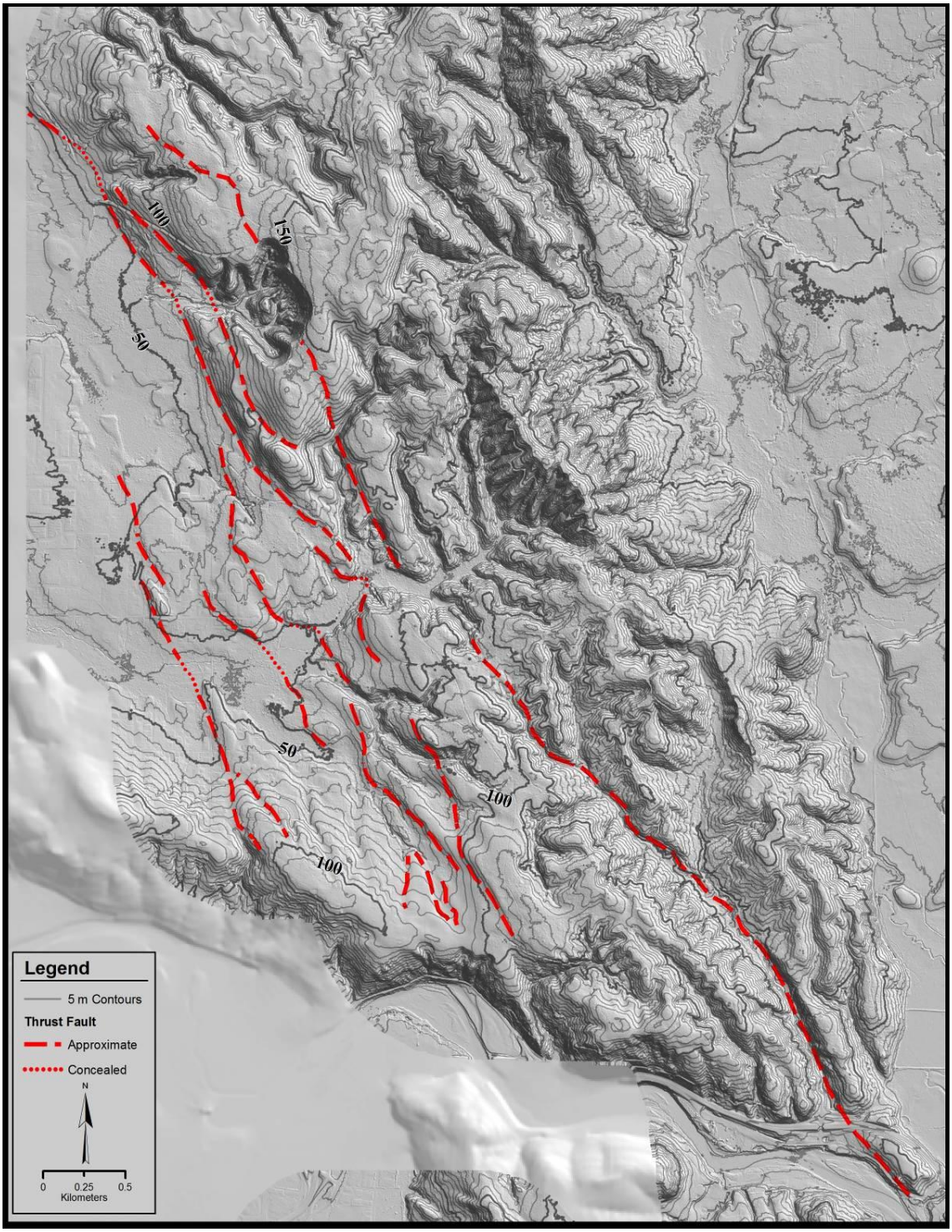

Figure 14: 45 degree hillshade and 5 m contour in the vicinity of the McKinleyville fault, north of the Mad River.

Profiles X-X’ through BB-BB’ (Appendix A) illustrate the degree of topographic relief along the fault traces. Faults are expressed in the southern-most profiles by a series of evenly spaced, low-gradient ridges. Directly south of Mill Creek, the faults displace MTS 2 terraces by approximately 45 m. To the north of Mill Creek, faults displace both MTS 3 and MTS 2 terraces by approximately 15 m and 8 m, respectively. Surface profiles are presented in *Fault Scarp Profiles* in Appendix A.

DISCUSSION

Late Pleistocene Marine Terraces

Actively uplifting coastlines provide ideal environments for marine terrace development and preservation (Muhs et al., 2003). Wave-cut terraces form when wave erosion in bedrock or other deposits occurs during a stable high sea stand (Muhs et al., 2003; Figure 15). The record preserved in a flight of emergent terraces consists of a tectonic component from the rising land mass and a glacio-eustatic component from the oscillating ocean surface (Lajoie, 1986). Muhs et al. (2003) postulate that emergent marine deposits on uplifting coastlines record interglacial periods. Timing for these interglacial periods is constrained using Uranium-series (U-series) dating and amino-acid racemization analysis on appropriate material found in the deposit.

Timing of previous sea level elevations is generally constrained by estimating ages of material deposited on stable land masses which have experienced little to no tectonic activity. Southern Florida provides an excellent record of late Pleistocene sea-level history in the northern hemisphere due to its location in a region that is tectonically stable and the presence of materials that are suitable for U-series and radiocarbon dating (Muhs et al., 2003). Florida appears to be one of the best areas to constrain high sea level elevations and respective ages in the northern hemisphere. However, due to the materials present (i.e. corals), the record left behind reflects the early part of sea level rise and the peak.

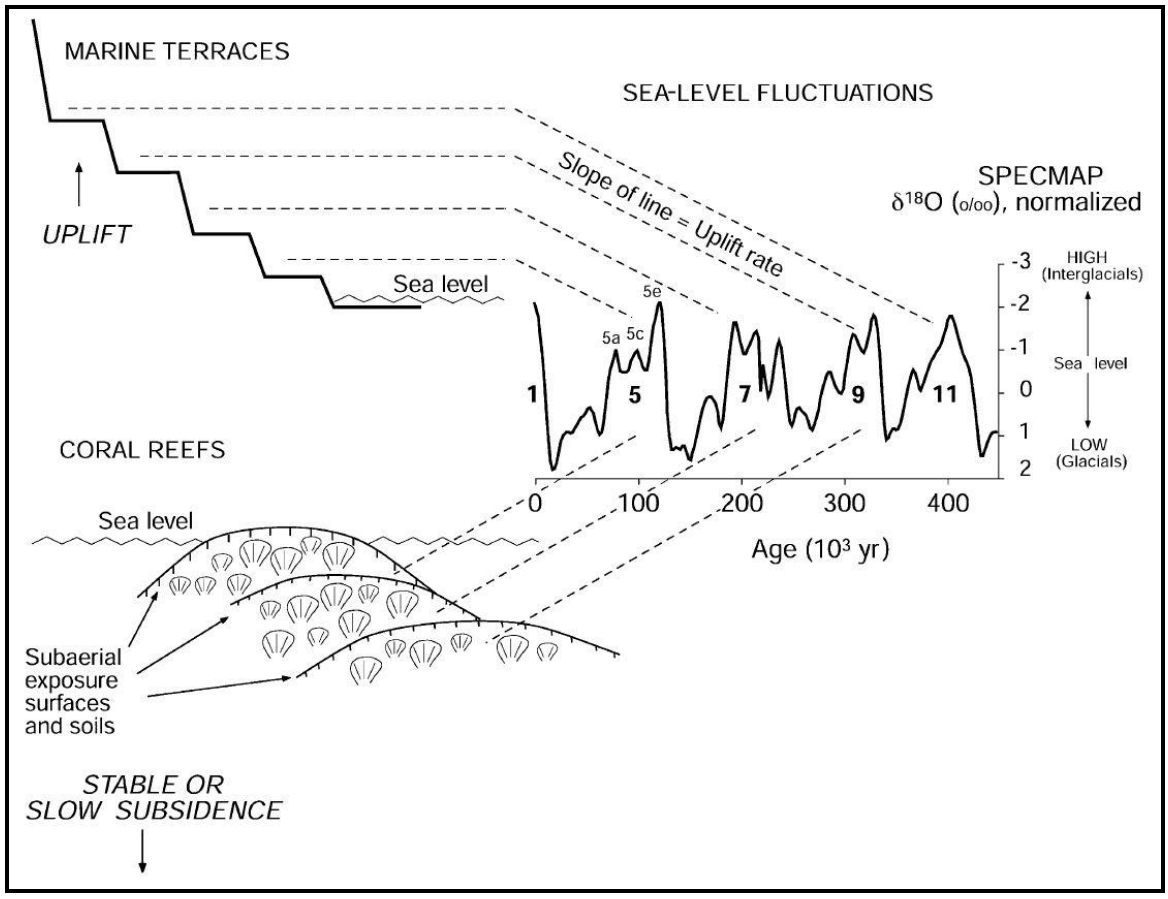

Figure 15: Diagram of hypothetical coastlines showing relations of oxygen isotope records in foraminifera of deep-sea sediments to emergent reef or wave-cut terraces on an uplifting coastline (upper) and a tectonically stable or slowly subsiding coastline (lower). Emergent marine deposits record interglacial periods. Oxygen-isotope data shown are from the SPECMAP record. Adapted from Muhs et al., 2003.

Fossils, such as marine mollusks, left behind in marine terrace remnants are thought to represent the peak of sea level or the early part of the regression (Bradley and Griggs, 1976). I have incorporated these ideas into my study realizing that there may be problems with definite age constraint. This study uses the ages and elevations of previous sea level highs acquired from material found along the Pacific coast. Studies

were not found that explore, in depth, the extent of sea level lowering during Oxygen Isotope Stage 5. Therefore I used a composite relative sea level curve produced by Muhs et al. (2012) to estimate the magnitude of sea level lowering during the last interglacial period along the California coast.

Sea Level Progression During OIS 5

It is important to understand sea level progression during the late-Pleistocene in order to envision an environment in which related geomorphic features formed. Global high sea level stand chronology developed by Bloom et al. (1974) and Chappell (1983) provided early understanding for the timing of different sea levels in the Pleistocene. The last inter-glacial period, Oxygen Isotope Stage (OIS) 5, lasted from approximately 130 ky to 80 ky (Muhs et al., 2003). Although this was considered a period of high sea level in the Pleistocene, OIS 5 consisted of three individual high stands (OIS 5e, 5c, and 5a) and two respective low stands (OIS 5d and 5b) prior to a much larger sea level lowering in OIS 4 (Figure 15). The initial sea level high stand during OIS 5e occurred between 130 ka and 120 ka and was considered to be up to 8 m above current sea found along the coast in Florida (Muhs et al., 2003). Coral fragments found in Florida limestone deposits date to approximately 130 ka to 121 ka during the main transgression period (Muhs et al., 2003). Based on optimum growth depths of these corals, sea level must have been at least 5 to 8 m above present (Muhs et al., 2003). For correlation of the OIS 5e high sea stand along the Pacific Coast, three coral-bearing localities in California provide

numerical age control indicating that OIS 5e could have lasted up to 9,000 years (Muhs et al., 2003). This record likely represents the sea level high stand and the regression that followed. According to a model presented by Waelbroeck et al. (2002), OIS 5d resulted in a drop in sea level to approximately 40 m below present around 110 ka. A subsequent high stand occurred at about 100 ky, during OIS 5c. Muhs et al. (2003; 2012) report that sea level during OIS 5c must have been close to present sea level elevation. Both 100 ky and 120 ky corals are found in terrace deposits at Cayucos and Point Loma, in southern California. Waelbroeck et al. (2002) suggest the 100 ky high stand re-occupied part of the 120 ky terrace, reworked it and eroded older fossils and deposited them with younger ones. OIS 5b took place at approximately 90 ky and was signaled by a drop in sea level to about 45 m below present (Waelbroeck et al., 2002).

The final sea level high stand of the period occurred around 80 ka (Muhs et al., 2003). U-series ages of solitary corals from Coquille Point, Oregon and numerous localities in California indicate that this high stand could have begun around 86 ky and lasted until around 76 ky, a duration of up to 10 ky (Muhs et al., 2003). As an indication of sea level elevation during this period, a shallow-water species of coral found seaward of the Florida Keys was identified at a depth of 15.2 m and dated to approximately 85 ka (Muhs et al., 2003). Muhs et al., (2012) report that U-series dates on corals from San Nicolas Island, California are consistent with ages found elsewhere in the northern hemisphere. Accurate elevation predictions for sea-levels high stands older than OIS 5 were not explored in this study.

Marine Terraces Along the Pacific Coast

Marine deposits have been identified along the Pacific coast from southern California to southern Oregon (Muhs et al., 1990; 2003; 2012; Polenz and Kelsey, 1999). Marine terraces in Cape Blanco and Coquille Point, Oregon approximately correlate to the 100 ky and 80 ky terraces (Muhs et al., 1990). At Pebble Beach, near Crescent City, California, cliff exposures reveal marine sands that are thought to be of intermediate age, probably deposited during the either the 80 ky or 105 ky sea level high stands (Polenz and Kelsey, 1998). Late-Pleistocene marine terraces are present for about 100 km for most of the coast north of Cape Mendocino to the vicinity of Big Lagoon, Humboldt County, California (Carver and Burke, 1992). Carver and Burke (1992) found that the terraces are glacio-eustatically controlled and coincident with late Pleistocene sea level high stands. Studies of numerous marine-terrace remnants spanning elevations from near sea level to greater than 400 m along many parts of the coastline, provide a means of determining longer term uplift rates (Merritts and Bull, 1989).

Detailed sea-level history during the last inter-glacial complex for the Pacific coast has recently been documented on San Nicolas Island, California (Muhs et al., 2003; Muhs et al., 2012). Paleo-sea level estimates for the 100 ka and the ~80 ka sea sands are higher than those estimated for the same sea stands on New Guinea, Barbados and (at 80 ka) for the Florida Keys (Muhs et al., 2012; Figure 16). In addition, the corresponding low stands between those periods were higher than estimated elsewhere. Muhs et al.

(2012) believe that the elevation differences can be attributed to glacial isostatic adjustment from continental glaciers relatively close to the west coast of California. Terraces present on San Nicolas Island, California represent each of the 3 major sea level high stands during OIS 5. Deposits indicate sea level elevations of +6 m at 120 ka (OIS 5e), approximately +2 m at 100 ka (OIS 5c), and at 80 ka (OIS 5a), -12 m (Figure 16).

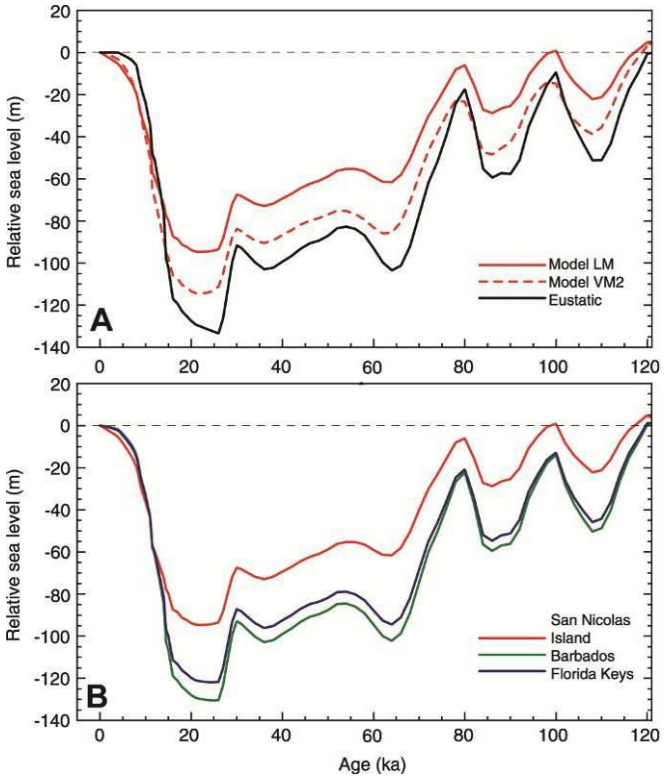

Figure 16: Late-Pleistocene sea-level curve illustrating numerical predictions of relative sea level (A) at San Nicolas Island based on radial viscosity profiles (dashed red line) VM2 or (solid red line) LM. The black line is the eustatic sea-level curve for the adopted ice history. (B) Predictions at (red line) San Nicolas Island, (Blue Line) Florida Keys and (green line) Barbados. Adapted from Muhs et al., 2012.

Marine Terraces in the Mad River Fault Zone

Carver and Burke (1992) assigned terrace ages by identifying the best matches between: (1) altitude sequences of local terrace remnants, and (2) unique terrace altitude sets produced by applying uniform average uplift rates to known ages and altitude of formation of New Guinea terraces (Carver and Burke, 1992; Chappell, 1983). The McKinleyville area served as one of two reference sections for terrace age assignment. Elevations of the terraces were plotted against the global sea level high stand curve using tie lines between the data sets (Figure 17). The slopes of the tie lines represent inferred uplift rates.

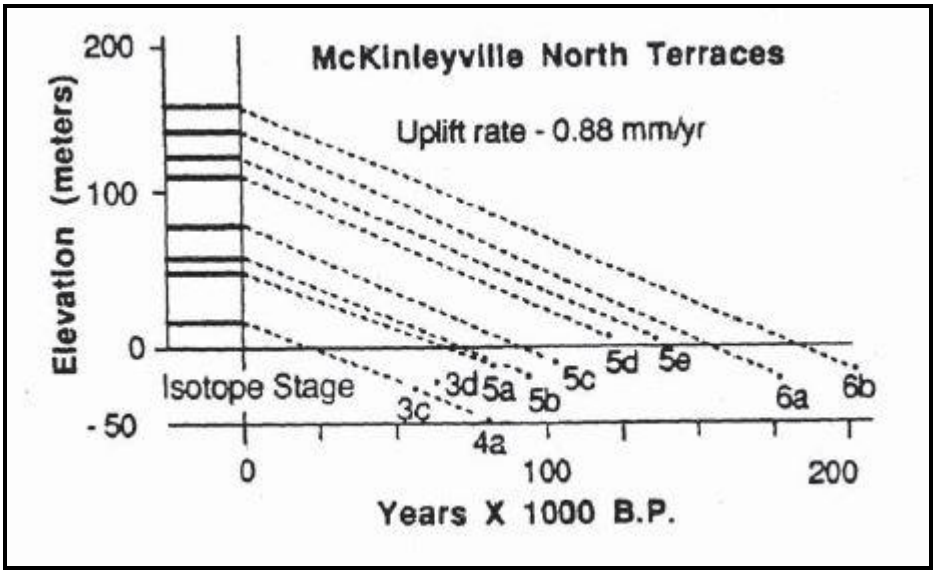

Figure 17: Uplift rate models for late Pleistocene marine terraces at McKinleyville (from Carver and Burke, 1992). Tie lines connect terrace elevations to sea level ages.

Utilizing methods proposed by Bull (1985) and Lajoie (1986), Carver and Burke (1992) assessed the uplift rates used for potential age assignment to test the validity of the constant uplift rate model and the best fit age assignment. They determined that the

lowest emergent terraces near McKinleyville had ages of approximately 83,000 years with the highest/oldest being approximately 176,000 years. In addition, they correlated terrace remnants across major thrust faults and between tectonic blocks based on the degree of soil development exhibited in the terrace cover sediments. Soils were differentiated into four age groups (Groups 1 through Group 4; Table 2); less than the total number of terraces recognized (Carver and Burke, 1992).

Table 2: Soil groups divided into age (Carver and Burke, 1992).

Soil Age Group	Terrace Age
Group 1	between 64 ky and 83 ky
Group 2	between 83 ky and 103 ky
Group 3	between 120 ky and 130 ky
Group 4	~ 200 ky

Marine terraces were further divided into 8 age groups. These groups (Figure 18) are summarized in Table 3, below.

The McKinleyville area is mapped (Carver and Burke, 1992) as having 6 different age terraces (Figure 18). The oldest of which being the A-Line terrace at approximately 176 ky (OIS7), while the youngest in the area is the Savage Creek terrace which

correlates to OIS 5a approximately 83 ka. The terrace treads are separated by risers that may represent the time and uplift between each period of deposition.

Table 3: Marine terrace age groups from Carver and Burke (1992)

Age (ka)	Oxygen Isotope Stage	Marine Terrace Name
64	4a	Patricks Point
83	5a	Savage Creek
96	5b	McKinleyville
103	5c	Westhaven
120	5d	Fox Farm
130	5e	Sky Horse
176	7a	A-Line
+200	--	Older Terraces

Having established the general location and elevation for different age marine terraces, Carver and Burke (1992) were able to plot the data against global sea level curve data (Bloom et al., 1974; Chappell, 1983) available at that time and estimate an average uplift rate to the fault zone. They determined uplift was on the order of 0.88 mm/yr (~1 m/ky) for the Mad River and McKinleyville faults, overall (Figure 17).

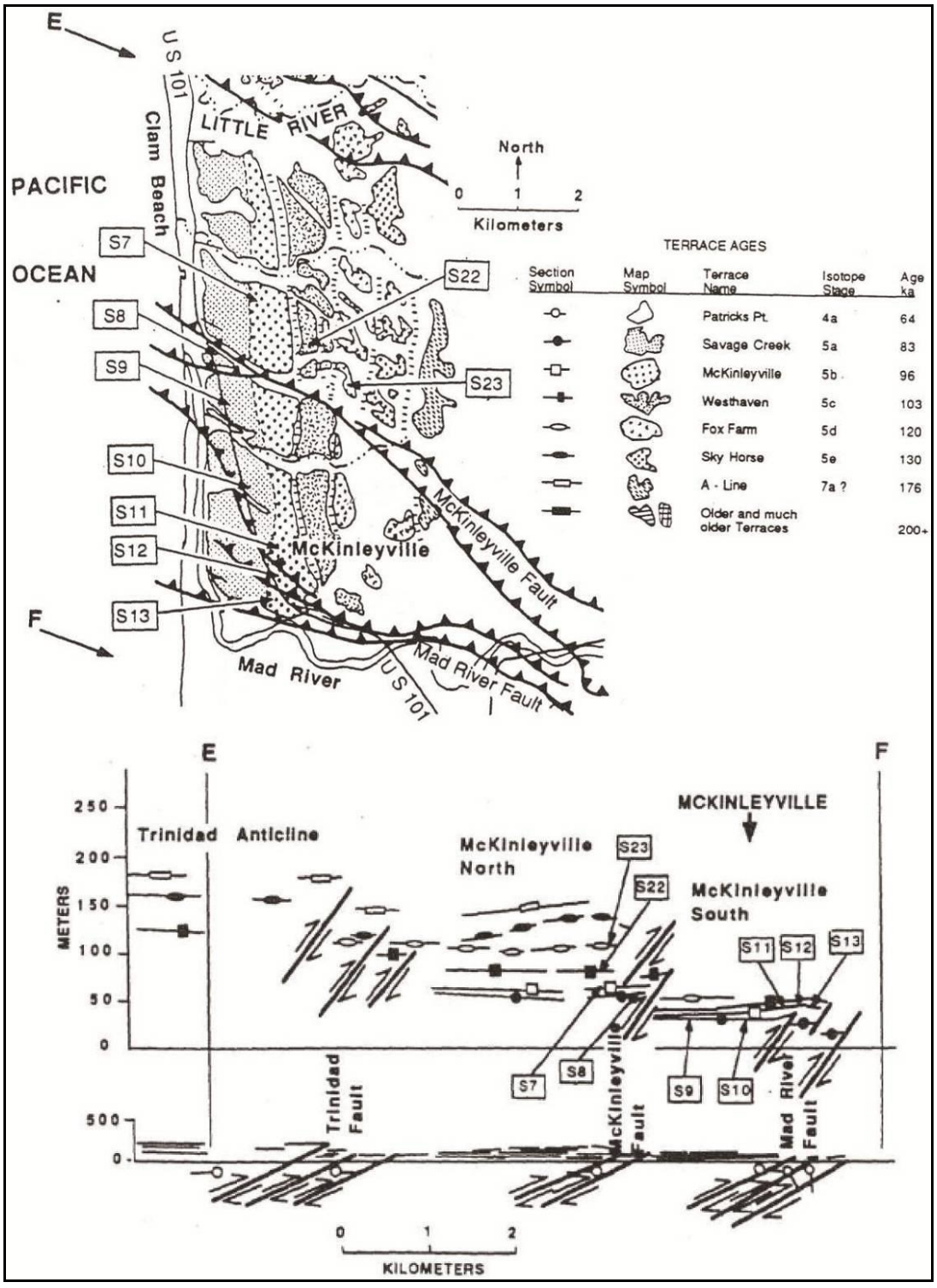

Figure 18: Map of raised, faulted, and folded late-Pleistocene marine terraces of the McKinleyville area (from Carver and Burke, 1992).

Tectonics in the Mad River Fault Zone

Active faulting was first identified in the region during the late 1970's and 1980's (Carver et al., 1982; Rust, 1982). They noted tectonic geomorphic features related to regional compression. In the Arcata-McKinleyville-Trinidad area, evidence of late-Quaternary fault displacement is well defined in a sequence of late-Pleistocene raised marine terraces (Carver et al., 1982). Many faults with smaller amounts of displacement also displace the terraces. Inland from the coastal belt of marine terraces the faults extend in a broad zone along the Mad River (Carver et al., 1982). Between Blue Lake and Maple Creek, low-angle reverse faults displace and juxtapose rocks of the Franciscan complex and late-Cenozoic marine, bay, and fluvial sediments of the Falor formation (Manning and Ogle, 1950). Carver et al. (1982) documented:

"Geomorphic expression of faults in Falor terraine includes aligned linear streams, aligned saddles, side hill ridges, and linear depressions. Juxtaposition by faulting of lithologies with different erosional characteristics has resulted in development of distinct boundaries between areas with contrasting drainage patterns and hillslope forms. These fault related geomorphic and topographic features are expressed as prominent lineaments on airphotos."

Carver (1985) noted that the Mad River Fault Zone (MRFZ) is about 15 km wide, trends N35°W, and contains five principle thrusts (Trinidad, Blue Lake, McKinleyville, Mad River, and Fickle Hill Faults) and numerous minor ones. The fault dips range from 15° - 25° NE at the coast to 35°– 45°NE to the southeast (Carver, 1985). Carver and Burke (1988) identified Holocene activity on the McKinleyville and Mad River faults.

Uplift/Sea-level Curve Model

I developed a model using the elevation and age of sea levels from the Pacific coast and an average fixed uplift rate. This helped in understanding coastline development with respect to inferred tectonic land-level changes. I utilized an average uplift rate of 1 m/ky and the most recent established sea-level curve for the Pacific coast from Muhs et al. (2012) (Figure 16). The model provided hypothetical target elevations of each sea level during OIS 5. I applied the model to two perspectives across the McKinleyville fault to visualize tectonic land-level changes and geomorphic development. The first perspective is to the northeast, perpendicular to fault strike (Figure 19) and the second view is to the northwest, parallel to fault strike (Figure 20).

This model demonstrates changes along the coast due to tectonic uplift, and differences in sea-level elevation through OIS 5 provide an ideal environment for the preservation of marine terraces and related geomorphology.

I generated target elevations based on uplift and paleo-sea-level parameters. To account for error associated with sea-level data and/or uplift rate, I allowed for an approximate range in elevation of 10 m for each sea-level high stand (Table 4). For example, the ~120 ky (OIS 5e) high stand of +6 m, has a generated target elevation of 126 m with a range from 120 m to 130 m. See Table 4 for the elevation range for each sea level high stand. Modeled contour sets are included in Appendix B.

Table 4: Table showing oxygen isotope stage, paleo-sea-level ages, paleo-sea-level elevations, approximate projected model elevations above modern sea-level, and elevation ranges of high stands generated from the model.

Oxygen Isotope Stage	Paleo Sea-Level Age	Paleo Sea-Level Elevation	Approximate Elevation Above Modern Sea-Level	Range of Elevations for High Stands
5a	***80 ka***	***-12 m***	***68 m***	***75 m to 65 m***
5b	85 ka	-30 m	55 m	--
5c	***100 ka***	***+2 m***	***102 m***	***105 m to 96 m***
5d	110 ka	-22 m	88 m	--
5e	***120 ka***	***+6 m***	***126 m***	***130 m to 120 m***

Marine and alluvial terrace geomorphology fit within the model parameters and elevation ranges; three of the MTSs and three alluvial terrace sets were recognized. MTS 3 appears to correlate to the OIS 5e elevation range, while MTS 2 fits within the OIS 5c target contours. The OIS 5a target contours correlate MTS 1 deposits to the 80 ka high stand. Some noted exceptions can be made, however. Marine Terrace Profiles A-A', F-F' and G-G' (Appendix A) illustrate that the terrace surfaces in general, are higher in elevation in the south than subsequent profiles for the same deposits to the north. MTS 3 and MTS 2 are more extensive in the north than model contours would suggest.

Alluvial terrace elevations do not directly correlate to the sea-level high stands, but appear to fall between the target elevations, indicating a gradual adjustment to sea level grade. Surface profiles with an approximate east-west trend were generated for the north and south ends of Fieldbrook Valley.

I included the model-generated elevations on the profiles to correlate features and estimate whether Fieldbrook Valley was devoid of marine influence during OIS 5 (Figure 21).

Marine Terrace Age Assignment

MTS 4

The elevation range (<160 m) and rounded, muted topography of MTS 4 marine terraces suggests that they were deposited much earlier than any of the subsequent terraces. The degree of soil development is consistent with older deposits. Surface profiles demonstrate this terrace set is the highest in the mapping area. Based on these characteristics and within the resolution of this study I have defined these deposits as older than 120 ka, OIS 5 (Figure 22). During subsequent sea-level high stands, these deposits would have persisted as narrow islands just off shore of the paleo coastline.

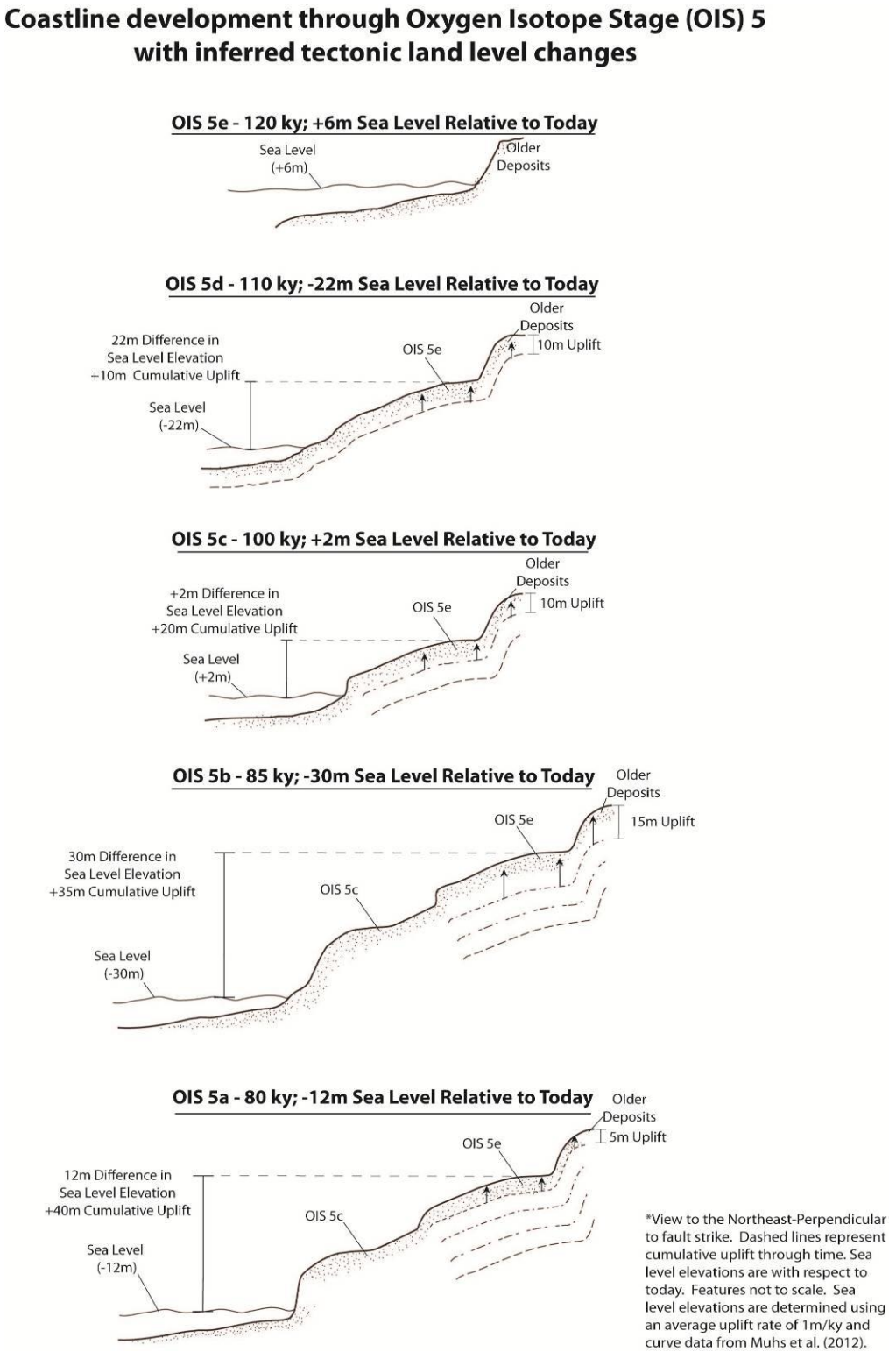

Figure 19: Modeled tectonic land level changes through OIS 5; view perpendicular to fault strike.

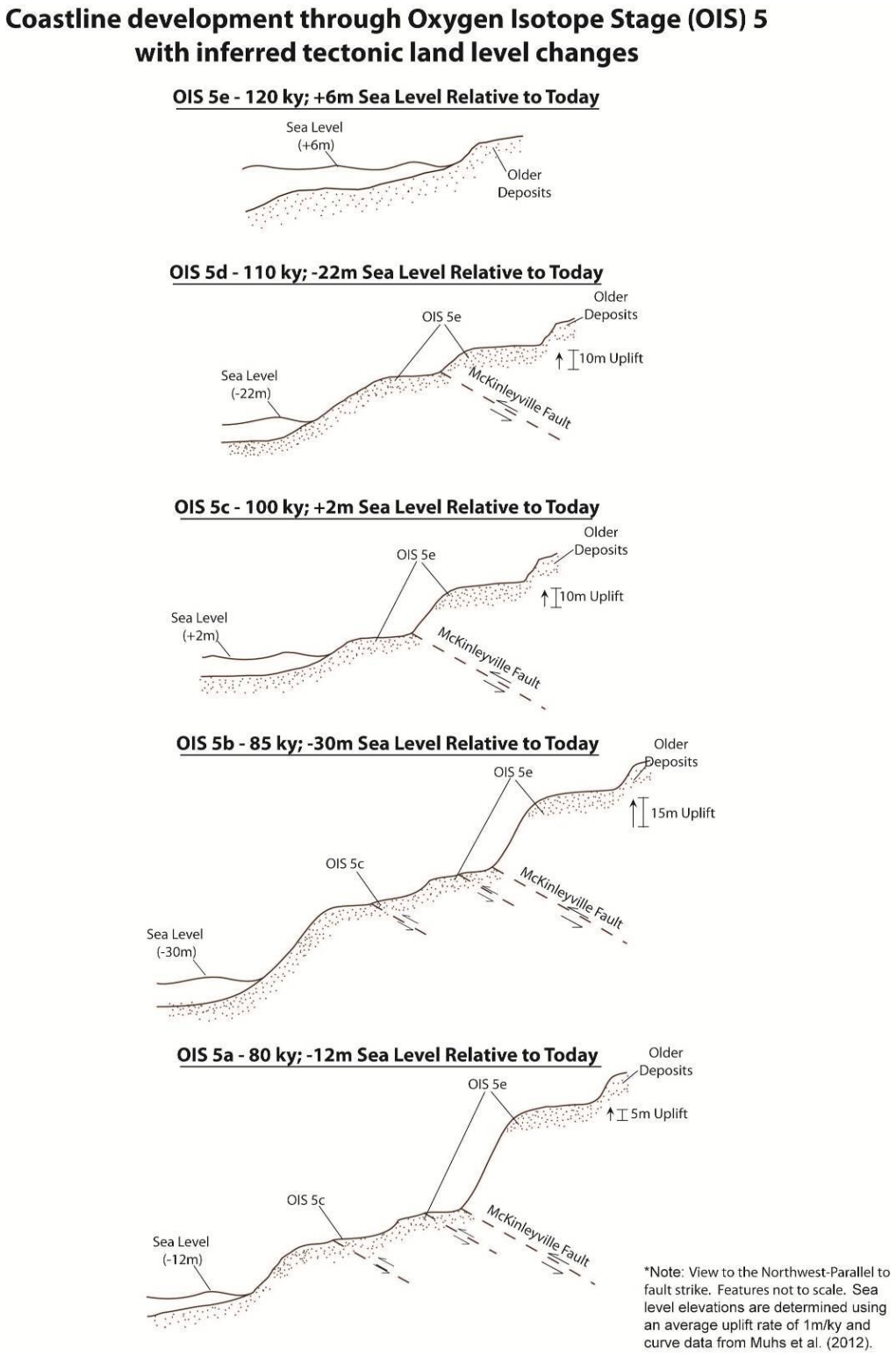

Figure 20: Modeled tectonic land level changes through OIS 5; view parallel to fault strike.

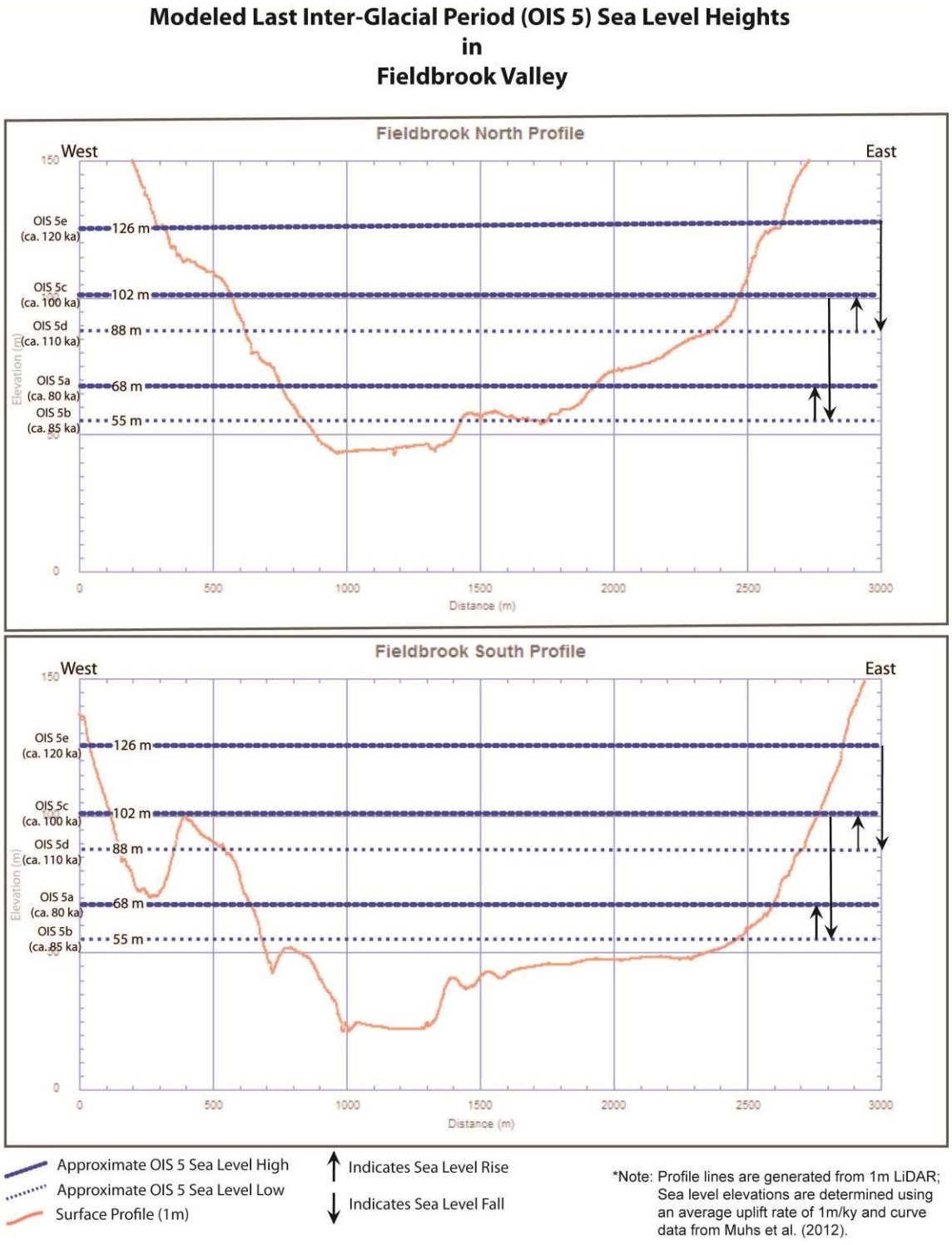

Figure 21: Modeled Last Inter-Glacial Period sea-level heights on modern topography in Fieldbrook Valley.

MTS 3

MTS 3 terraces appear over a broad range of elevations in the mapping area (Figure 7), but all exhibit similar surface morphology. Low-gradient, relic drainages suggest formation during a period of time when the surface was closer to sea-level. The hummocky topography and fine-grained nature of the surface soil is attributed to paleo-dune fields, similar to what is deposited on modern emergent beaches (Carver and Burke, 1992). Discontinuous features along the western hills of Fieldbrook Valley and adjacent to Mather Creek, suggest that much of these deposits have been eroded. No evidence for this terrace set is identified along the eastern slope of Fieldbrook Valley. This hillslope has active earth flows and landslides; preservation of the terrace deposits under those conditions is unlikely. Elevations of this surface, identified north of Mill Creek, are inconsistent with the terrace elevations found elsewhere in the mapping area. The main trace of the Mad River fault is located nearby (Figure 22), suggesting that the elevation difference may be techtonically induced. Additionally, low-relief linear topographic features observed on the surface, north of Mill Creek, are attributed to localized tectonics.

The firm nature of the soil implies a moderate degree of weathering has occurred. Based on the high elevation, discontinuous surfaces and mature soil character, I defined these deposits as correlating to 120 ky, OIS 5e sea-level high stand (Figure 22). The locations of these deposits and potential age imply that Fieldbrook Valley was inundated with marine water. This would result in a low-energy embayment at about OIS 5e time (OIS 5e, Figure 21; Appendix C).

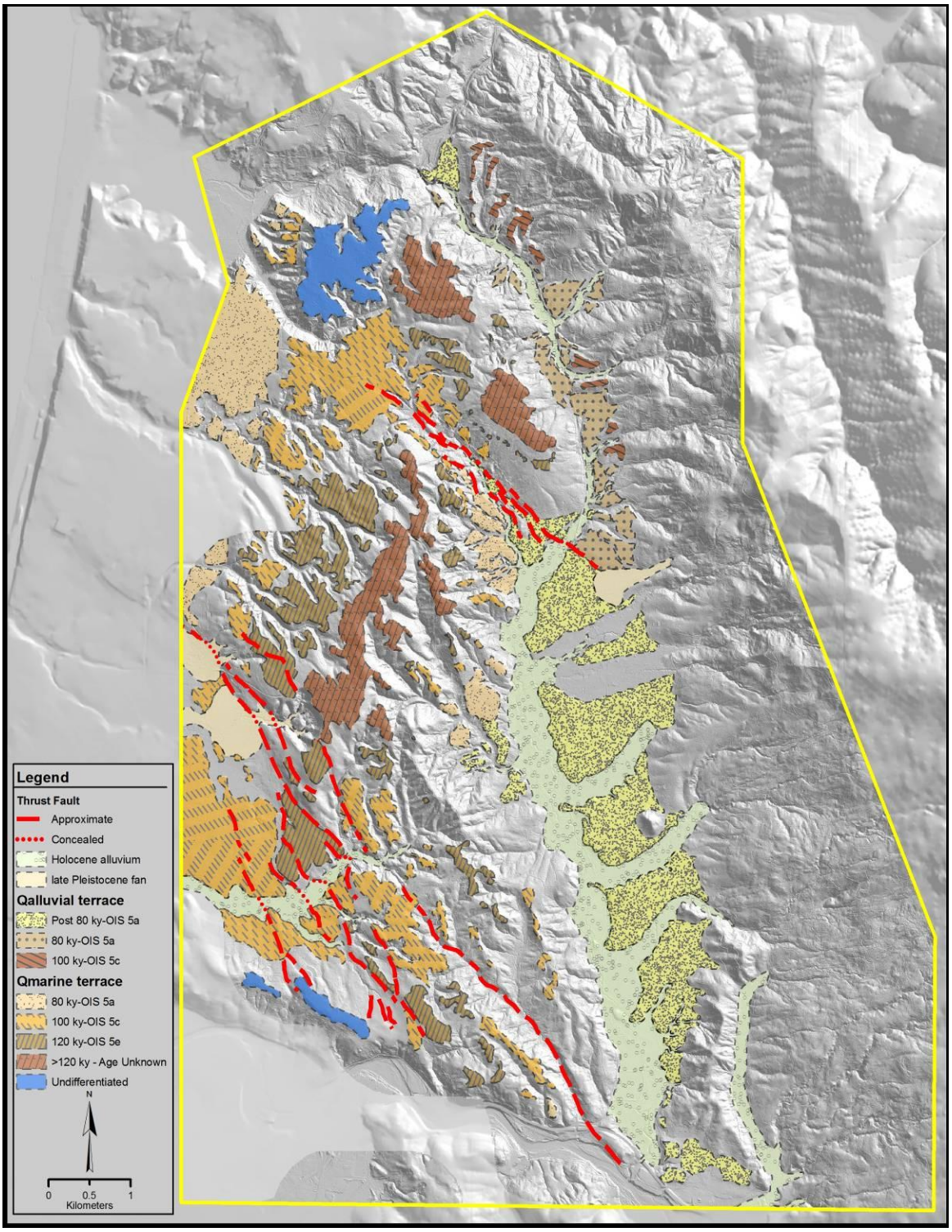

Figure 22: Geomorphology of the Mad River Fault Zone on 1m LiDAR topographic base. Study area boundary indicated by yellow line.

Additionally, this terrace set appears to be folded from compression associated with the McKinleyville fault, and exhibits northwest-southeast trending fold axes (see profiles in Appendix A).

MTS 2

Within the mapping area, MTS 2 lies almost entirely within the OIS 5c contour model (OIS 5c,Table 4; Appendix B). The relatively broad, low-gradient nature of this surface suggests less deformation than the MTS 3 terraces (Figure 7). However, deeply incised drainages indicate relatively mature drainage systems. MTS 2 terraces are less fragmented and more extensive than MTS 3 terraces suggesting that they are younger. Similar to MTS 3, in the western portion of the mapping area, north of Mill Creek, terrace surfaces are found at elevations inconsistent with other MTS 2 surfaces found elsewhere in the mapping area. The difference in elevation along low-relief linear topographic features, observed on the surface (Figure 23), indicates tectonic activity along the Mad River fault.

I correlate these terraces to the 100 ky, OIS 5c sea-level high stand (Figure 22). These deposits may represent a time when more land was exposed than any of the previous sea-level high stands from ongoing deformation resulting from regional tectonic uplift. The location of these deposits also implies that Fieldbrook Valley was submerged during the sea level high stand (OIS 5c, Figure 21; Appendix C). Furthermore, this

terrace set appears folded from compression along the McKinleyville fault, and exhibits northwest-southeast trending fold axes (see profiles in Appendix A).

MTS 1

MTS 1 surfaces occur at relatively consistent elevations through out the mapping area (Figure 7). They are located within the model-generated contours associated with the OIS 5a sea-level high stand (Table 4; Appendix B). I identified this terrace set at the lowest elevations of all the terrace surfaces in the mapping area. The surfaces are low-gradient and planar. They are incised by well-established drainages, and demonstrate the lowest amount of surface deformation. With respect to the other marine terrace sets adjacent to Mather Creek, MTS 1 terraces are the most continuous (Figure 7; Figure 22). Soils are relatively poorly developed within this deposit, suggesting it has experienced less weathering than MTS 2, 3, or 4 soils. The surface is characterized by subtle topography (Figure 10a). Based on these characteristics I correlate this surface and associated deposits to 80 ky, OIS 5a sea-level high stand (Figure 22). The location of this MTS 1 suggests that more land was exposed during this time period than during any of the previous sea-level high stands. Fieldbrook Valley was submerged (OIS 5a, Figure 21; Appendix C). Furthermore, this terrace set appears to be folded from compression associated with the McKinleyville fault, and exhibits a southwest sloping surface (see profiles in Appendix A).

Alluvial Terrace Age Assignment

ATS 3

Elevations of ATS 3 features are generally positioned between the OIS 5e and OIS 5c model-generated contours (Table 4; Appendix B). The ATS 3 surfaces are present on ridges that trend north-south with consistent surface morphology and relief to active creeks (Figure 7). The orientation of these surfaces implies a south-flowing stream system during the time of deposition, however imbricated gravels were not observed. Fine- to medium-grained fluvial gravel and sand is located well above modern, active fluvial channels. ATS 3 surfaces are higher than those of the OIS 5c model contours (Table 4; Appendix B) and MTS 2 (OIS 5c) surfaces. Considering that fluvial systems adjust to base level and fluvial deposits progressively become higher in elevation away from active base level, I believe the ATS 3 surfaces correlate to the ~ 100 ka, OIS 5c sea-level high stand (Figure 22). I attribute these deposits to be associated with a paleo-Little River drainage (OIS 5c, Appendix C). This would imply that Little River flowed to the south, into the north end of Fieldbrook Valley. The river would have encountered a marine inlet (OIS 5c, Figure 21) in Fieldbrook Valley, its outlet.

ATS 2

The elevation range for ATS 2 surfaces is within the model-generated contours for OIS 5a (Table 4; Appendix B) however, the upper end of the range falls within the modeled OIS 5c contours. Relief of the terrace surfaces above modern streams is less

than ATS 3 surfaces. This terrace set marks the major drainage divide between South Fork Little River (Little River drainage basin) and Lindsey Creek (Mad River Drainage basin) (Figure 7; Alluvial Terrace Profiles J-J' and K-K', Appendix A). At the head-waters to South Fork Little River (SFLR) and Lindsey Creek (Figure3) stream power is low and would not carry enough energy to modify ATS 2 surfaces. I observed terrace treads cut into this deposit along the flanks of the upper reach of SFLR and assume this surface was more continuous at one time and has since been eroded. ATS 2 also contains coarse-grained deposits consistent with fluvial processes and are situated above modern, active streams. I consider the ATS 2 deposits roughly correlate to the ~ 80 ka, OIS 5a sea-level high stand (Figure 22) suggested by current elevations and model contours (OIS 5a, Table 4). Similar to ATS 3, I attribute these deposits to a paleo-Little River drainage (OIS 5c-OIS 5a, Appendix C). However, I believe it is at some point during or after OIS 5a that the drainage divide between Little River and Lindsey Creek may have developed as a result of regional tectonic uplift and stream piracy.

ATS 1

This group of terrace surfaces is situated at the lowest elevations of all the alluvial terrace sets. ATS 1 features are generally lower in elevation than the model-generated contours for OIS 5a (OIS 5a, Table 4; Appendix B). They are continuous in Fieldbrook Valley with primary erosive processes originating from Lindsey Creek and its lateral tributaries, and Little River, in the northern portion of the mapping area. ATS 1 deposits

contain the most grain size variability of all the alluvial terrace sets. The northern deposits are coarse-grained, while the southern deposits are more fine-grained (Figure 7). This suggests a higher energy environment persisted for some time at the north end of Fieldbrook Valley, while the southern end experienced a quieter energy environment. The deposits support the idea that the mouth of Little River was once present at the north end of the valley and a lower energy marine embayment largely occupied the southern portion of the valley (OIS 5c-OIS 5a, Appendix C). The elevation and youthful character of this terrace set suggests primary deposition post-dates the OIS 5a sea-level high stand (Figure 22). It also seems likely that piracy of Little River occurred around or after OIS 5a following a subsequent fall of sea-level to elevations lower than any during OIS 5.

Implications for Tectonic Activity

Trinidad Fault

The Trinidad fault has been identified in the town of Trinidad, California and projects to the southeast along the north side of Little River and to the north end of Fieldbrook Valley (Appendix D). Little has been found documenting the location of the Trinidad fault in the north end of Fieldbrook Valley, however the map *Quaternary Faults of the Mad River Fault Zone* produced by Carver et al. (1982) depicts the fault location northeast of the Murray Road, Fieldbrook Road interchange (Appendix D). On the map structural information for this location is scarce but shows KJ Franciscan bedrock thrust southwestward over Quaternary sand with a general northwest orientation. Carver and

Stephens (1984) project the fault through the top of the northwest trending ridge, north of the confluence of Mather Creek and Lindsey Creek (Figure 4), while Carver et al. (1982) project the fault into the valley and along the northern flank of Mather Creek. This discrepancy may be attributed to error in subsequent map transcription. There is no indication in either of the mapping efforts, however, of definitive evidence for the fault northwest of the Fieldbrook site. Topography and bedrock variability however, suggest the presence of tectonic structures in the bottom of Mather Creek valley. Many of the prominent drainages appear to be structurally controlled in an area with relatively low stream power. This is evident by the linear nature of the stream, aligned saddles and side hill drainages, and linear depressions (Figure 13). The side drainages are along a trend that is consistent with other tectonic geomorphic features in the area such as those found along the Mad River fault (Figure 14).

I was unable to identify apparent topographic expression of faulting in MTS 2 (OIS 5c), MTS 1 (OIS 5a) or ATS 1 (post OIS 5a; Figure 15; Figure 23). The discontinuous, linear, bedrock ridges present in Mather Creek do not project into the younger valley deposits. This may be due to active channel erosion and may indicate cessation of tectonic activity or a period of quiescence along this portion of the fault. Additionally, the surface of MTS 2 at the northwest end of Mather Creek (Figure 13; Figure 23) does not exhibit thrust fault features similar to those identified elsewhere in the mapping area. The lower reach of Bulwinkle Creek (Figure 3) has a similar trend to that of the fault geomorphology found in Mather Creek. A lack of surface expression to

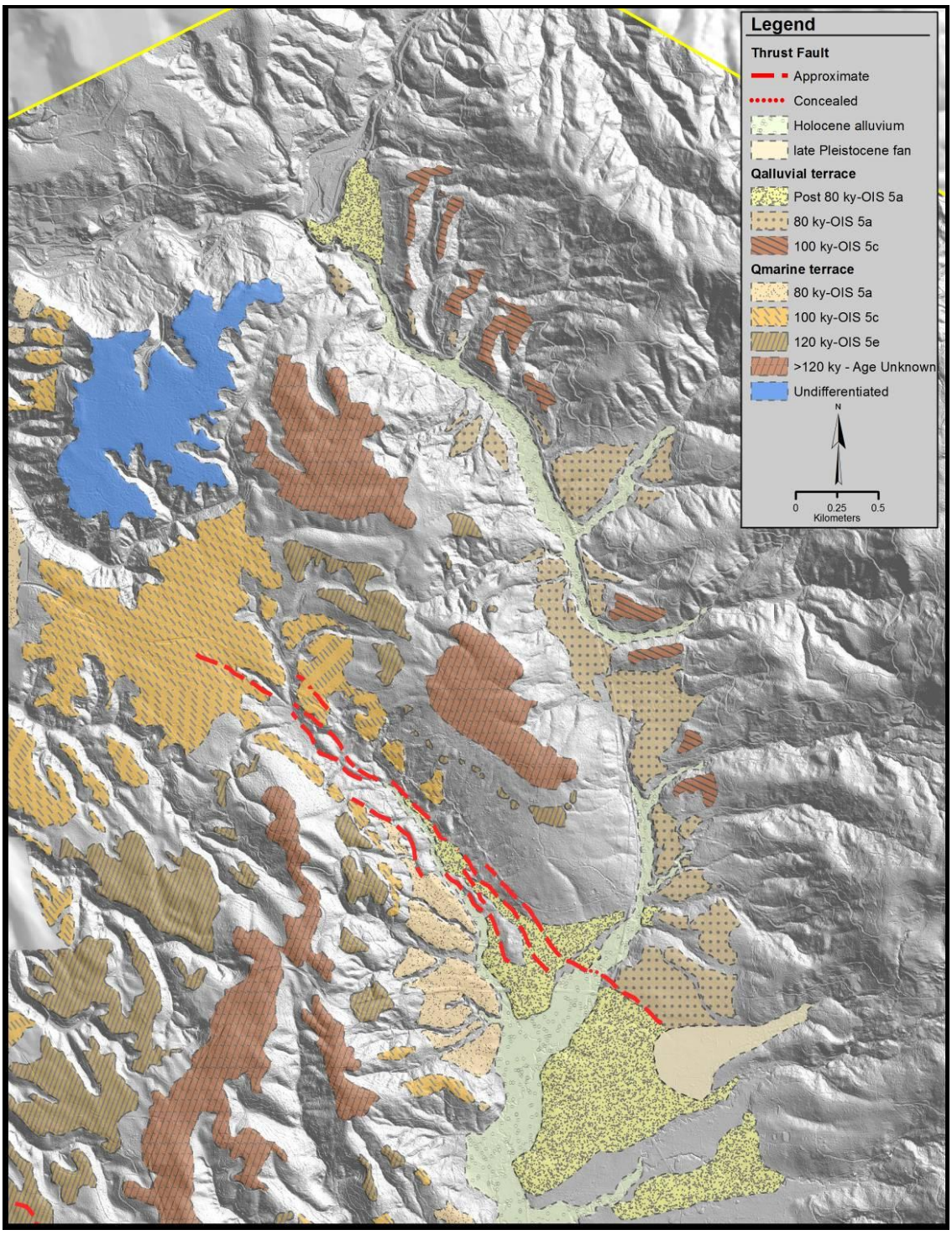

Figure 23: Geomorphology of the area in the vicinity of the Trinidad fault.

the south of the confluence of Little River and Bulwinkle Creek (Figure 3) also appears to demonstrate structural fault control as oppose to recent fault activity in this region.

McKinleyville Fault

I interpret several topographic features in the mapping area to be associated with the McKinleyville fault (Figure 14). The fault crosses the coastline at the Eureka/Arcata Airport (Figure 3) where it offsets a late-Pleistocene marine terrace and forms a broad rounded scarp about 35 m high (Coppersmith et al., 1982). East of the airport the fault has been mapped along the base of the hills east of McKinleyville to the Mad River "*near the Humboldt Bay Water District pump station no. 1"* (Carver and Burke, 1988). Carver and Burke (1988) report that

"south of the river, the fault continues southeast along the north side of Warren Creek valley to the broad Mad River terraces west of the Mad River fish hatchery near Blue Lake, California".

They determined Holocene activity for the McKinleyville fault, with at least one Holocene slip event. This recent activity was documented based on a faulted late-Pleistocene fluvial terrace near Blue Lake.

Fault Scarp Profiles T-T' to W-W' (Appendix A), north of the Mad River, demonstrate greater complexity of the faults in the south that a more defined single fault trace at the west-central mapping boundary (Fault Scarp Profiles X-X' to BB-BB'). Individual traces in the south have lower topographic relief than the main trace to the

north. This may indicate that in the south, slip within the fault zone may be accommodated along multiple traces, where as in the north slip is concentrated along a single trace.

Given the proximity of these individual faults to the Mad River fault, the subtle topography in the southern portion of this zone may be attributed to deformation on the Mad River fault to the southwest. This subtle topography is apparent in the OIS 5e and OIS 5c marine terraces (Figure 24). The OIS 5e terrace appears to have experienced the greatest amount offset, suggesting that the McKinleyville fault may have been active during the initial phases of the Last Inter-Glacial Period. Refer to Figure 12 for inferred tectonic land level changes during OIS 5 with a view parallel to fault strike, developed from the uplift/sea-level model. I was unable to identify evidence for significant fault activity in the young stream deposits of Mill Creek or the alluvial fan deposits to the north (Figure 23). Both the Mill Creek deposits and the alluvial fan deposits appear to post-date the most recent fault activity on the McKinleyville fault.

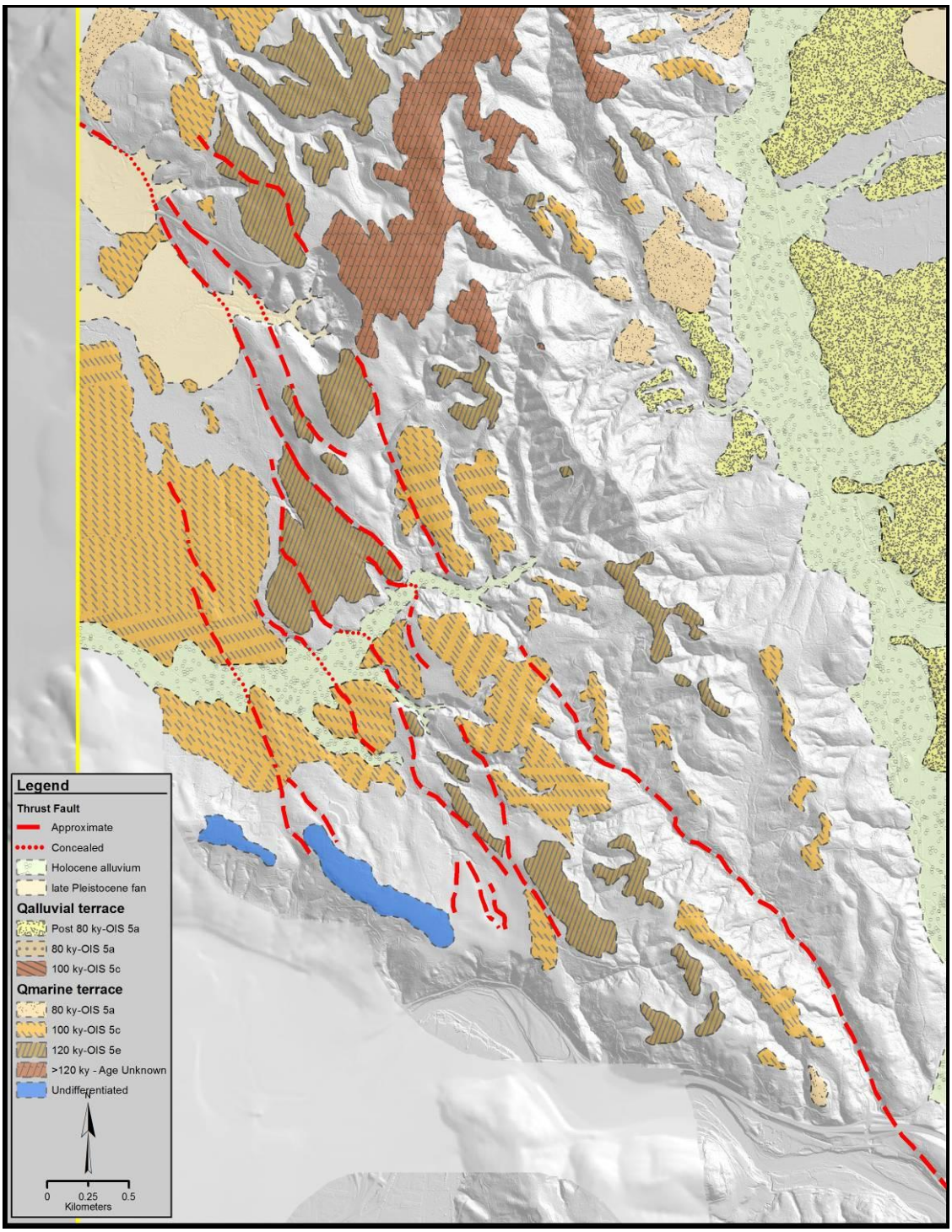

Figure 24: Geomorphology of the area in the vicinity of the McKinleyville fault.

CONCLUSIONS

A flight of four marine terraces is observed in the mapping area. Three of the flights correlate to the Last Inter-Glacial Period, OIS 5, from ~80 ka to 120 ka. MTS 4 is thought to precede OIS 5, while MTS 3 can be attributed to the +6 m sea-level high stand at ~120 ka. MTS 2 best represents the +2 m OIS 5c sea-level high stand at ~100 ka, and MTS 1 correlates to the -12 m OIS 5a sea-level high stand at ~80 ka. ATS 3 appears to have been controlled by a +2 m sea level during OIS 5c, while Alluvial Terrace Set 2 graded to the -12 m sea-level during OIS 5a. The ATS 1 deposits appear to represent an on-going marine embayment and are though to post-date deposits associated with OIS 5a sea-level. These deposits indicate that through all of OIS 5 time, Fieldbrook Valley was inundated with marine water. More and more land became exposed through uplift and subsequent lower sea-levels, until, post OIS 5a, sea-level fell to elevations so low, the Fieldbrook terraces emerged for the first time and Lindsey Creek cut to a new lower base level. Stream piracy of Little River appears to have occurred during or after OIS 5a, but due to the limited scope of this project, precise timing is unknown. Appendix C demonstrates reconstructed coastlines through the Last Inter-Glacial Period.

Tectonic activity on the trace of the Trinidad fault present in the mapping area appears to have ceased sometime before deposition of the OIS 5c marine terrace deposits. The fault structure present is structurally controlled and may have been revealed through erosion of overlying marine deposits.

The McKinleyville fault appears to have experienced on-going activity through all of the Last Inter-Glacial Period as well as after OIS 5. Several smaller topographic features appear to deform deposits associated with the OIS 5e and OIS 5c sea-level high stands. These faults may be attributed to subsequent activity along the Mad River fault to the southwest. A lack of fault expression in the young deposits of Mill Creek and the Alluvial fans may indicated that those deposits are latest-Holocene in age, or that fault activity on this portion of the McKinleyville fault pre-dates the Holocene.

The expression of these faults through time would suggest that principal thrust activity migrates to the southwest on newly emergent fault structures.

REFERENCES

Birkeland, P. W., 1999. Soils and Geomorphology, Third Edition. New York Oxford, Oxford University Press.

Bloom, A. L., Broecker, W. S., Chappell, J., Matthews, R. K., and Mesolella, K. J., 1974. Quaternary sea level fluctuations on a tectonic coast: new Th/U dates from the Huon Peninsula. New Guinea: Quaternary Research 4. p. 185-205

Bradley, W. C., and Griggs, G. B., 1976. Form, Genesis, and Deformation of Central California Wave-Cute Platforms. Geological Society of America Bulletin. no.3. p 433-449

Bull, W. B., 1985. Correlation of flights of global marine terraces in Tectonic geomorphology (Morisawa, M., and Hack, J,. eds.): Binghamton Symposia in Geomorphology: International Series, 15. p. 129-152

Carver, G. A., 1985. Quaternary Tectonics North of the Mendocino Triple Junction The Mad River Fault Zone. in Kelsey, H.M., Lisle, T.E., and Savina, M.E., eds., Redwood Country Guidebook: American Geomorphological Field Group 1985 Field Trip. p. 155-167

Carver, G. A., Stephens, T. A., and Young, J. C., 1982. Quaternary Faults-Mad River Fault Zone. Friends of the Pleistocene, 1982 Pacific Cell Field Trip, Late Cenozoic History and Forest Geomorphology of Humboldt County, California. 7.5 Minute Quad Maps. p 93-99

Carver, G. A. and Stephens, T. A., 1984. Quaternary Geology of the Mad River Fault Zone. Unpublished Geologic Map Series.

Carver, G.A. and Burke, R.M., 1988. Trenching investigations of northwestern California faults, Humboldt Bay region: Technical report to U.S. Geological Survey, Reston, Virginia, under Contract 14-08-0001-G1082, 53 pp.

Carver, G. A. and Burke, R. M., 1992. Late Cenozoic Deformation on the Cascadia Subduction Zone in the Region of the Mendocino Triple Junction. Pacific Cell, Friends of the Pleistocene, Guidebook for the Field Trip to Northern Coastal California. p. 31-63

Chappell, J., 1983, A revised sea level record for the past 300,000 years on Papua New Guinea: a numerical calculation: Quaternary Research 9. p. 265-287

Clarke, S. H. Jr. and McLaughlin, R. J., 1992. Neotectonic Framework of the Southern Cascadia Subduction Zone-Mendocino Triple Junction Region. Pacific Cell, Friends of the Pleistocene, Guidebook for the Field Trip to Northern Coastal California. p. 64-72

California Geologic Survey, CGS, 2007. Bryant, W.A., and Hart, E.W., Fault-Rupture Hazard Zones in California, Alquist-Priolo Earthquake Fault Zoning Act With Index to Earthquake Fault Zones Maps, Special Publication 42, Interim Revision 2007, Department of Conservation, California Geological Survey

Coppersmith, K. J., Stephens, T. A., Swan, III, F. H., Denning, N. E., and Malek, K. A., 1982. Near-surface behavior of thrust faults in the Humboldt Bay area, California. Friends of the Pleistocene, 1982 Pacific Cell Field Trip, Late Cenozoic History and Forest Geomorphology of Humboldt County, California. p. 63-92

Green Diamond Resource Company, 2011. Proprietary 1-meter resolution LiDAR data sets

Kelsey, H. M. and Carver, G. A., 1988. Late Neogene and Quaternary Tectonics Associated With Northward Growth of the San Andreas Fault, Northern California. Journal of Geophysical Research, v. 93, no. B5, p. 4797-4819

Lajoie, K. R. 1986. Coastal tectonics in Active tectonics (Wallace, R. E., Chair) in the series Studies in Geophysics: Washington D. C., National Academic Press. p. 95-124

Manning, G. A. and Ogle, B. A., 1950. Geology of the Blue Lake Quadrangle: California Department of Natural Resources, Divisions of Mines, Bulletin 148

Merritts D. and Bull, W. B., 1989. Interpreting Quaternary uplift rates at the Mendocino triple junction, northern California, from uplifted marine terraces. Geology, v. 17. p. 1020-1024

Muhs, D. R., Kelsey, H. M., Miller, G. H., Kennedy, G. L., Whelan, J. F., and McInelly, G. W., 1990. Age Estimates and Uplift Rates for Late Pleistocene Marine Terraces' South Oregon Portion of the Cascadia Forearc. Journal of Geophysical Research, vol. 95, no. B5, p. 6685-6698.

Muhs, D. R., Wehmiller, J. F., Simmons, K. R., and York, L. L., 2003. Quaternary sea-level history of the United States. Developments in Quaternary Science, v. 1, p. 147-183

Muhs, D. R., Simmons, K. R., Schumann, R. R., Groves, L. T., Mitrovica, J. X., and Laurel, D., 2012. Sea-level history during the Last Interglacial complex on San Nicolas Island, California: implications for glacial isostatic adjustment processes, paleozoogeography and tectonics. Quaternary Science Reviews 37, p. 1-25

Petersen, M., Frankel, A., Harmsen, S., Mueller, C., Haller, K., Wheeler, R., Wesson, R., Zeng, Y., Boyd, O., Perkins, D., Luco, N., Field, E., Wills, C., and Rukstales, K., 2008, Documentation for the 2008 Update of the United States National Seismic Hazard Maps: U.S. Geological Survey Open-File Report 2008-1128, 61 pp

Polenz, M. and Kelsey, H. M., 1999. Development of a Late Quaternary Marine Terraced Landscape during On-Going Tectonic Contraction, Crescent City Coastal Plain, California. Quaternary Research 52, p. 217-228

Rust, D., 1982. Late Quaternary Coastal Erosion, Faulting and Marine Terraces in the Trinidad Area, Humboldt County, Northern California. Friends of the Pleistocene, 1982 Pacific Cell Field Trip, Late Cenozoic History and Forest Geomorphology of Humboldt County, California. p. 107-129

USGS Seamless Server, 2011, http://nationalmap.gov/viewer.html.

Waelbroeck, C., Labeyrie, L., Michel, E., Dublessy, J. C., McManus, J. F., Lambeck, K., Balbon, E., and Labracheri, M., 2002. Sea-level and deep water temperature changes derived from benthic foraminifera isotopic records. Quaternary Science Reviews 21, p. 295-305

APPENDICIES

Appendix A

Marine Terrace Profiles

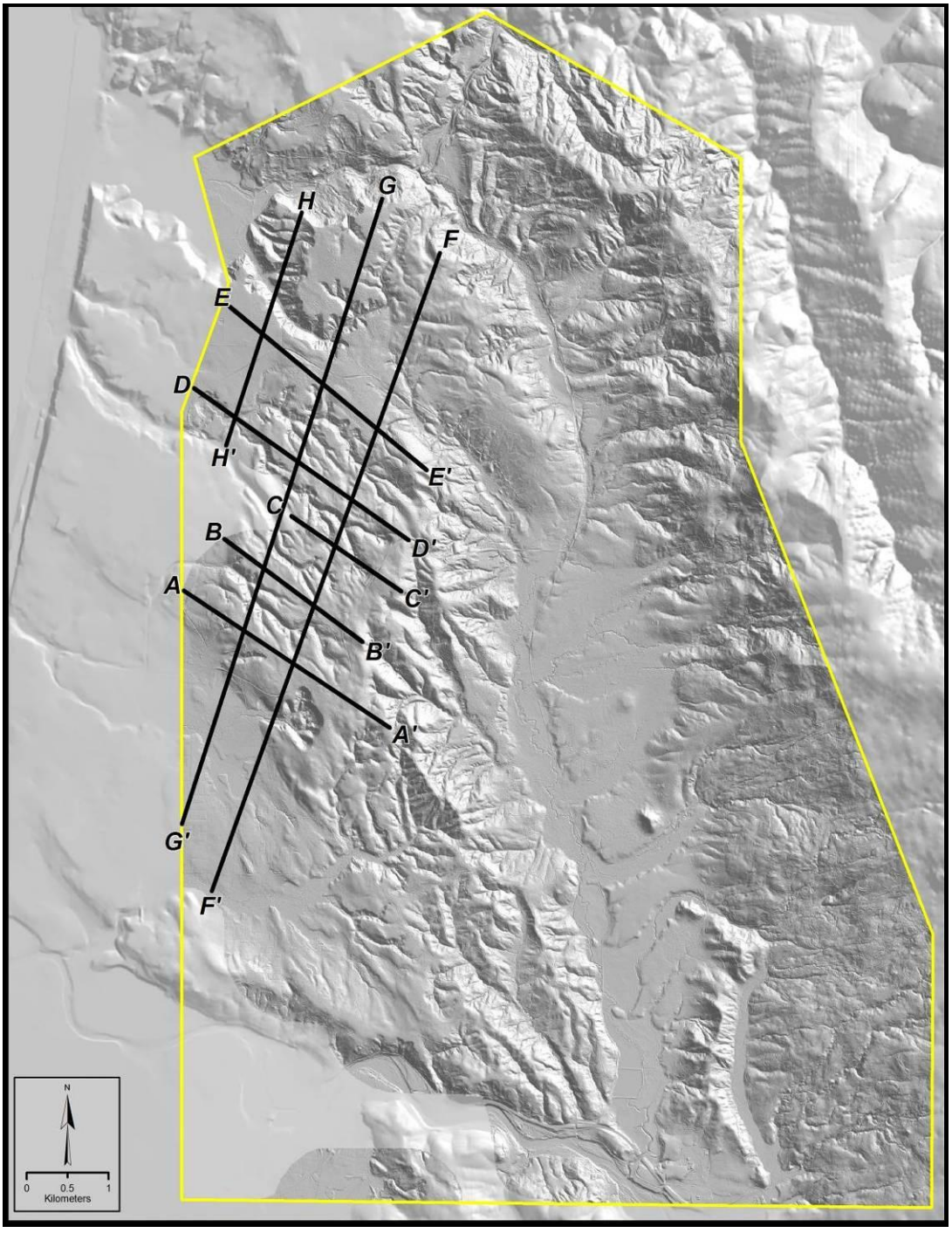

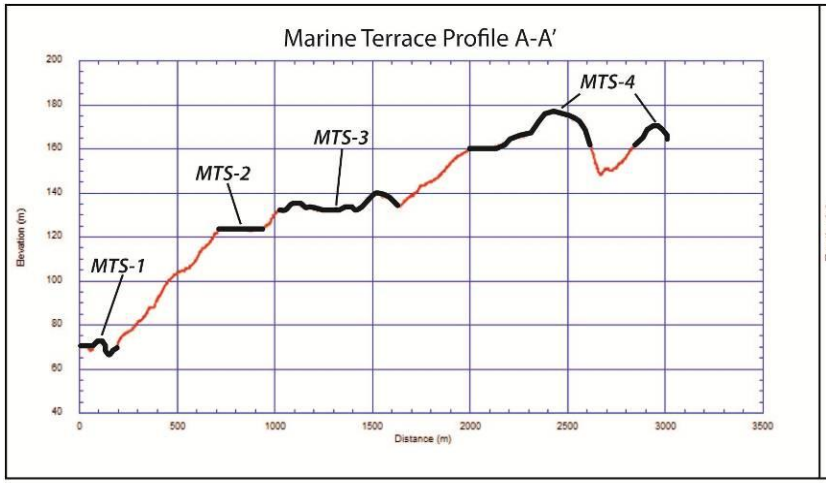
Marine Terrace Profile A-A′
MTS-1
MTS-2
MTS-3
MTS-4
Elevation (m)
Distance (m)

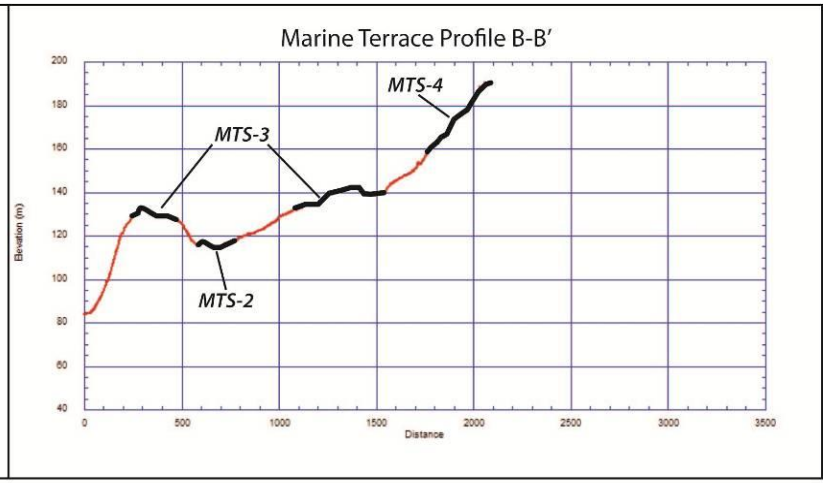
Marine Terrace Profile B-B′
MTS-2
MTS-3
MTS-4
Elevation (m)
Distance

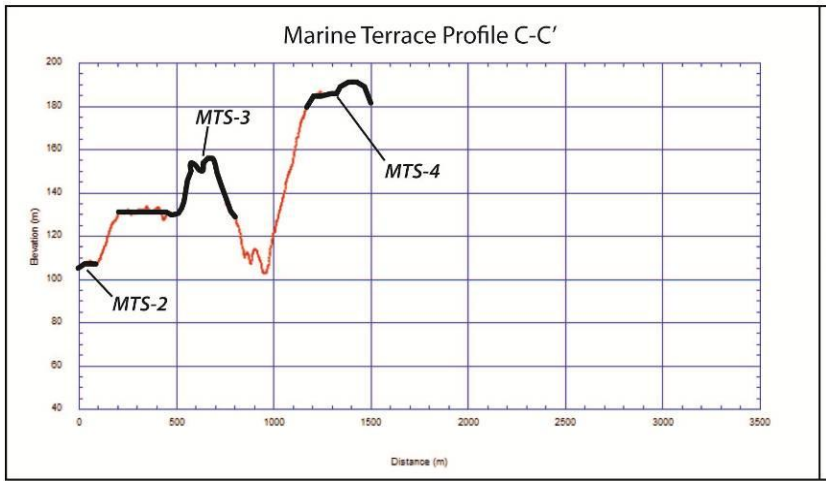
Marine Terrace Profile C-C′
MTS-2
MTS-3
MTS-4
Elevation (m)
Distance (m)

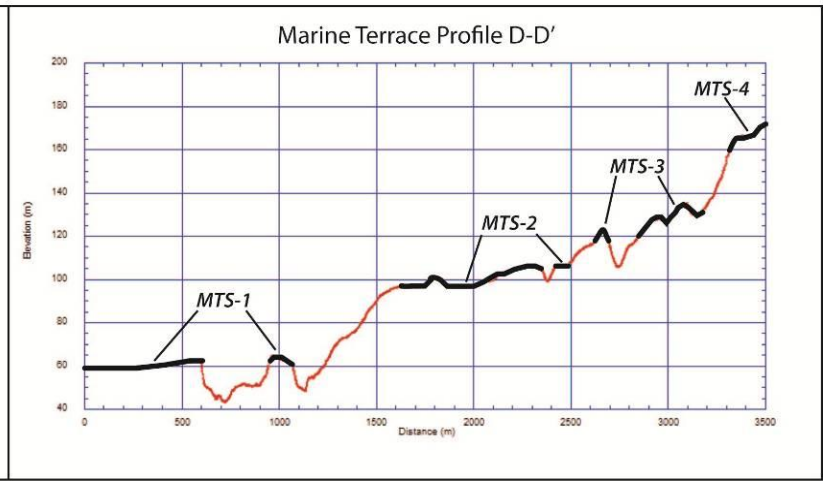
Marine Terrace Profile D-D′
MTS-1
MTS-2
MTS-3
MTS-4
Elevation (m)
Distance (m)

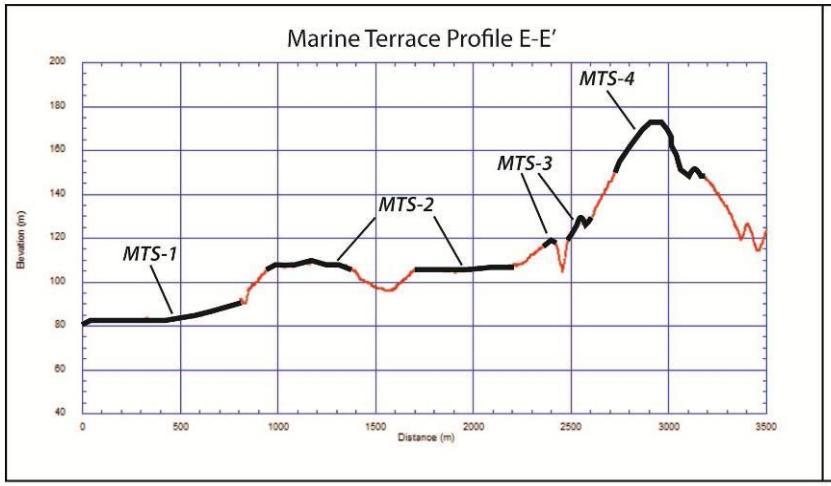
Marine Terrace Profile E-E′
MTS-4
MTS-3
MTS-2
MTS-1
Elevation (m)
Distance (m)

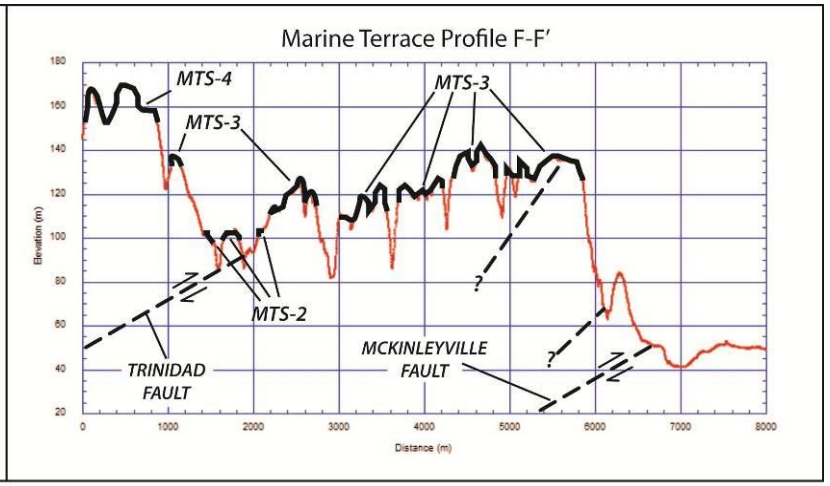
Marine Terrace Profile F-F′
MTS-4
MTS-3
MTS-3
MTS-2
TRINIDAD FAULT
MCKINLEYVILLE FAULT
Elevation (m)
Distance (m)

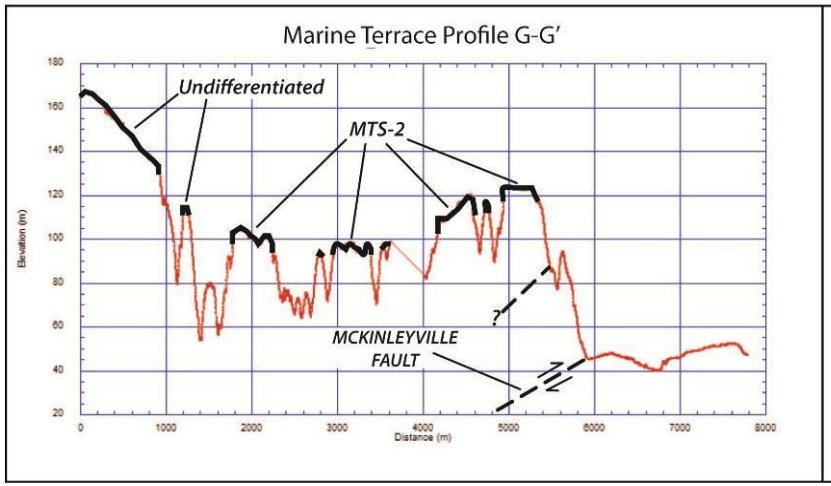
Marine Terrace Profile G-G′
Undifferentiated
MTS-2
MCKINLEYVILLE FAULT
Elevation (m)
Distance (m)

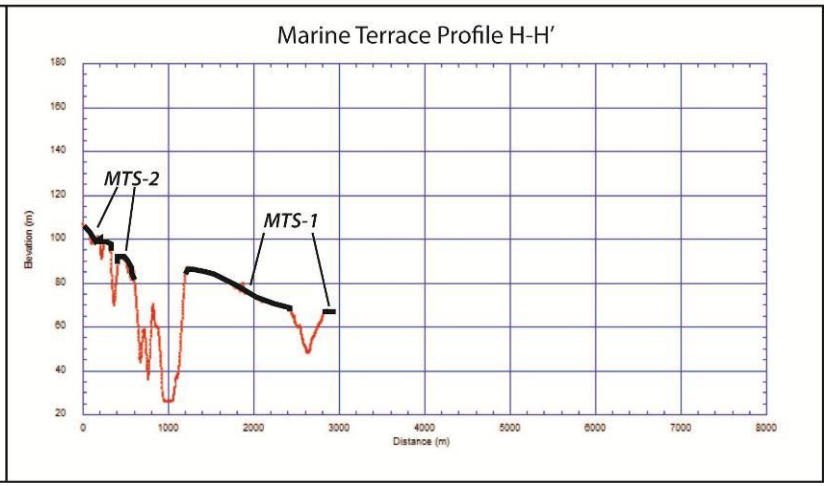
Marine Terrace Profile H-H′
MTS-2
MTS-1
Elevation (m)
Distance (m)

Alluvial Terrace Profiles

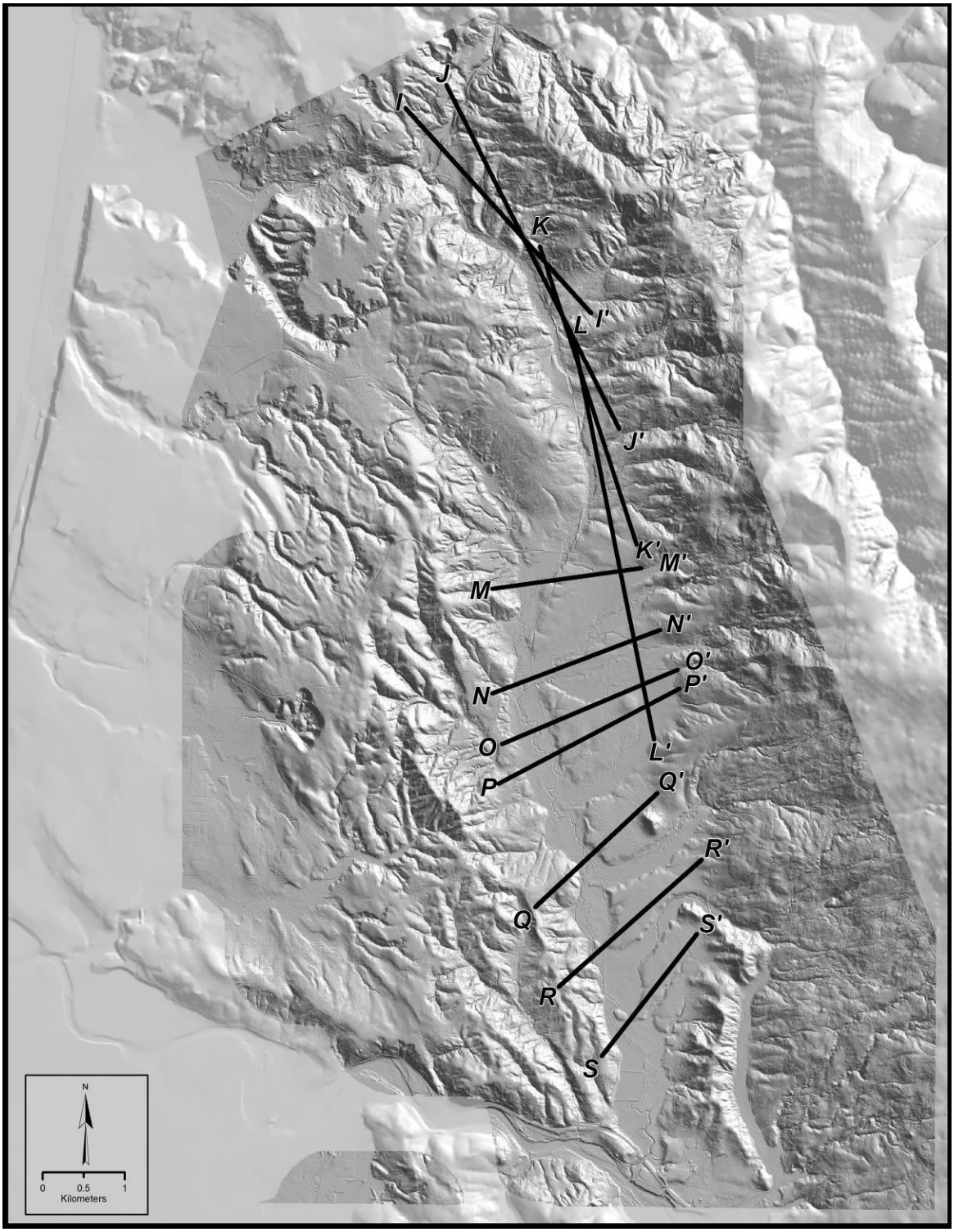

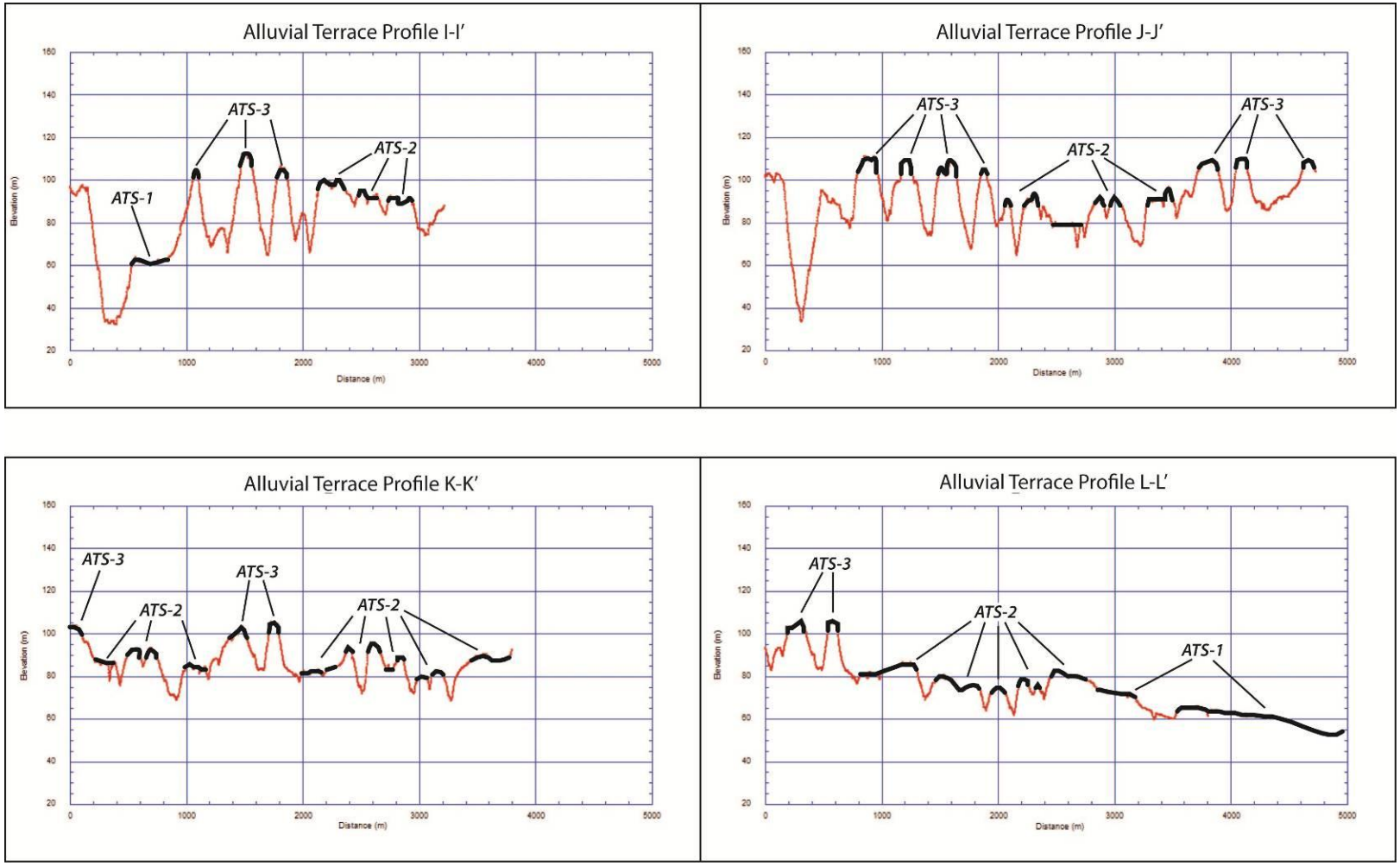
Alluvial Terrace Profile I-I'
ATS-1
ATS-3
ATS-2
Elevation (m)
Distance (m)
Alluvial Terrace Profile J-J'
ATS-3
ATS-2
ATS-3
Elevation (m)
Distance (m)
Alluvial Terrace Profile K-K'
ATS-3
ATS-2
ATS-3
ATS-2
Elevation (m)
Distance (m)
Alluvial Terrace Profile L-L'
ATS-3
ATS-2
ATS-1
Elevation (m)
Distance (m)

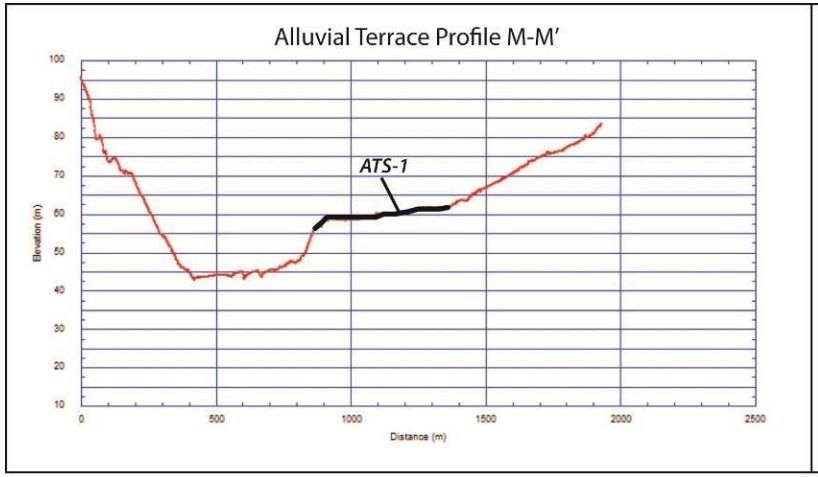
Alluvial Terrace Profile M-M′
ATS-1
Elevation (m)
Distance (m)

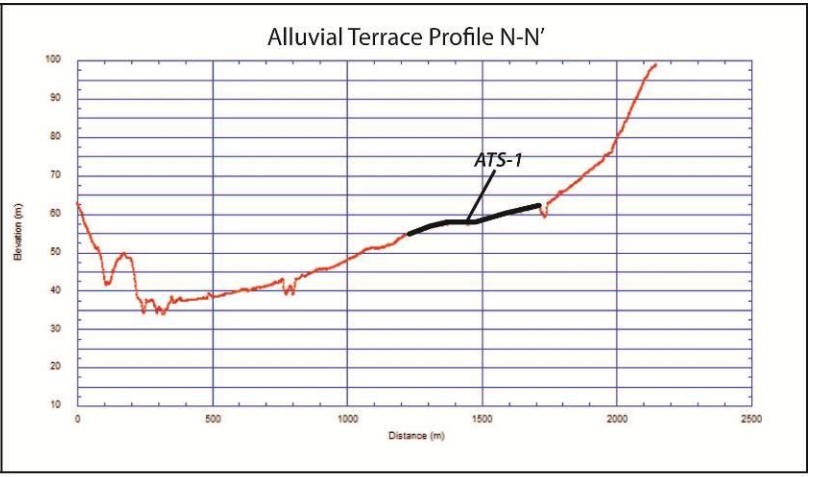
Alluvial Terrace Profile N-N′
ATS-1
Elevation (m)
Distance (m)

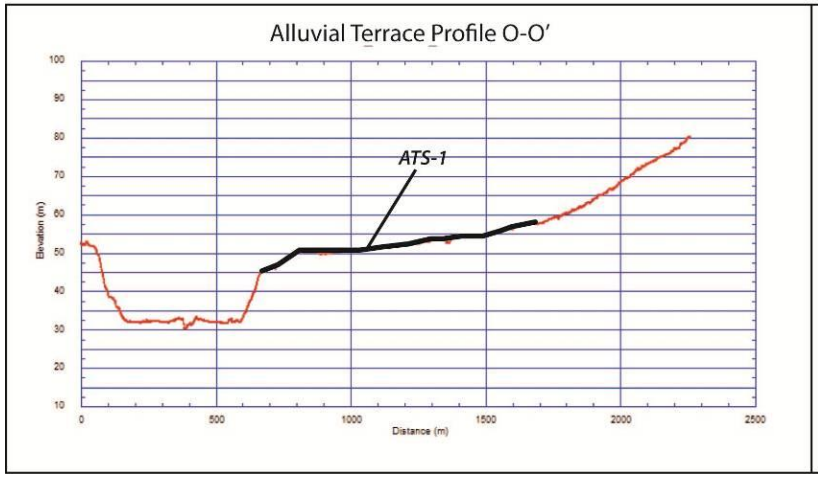
Alluvial Terrace Profile O-O′
ATS-1
Elevation (m)
Distance (m)

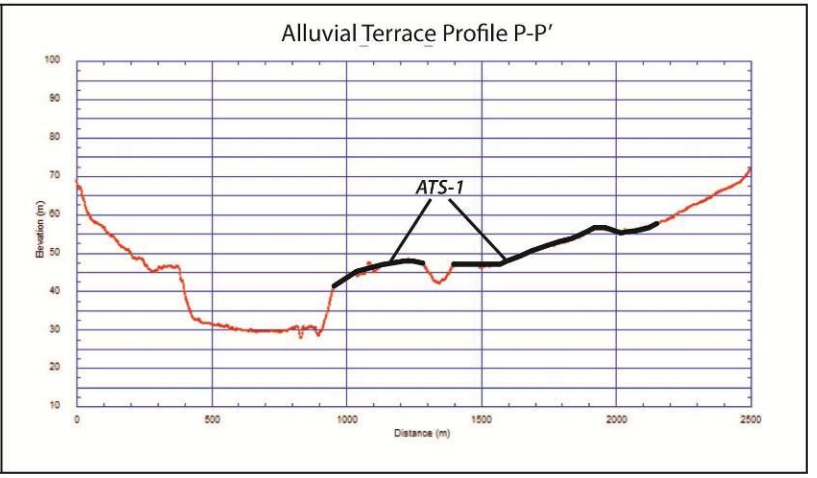
Alluvial Terrace Profile P-P′
ATS-1
Elevation (m)
Distance (m)

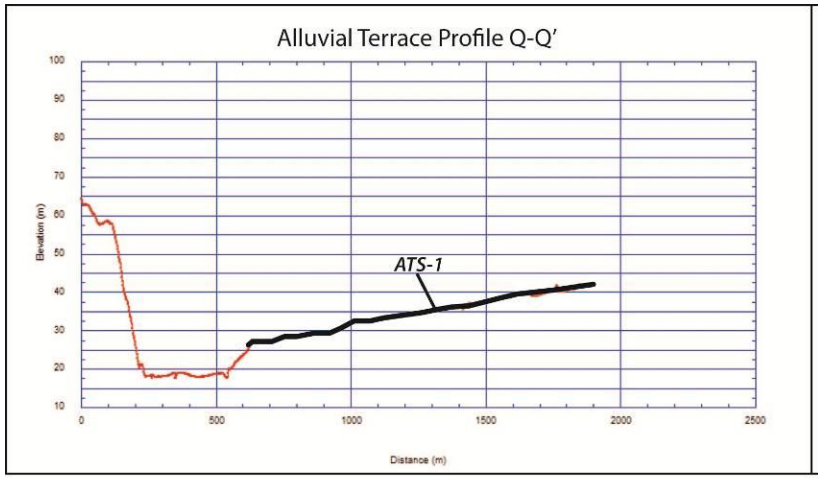
Alluvial Terrace Profile Q-Q'
Elevation (m)
Distance (m)
ATS-1

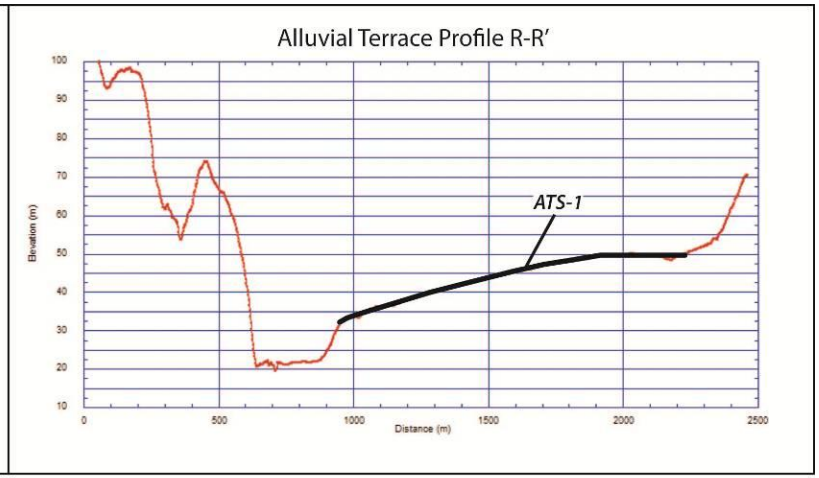
Alluvial Terrace Profile R-R'
Elevation (m)
Distance (m)
ATS-1

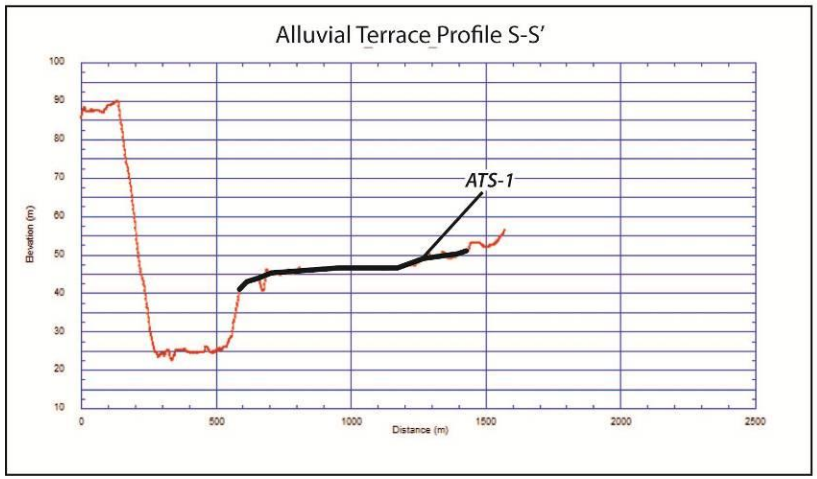
Alluvial Terrace Profile S-S'
Elevation (m)
Distance (m)
ATS-1

Tectonic Geomorphology Profiles

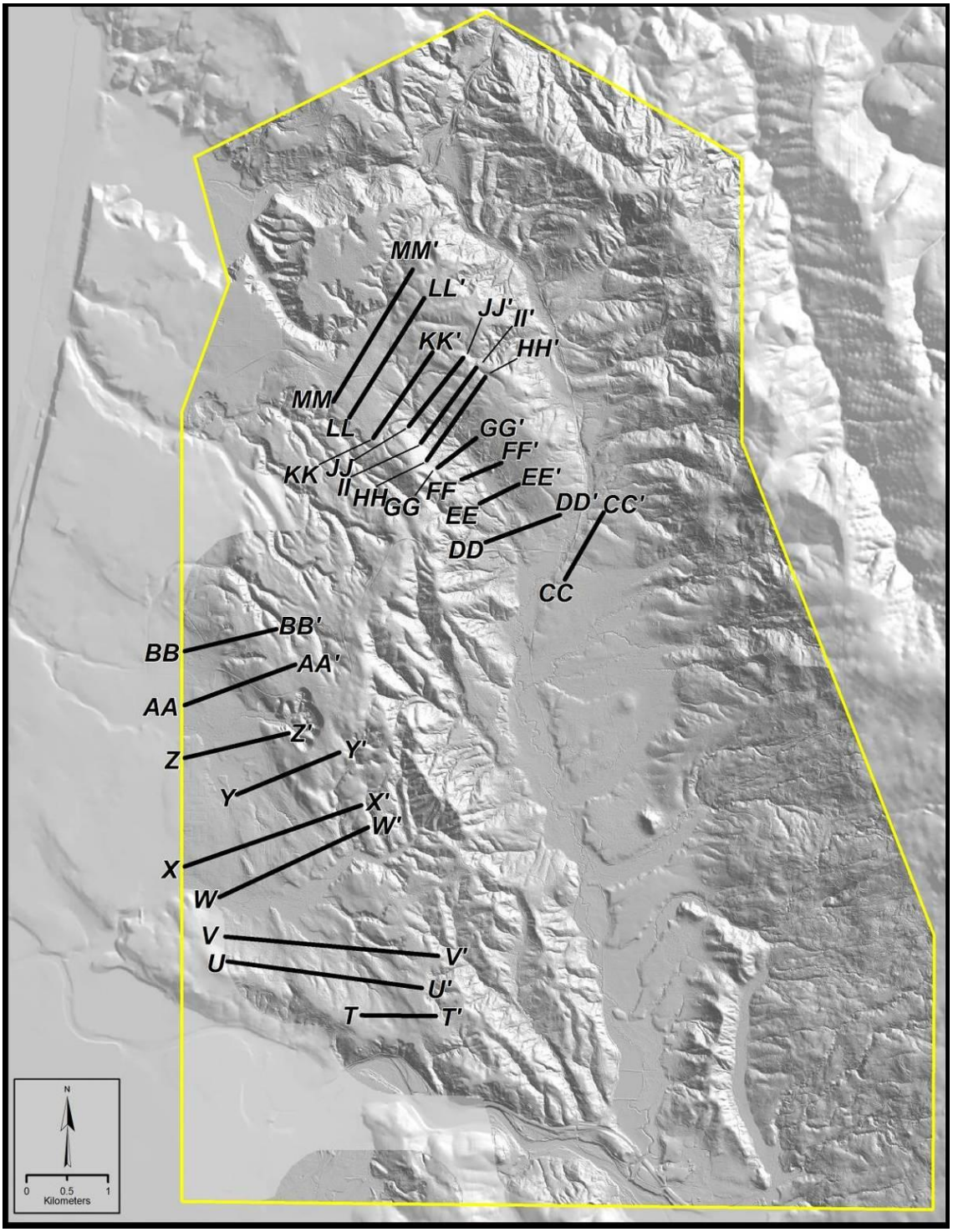

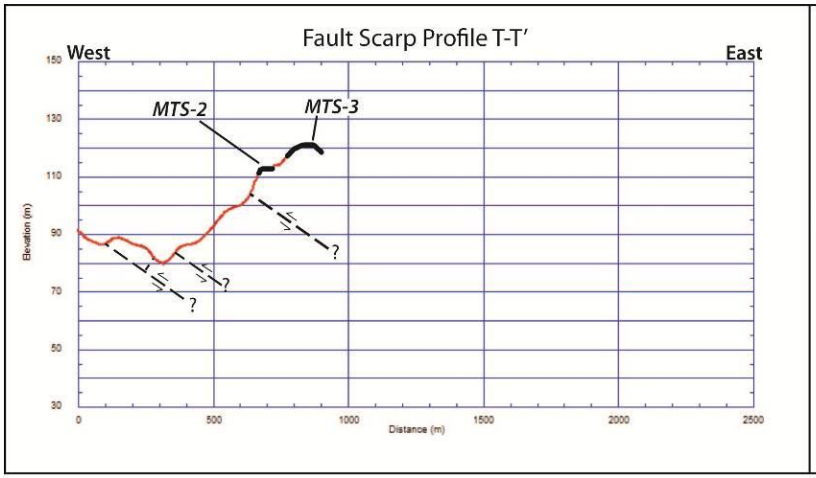
Fault Scarp Profile T-T′
West
East
MTS-2
MTS-3
Elevation (m)
Distance (m)

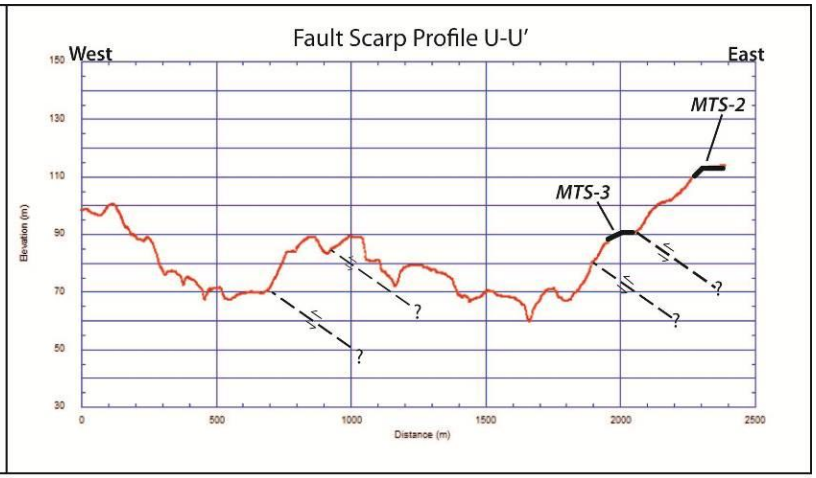
Fault Scarp Profile U-U′
West
East
MTS-2
MTS-3
Elevation (m)
Distance (m)

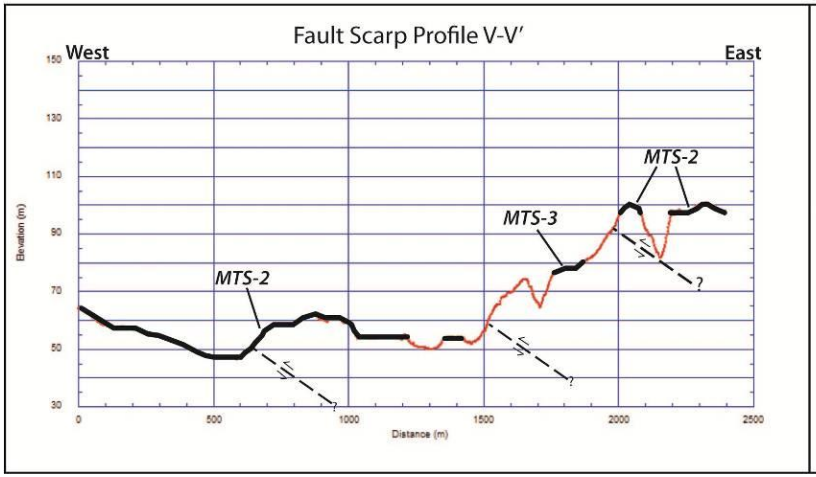
Fault Scarp Profile V-V′
West
East
MTS-2
MTS-3
MTS-2
Elevation (m)
Distance (m)

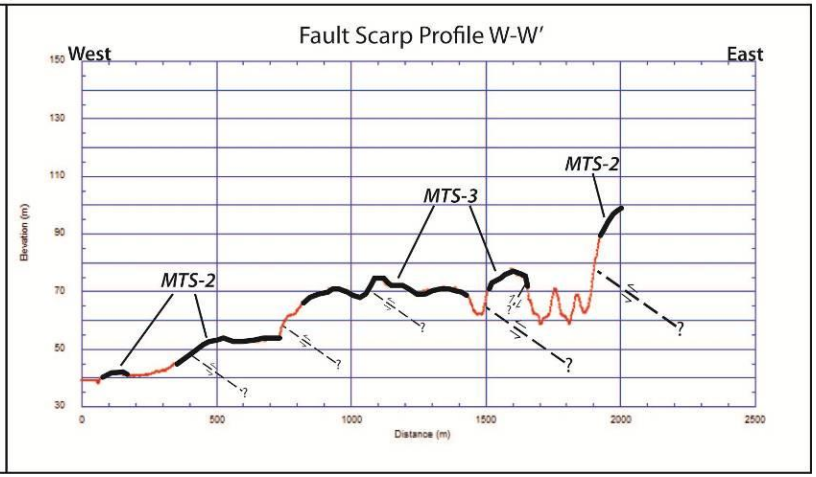
Fault Scarp Profile W-W′
West
East
MTS-2
MTS-3
MTS-2
Elevation (m)
Distance (m)

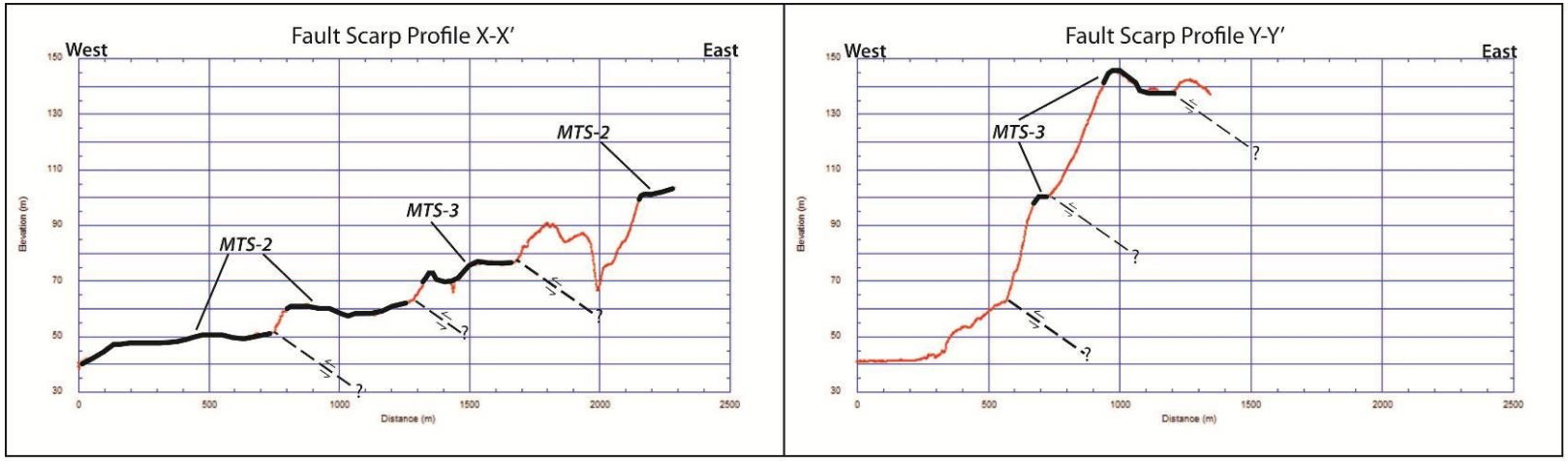
Fault Scarp Profile X-X′
West
East
MTS-2
MTS-3
MTS-2
?
?
?
Elevation (m)
Distance (m)

Fault Scarp Profile Y-Y′
West
East
MTS-3
?
?
?
Elevation (m)
Distance (m)

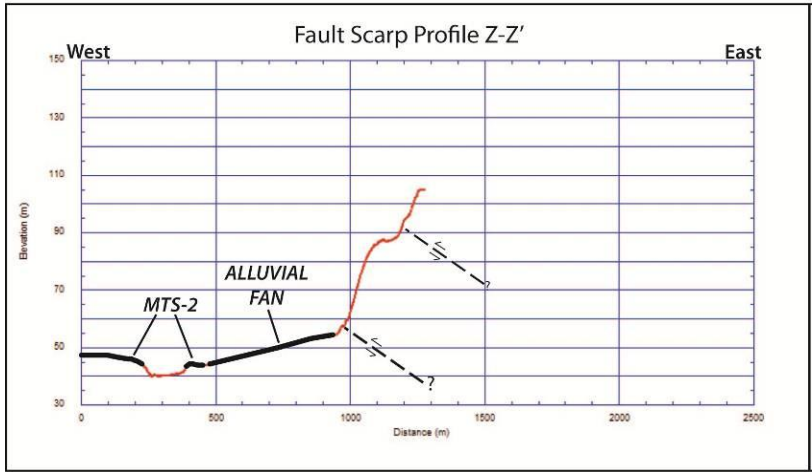
Fault Scarp Profile Z-Z′
West
East
ALLUVIAL
FAN
MTS-2
?
Elevation (m)
Distance (m)

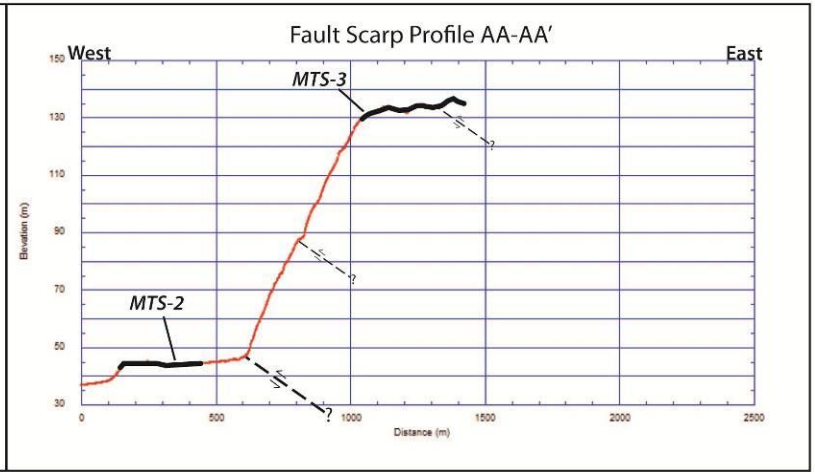
Fault Scarp Profile AA-AA′
West
East
MTS-3
MTS-2
?
?
Elevation (m)
Distance (m)

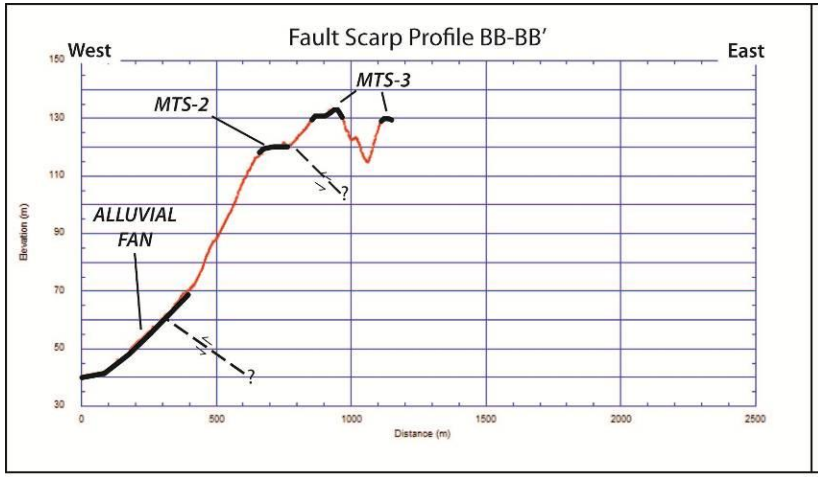
Fault Scarp Profile BB-BB'
West
East
MTS-3
MTS-2
ALLUVIAL
FAN
?
?
Elevation (m)
Distance (m)

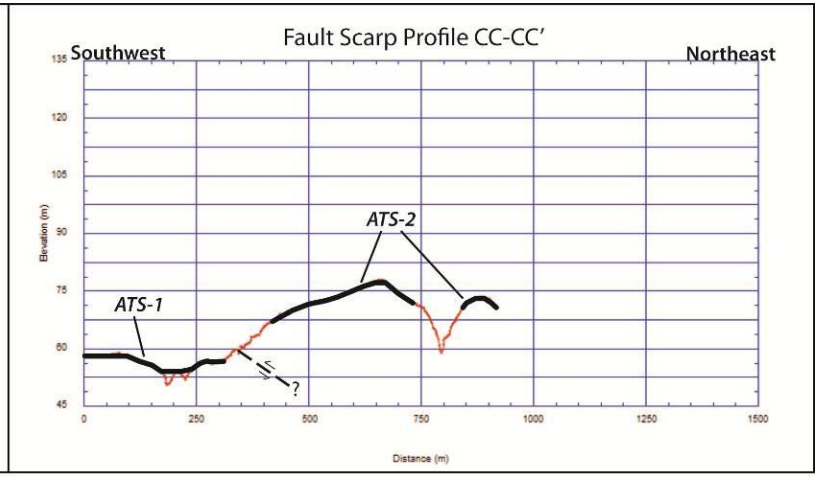
Fault Scarp Profile CC-CC'
Southwest
Northeast
ATS-2
ATS-1
?
Elevation (m)
Distance (m)

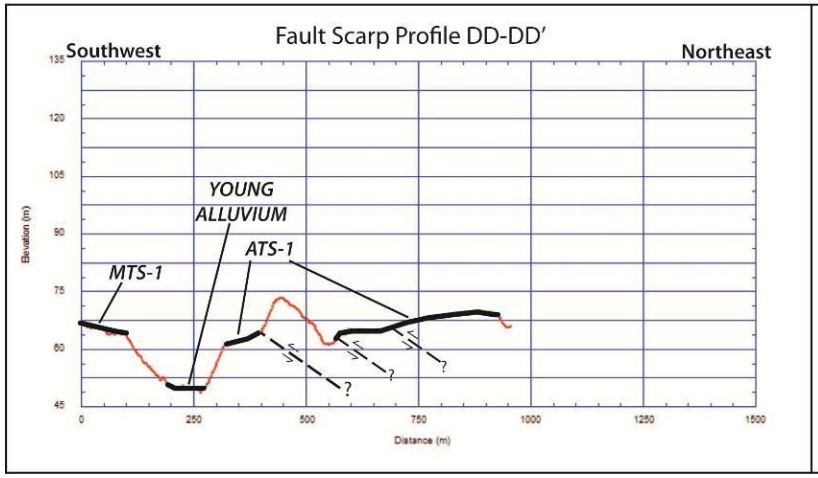
Fault Scarp Profile DD-DD'
Southwest
Northeast
YOUNG
ALLUVIUM
ATS-1
MTS-1
?
?
?
Elevation (m)
Distance (m)

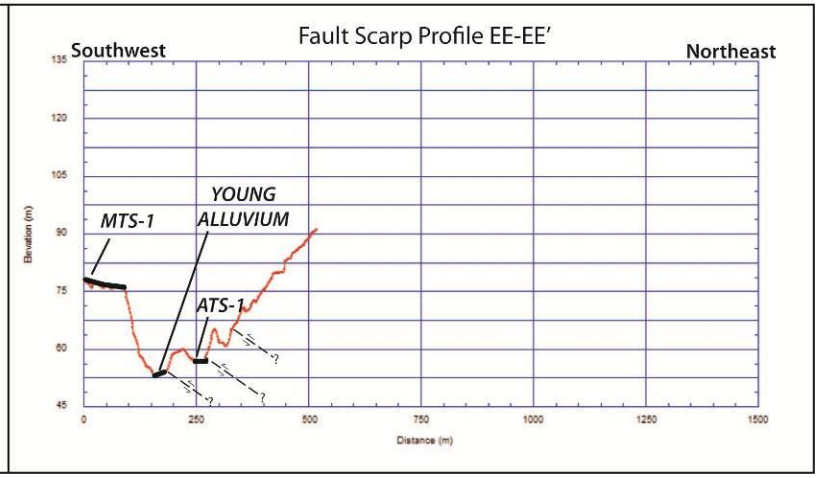
Fault Scarp Profile EE-EE'
Southwest
Northeast
YOUNG
ALLUVIUM
MTS-1
ATS-1
?
?
?
Elevation (m)
Distance (m)

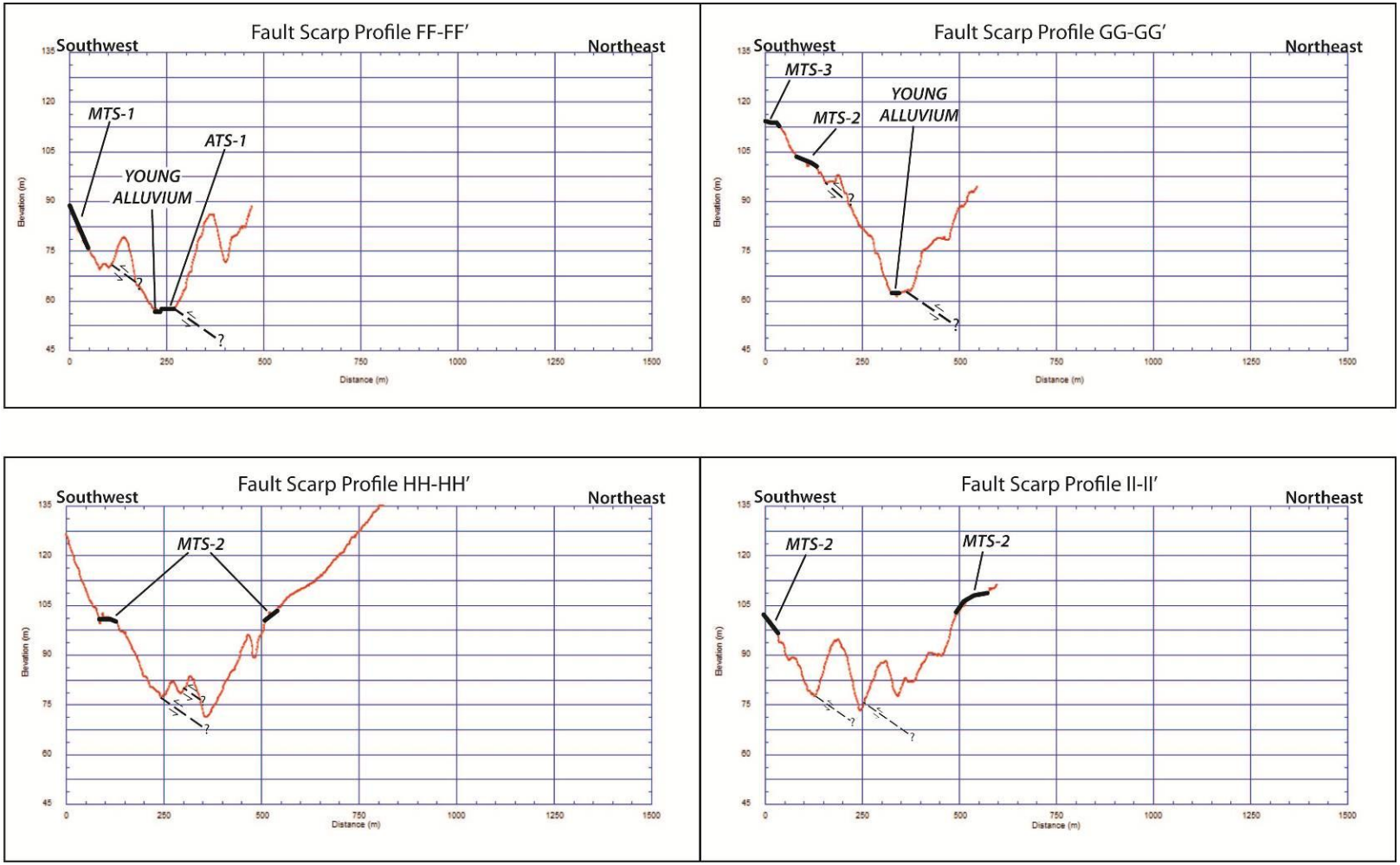
Fault Scarp Profile FF-FF'
Southwest
Northeast
MTS-1
ATS-1
YOUNG
ALLUVIUM
Elevation (m)
Distance (m)
Fault Scarp Profile GG-GG'
Southwest
Northeast
MTS-3
MTS-2
YOUNG
ALLUVIUM
Elevation (m)
Distance (m)
Fault Scarp Profile HH-HH'
Southwest
Northeast
MTS-2
Elevation (m)
Distance (m)
Fault Scarp Profile II-II'
Southwest
Northeast
MTS-2
MTS-2
Elevation (m)
Distance (m)

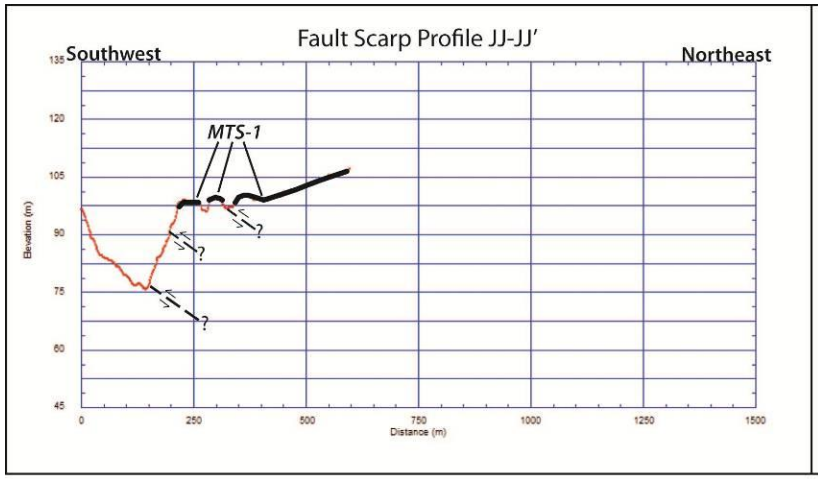
Fault Scarp Profile JJ-JJ'
Southwest
Northeast
MTS-1
?
?
?
Elevation (m)
135
120
105
90
75
60
45
0
250
500
750
1000
1250
1500
Distance (m)

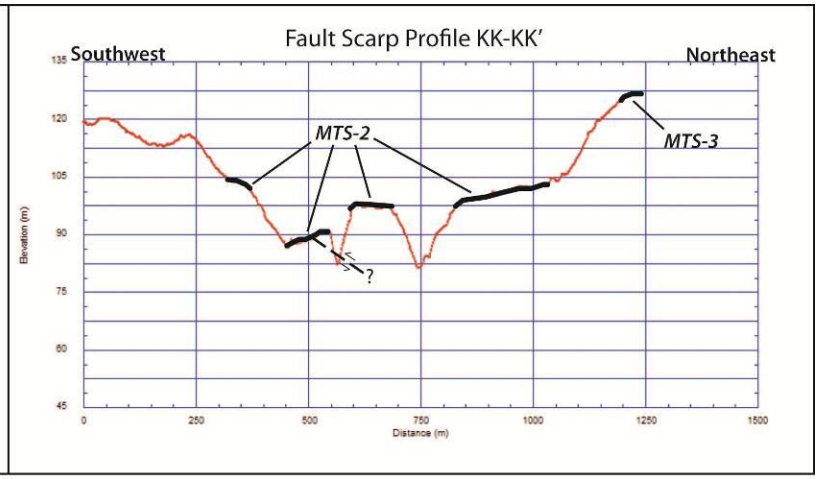
Fault Scarp Profile KK-KK'
Southwest
Northeast
MTS-2
MTS-3
?
Elevation (m)
135
120
105
90
75
60
45
0
250
500
750
1000
1250
1500
Distance (m)

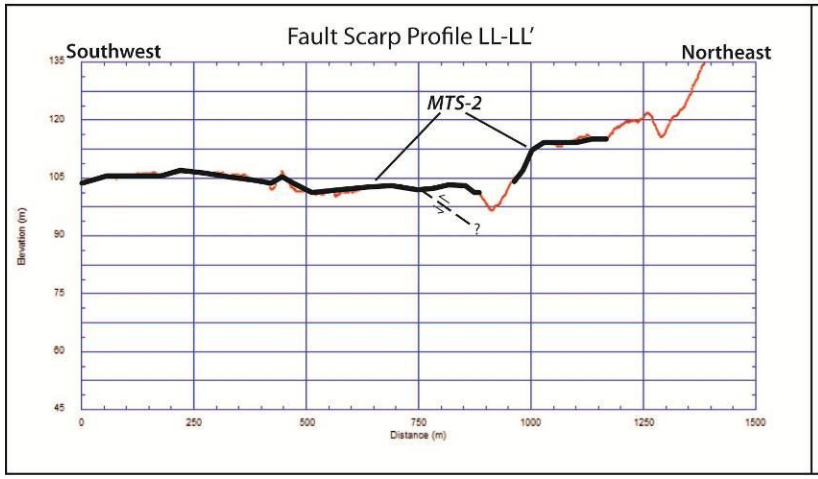
Fault Scarp Profile LL-LL'
Southwest
Northeast
MTS-2
?
Elevation (m)
135
120
105
90
75
60
45
0
250
500
750
1000
1250
1500
Distance (m)

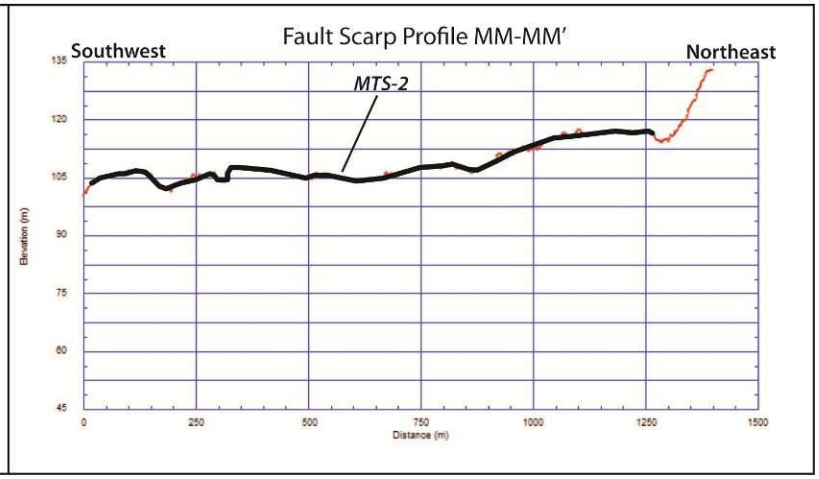
Fault Scarp Profile MM-MM'
Southwest
Northeast
MTS-2
Elevation (m)
135
120
105
90
75
60
45
0
250
500
750
1000
1250
1500
Distance (m)

Appendix B

OIS 5e Model Contours

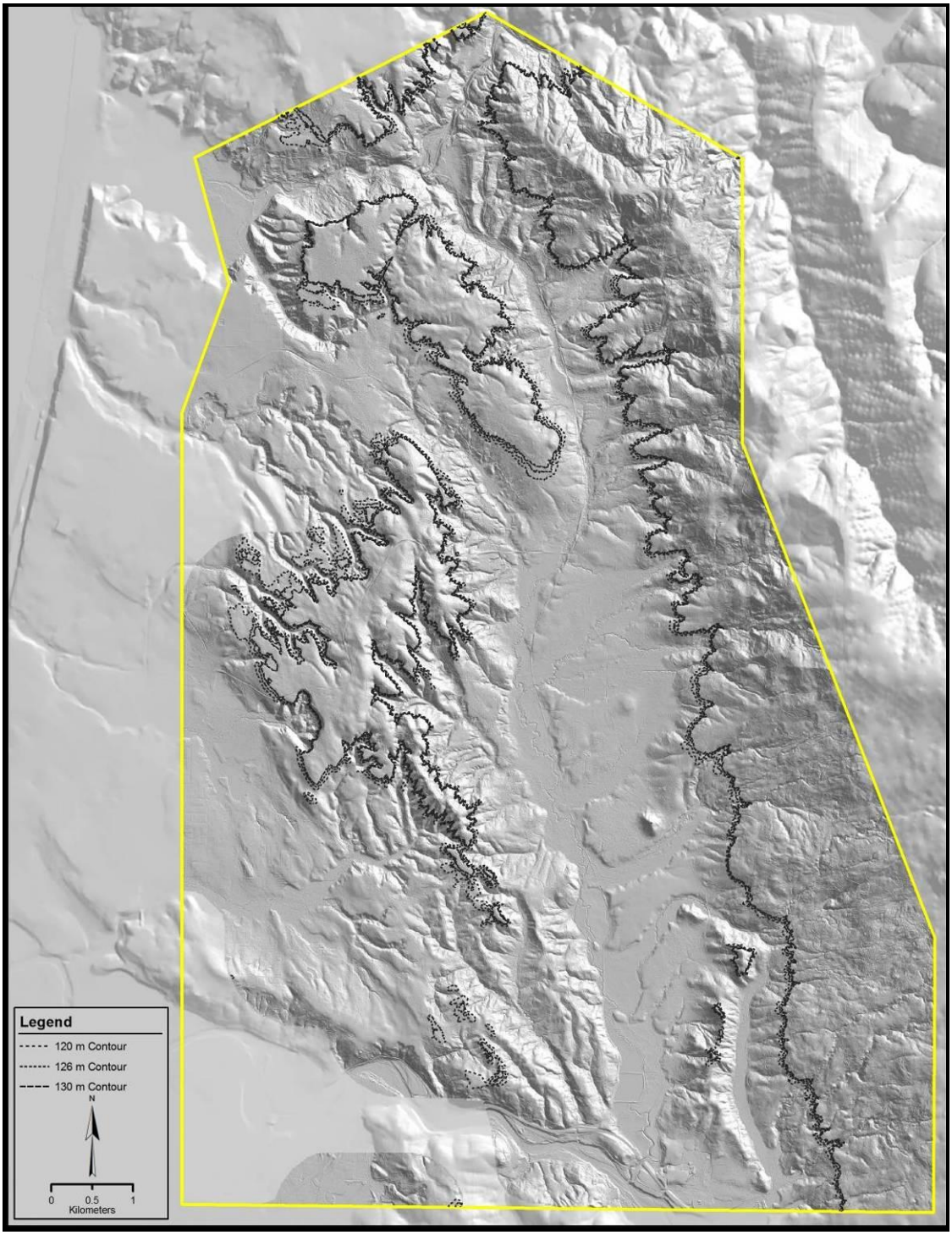

OIS 5c Model Contours

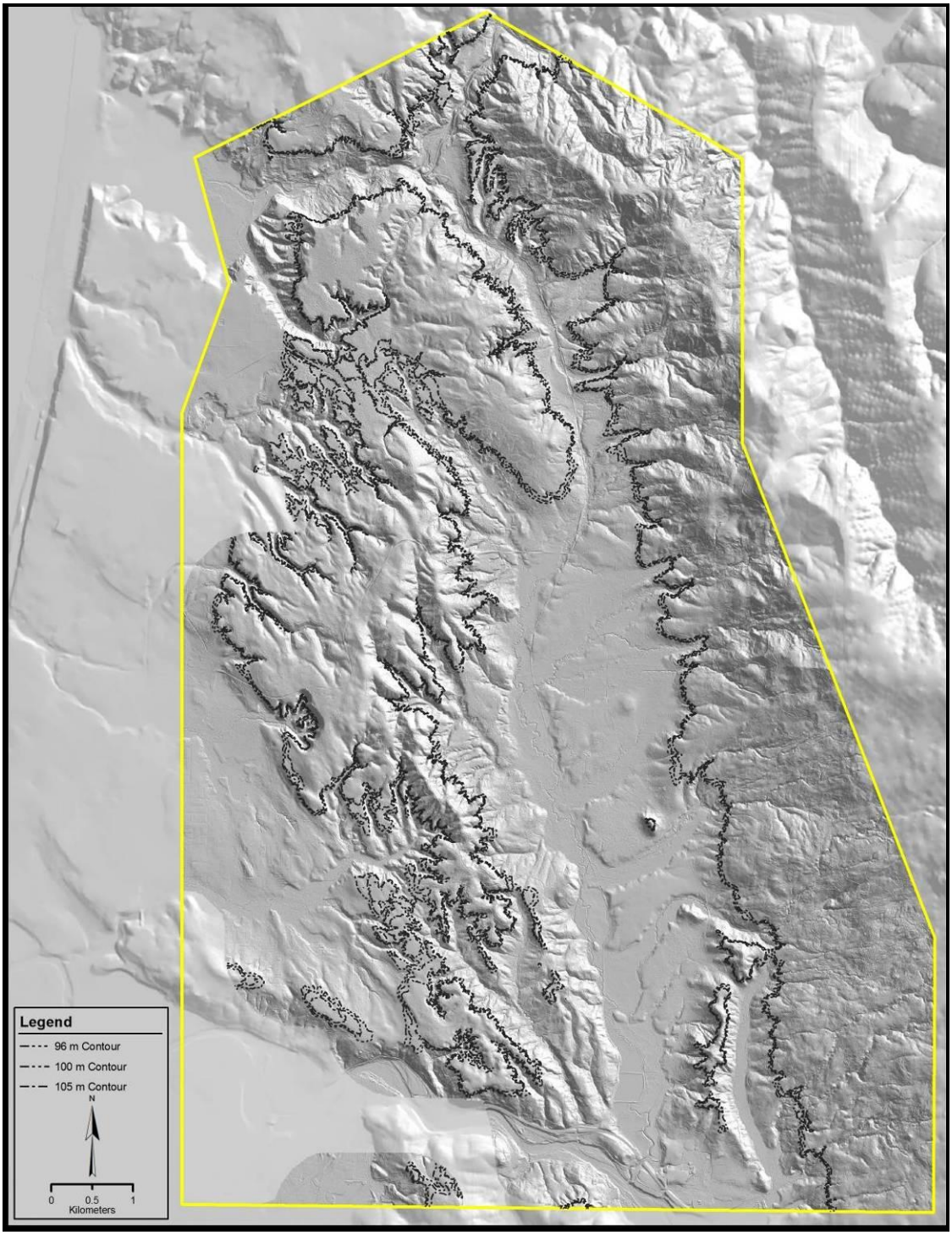

OIS 5a Model Contours

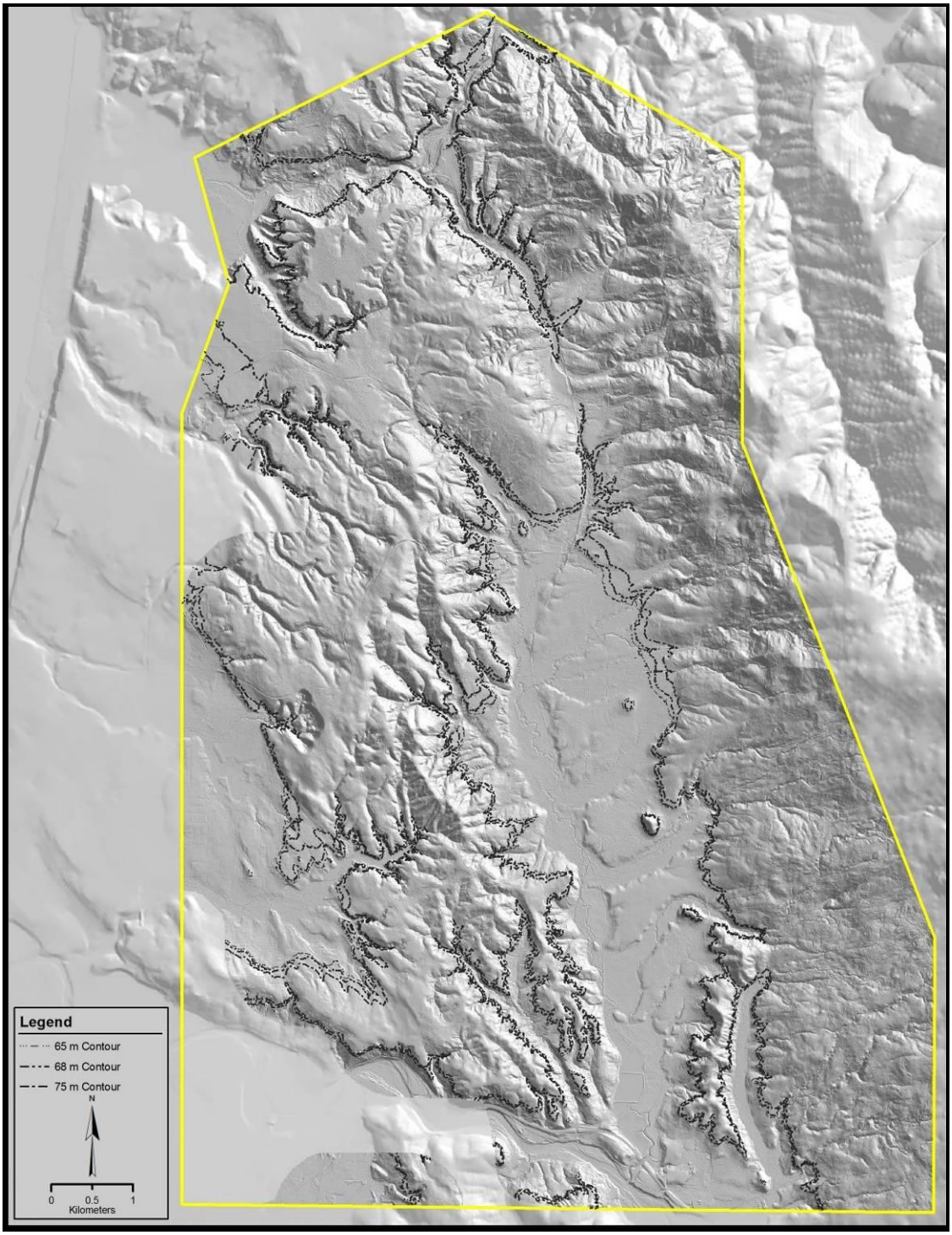

Appendix C

Reconstructed Coastlines through Last Inter-Glacial Period

OIS 5e

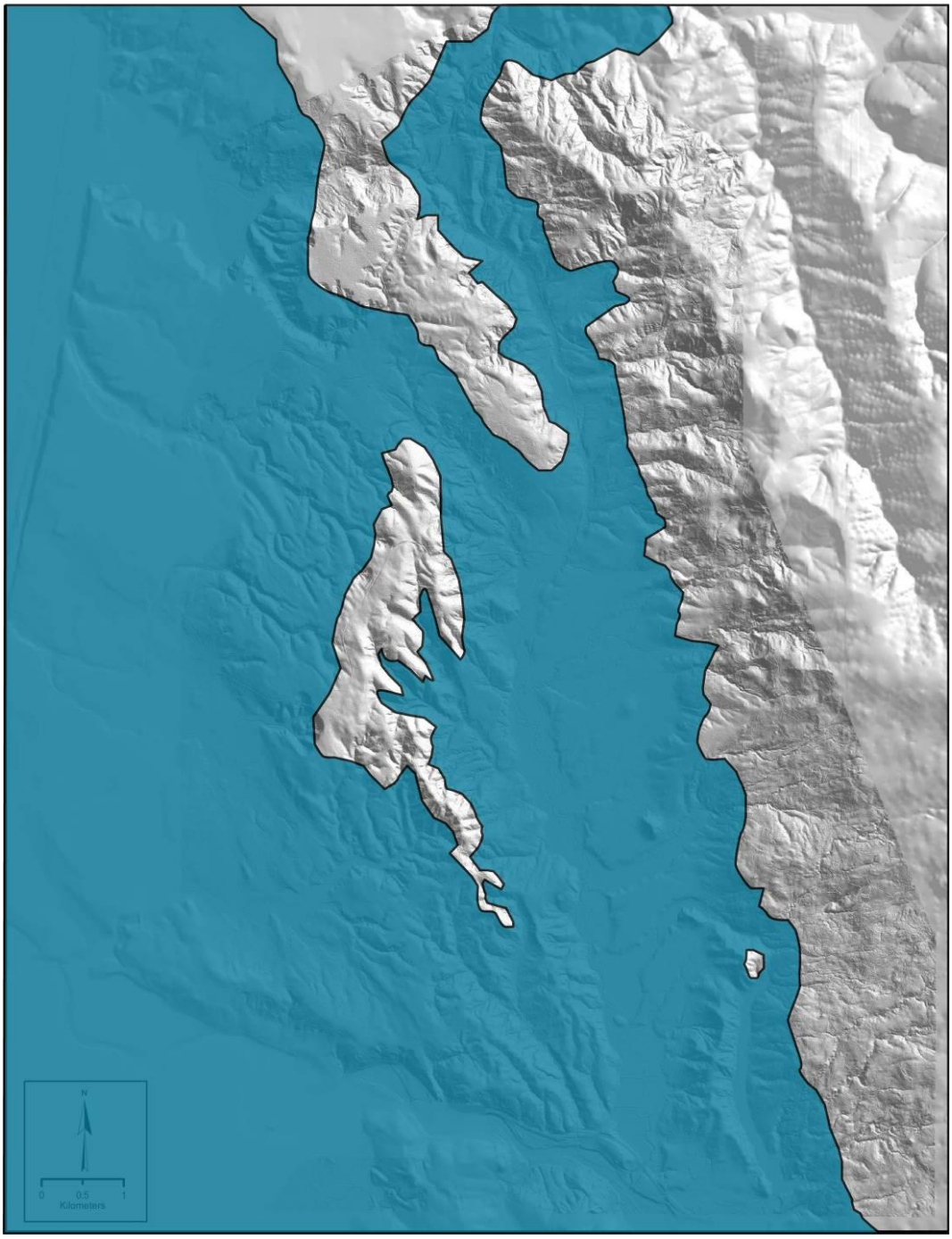

OIS 5c

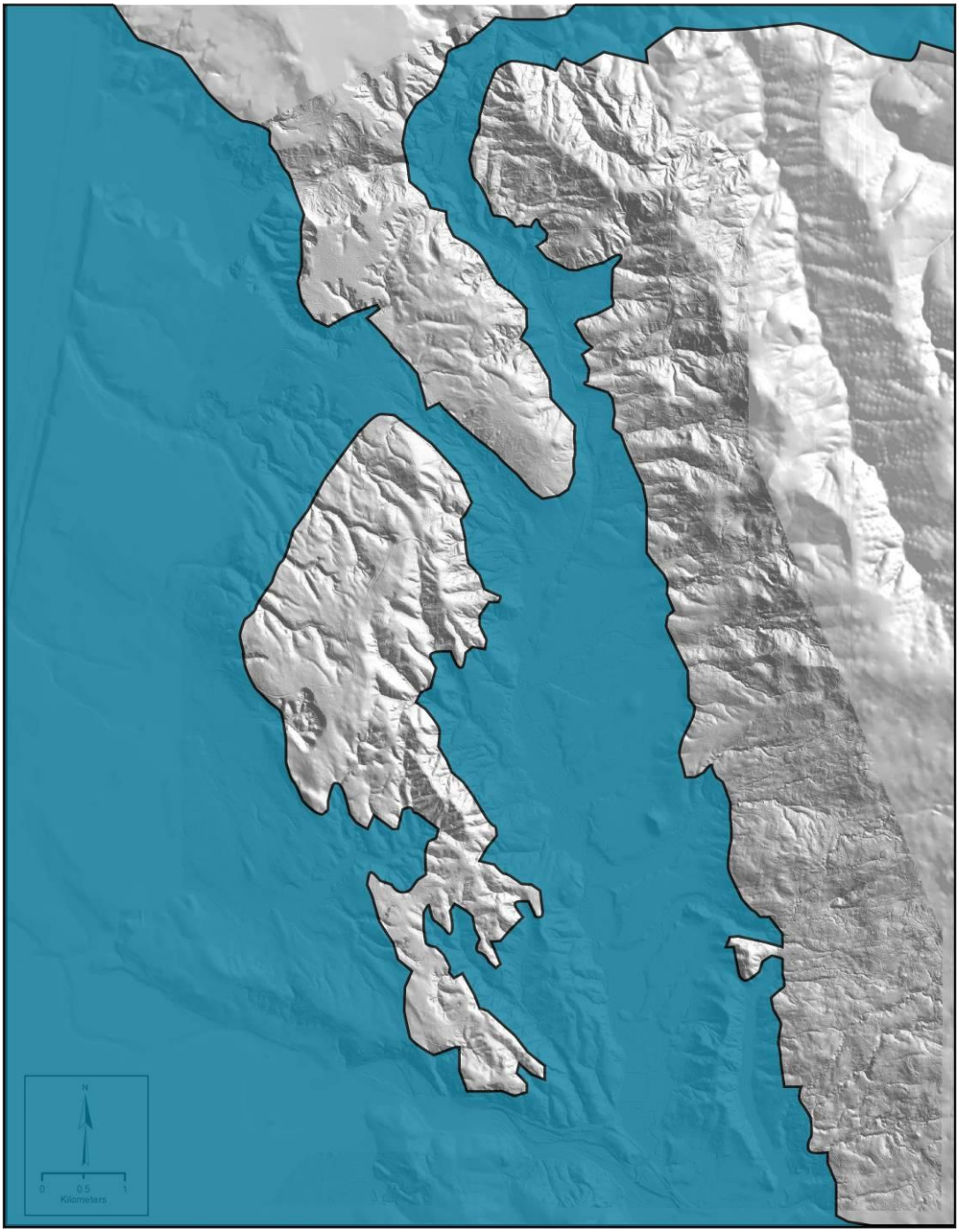

OIS 5a

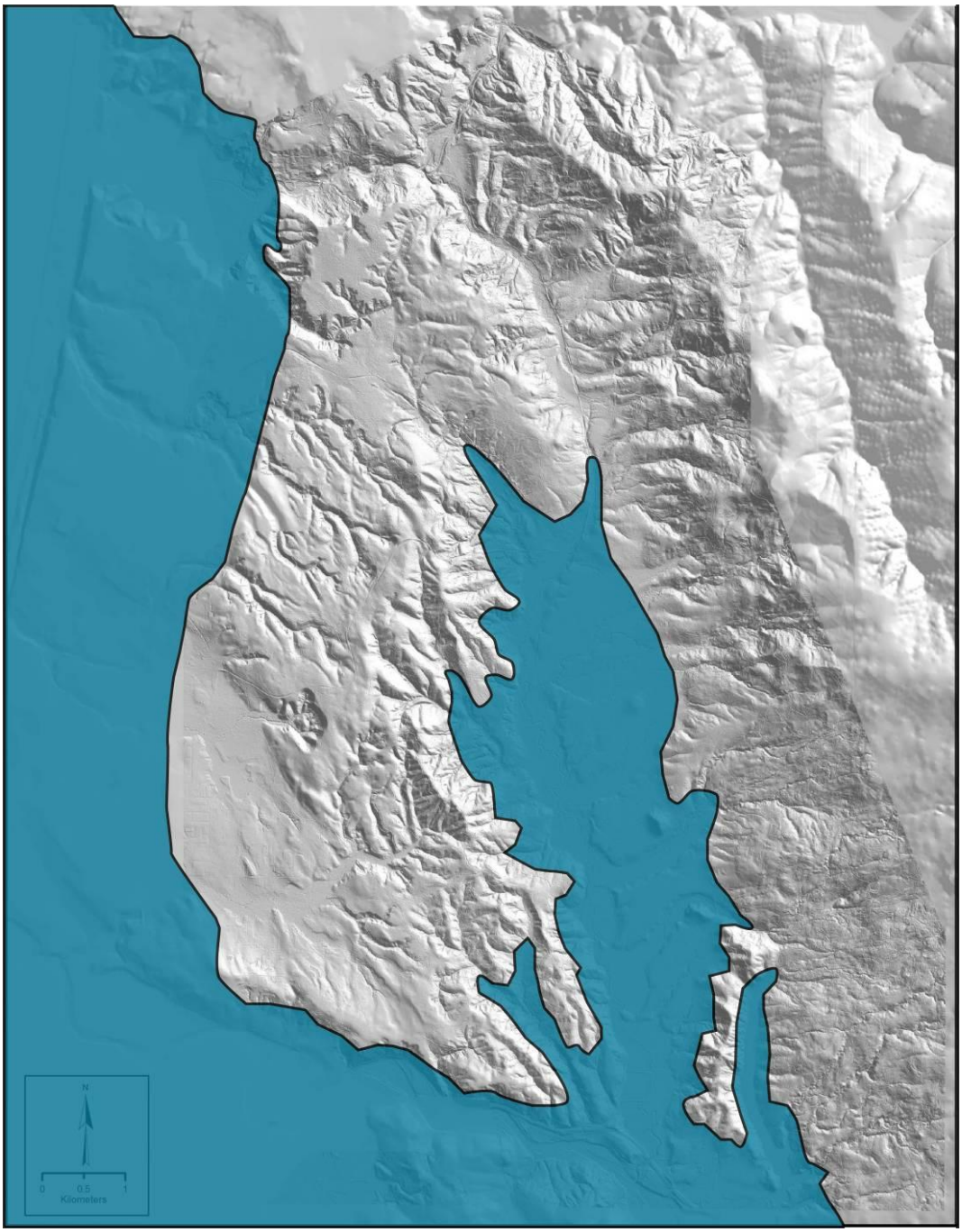

Appendix D

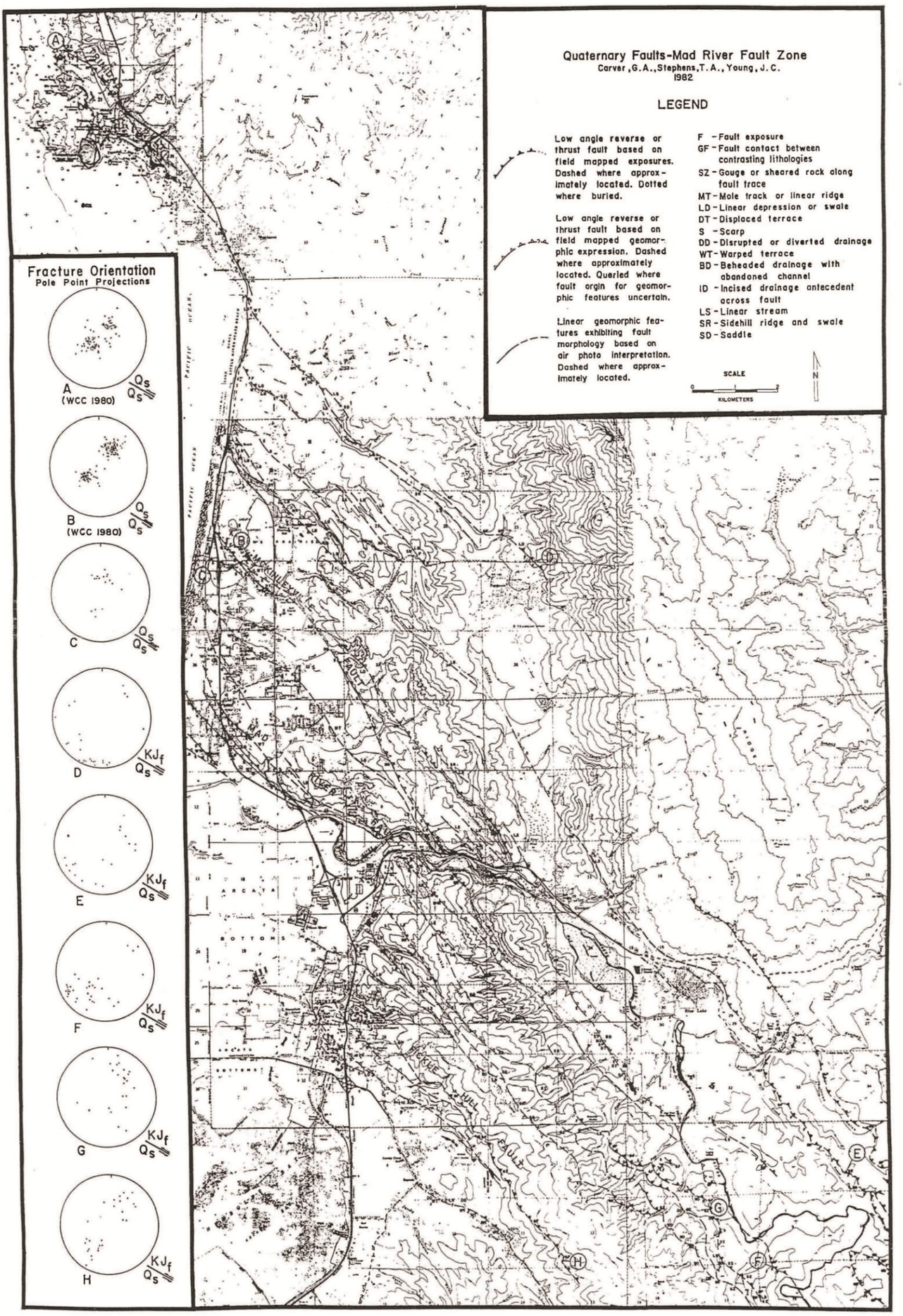
Quaternary Faults-Mad River Fault Zone
Carver, G.A., Stephens, T.A., Young, J.C.
1982
LEGEND
Low angle reverse or thrust fault based on field mapped exposures. Dashed where approximately located. Dotted where buried.
Low angle reverse or thrust fault based on field mapped geomorphic expression. Dashed where approximately located. Queried where fault orgin for geomorphic features uncertain.
Linear geomorphic features exhibiting fault morphology based on air photo interpretation. Dashed where approximately located.
F - Fault exposure
GF - Fault contact between contrasting lithologies
SZ - Gouge or sheared rock along fault trace
MT - Mole track or linear ridge
LD - Linear depression or swale
DT - Displaced terrace
S - Scarp
DD - Disrupted or diverted drainage
WT - Warped terrace
BD - Beheaded drainage with abandoned channel
ID - Incised drainage antecedent across fault
LS - Linear stream
SR - Sidehill ridge and swale
SD - Saddle
SCALE
KILOMETERS
N
Fracture Orientation
Pole Point Projections
A (WCC 1980)
B (WCC 1980)
C
D
E
F
G
H
Qs
KJf
ARCATA
BOTTOMS
EUREKA
FAULT